GAIT AND LOCOMOTION ANALYSIS FOR TRIBOLOGICAL APPLICATIONS

by

Md Hayder Ali

A Thesis Submitted in

Partial Fulfilment of the

Requirements for the Degree of

Master of Science

in Engineering

at

The University of Wisconsin-Milwaukee

December 2013

ABSTRACT
GAIT AND LOCOMOTION ANALYSIS FOR TRIBOLOGICAL APPLICATIONS

by

Md Hayder Ali

The University of Wisconsin-Milwaukee, 2013
Under the Supervision of Professor Michael Nosonovsky

The control of friction during walking is important to prevent slips and falls at workplace or other situations. Gait type is a crucial factor in walking. When person is walking, there is high possibility of slips and falls depending on the surface conditions friction, and gait. In this research, we survey these factors. Based on this, the study has focused on biometric system of gait and locomotion analysis. Biometric systems have become popular systems in recent decades. They are normally used for security systems such as access control and surveillance, human computer interaction, and multimedia management. In this thesis, Principal Component Analysis (PCA) with and without Radon Transform (RT) were used. Principal Component Analysis (PCA) technique is used to reduce the dimension of images without much loss of information. For the numerical experiments, we have selected CMU MoBo gait database. Two features were used for gait recognition: silhouette and Gait Energy Image (GEI). Only side view images with three walking styles were considered. To evaluate the system performance, the Equal Recognition Rate (ERR) criteria was used. Using the silhouette feature, Equal Recognition Rates (ERR) of 90.78%, 90.26%, and 87.75% were achieved for PCA-only

technique and 90.92%, 90.20% and 87.76% for PCA with RT technique for slow walk, fast walk and "carrying-a-ball" walk respectively. The GEI-based template system achieved Equal Recognition Rates (ERR) of 91.62%, 90.90% and 92.34% using the PCA-only method and 91.70%, 90.88% and 92.34% using PCA with RT technique for slow, fast and carrying-a-ball respectively. Thus, the GEI-based template system achieved better recognition rates applying PCA with and without RT techniques compared to silhouettes-based system using PCA with and without RT techniques. The implications for friction are discussed.

TABLE OF CONTENTS

LIST OF FIGURES

LIST OF TABLES

ACKNOWLEDGEMENTS

I would like to express my deepest gratitude and appreciation to my advisor Dr. Michael Nosonovsky, Department of Mechanical Engineering program, Engineering Mathematics and Science, University of Wisconsin-Milwaukee (UWM) for all his guidance, never ending support in the completion of this thesis, and giving me the opportunity to embark on this research and enhanced my knowledge on the given subject. This piece of work has attained the present shape due to his helping hand.

I would like to express my heartfelt thanks to one of my professor Jamal A. Dargham department of computer Engineering, University of Malaysia Sabah (UMS), for his proper guidance, encouragement and moral support throughout my study period at University of Malaysia Sabah (UMS) and University of Wisconsin-Milwaukee (UWM). I started working on gait identification problems on UMS in 2010 in professor Jamal A. Dargham lab and continue this work at UWM.

I also express my heartfelt thanks for one of my UMS lab mate Ervin Gobin Moung who helped me to develop the Matlab code to get the desired results.

Finally, I would like to thank my beloved parents, my younger brother Eklas Hossain, my Elder brother Dr. Ahad Ali, wife Masuma S. Bithi, daughter Mahreen A. Ali and son Muhammed S. Ali for their patience, understanding and encouragement in every aspect of the study. They have been my strongest support emotionally and spiritually.

CHAPTER 1

INTRODUCTION

1.1 Over View of Slips and Falls

When person is walking on the street or any place, including workplace, it is possible accident of sudden falling or some environmental hazard happened. Nowadays, researchers found out that significantly increased accident any place and becoming serious injured. However, it may cause fatal or non-fatal injured for pedestrians.

Slipping is the major cause of falling for the young or older individuals during walking. The individual can face serious back pain or muscular strain illness or ever injury cause for slipping. It is therefore very important to understand causes of slipping for humans. Various environmental and other factors were studied as causes of slip and fall including surface roughness, compliance, topography, adjacent area, contaminants, shoe, foot and others. However, lighting and contrastness levels are also causes of slip while walking. Even, weather and climate factors such as ice and snow may increase slipping. The human health conditions are also a factor to slip when person is walking.

The most important point of slip is complicated conduct friction when subjects are walking. So if individuals are able to control gait not to exceed limitation of friction then individuals would not slip on the surface or any walking place. There are different types of walking style such as carrying with load, walking up hill, level walking, and each walking style requires different friction. Each walking style has different friction and

different techniques to prevent surface slipping. The gait analysis may reduce slip and fall accidents and may bring a good condition for the individuals. The gait analysis may be improved to reduce the friction whether it's happened by shoe, walking surface or combination of both for walking person. The tribometric instruments may be applied for friction situation that faced by person. If the person gait known about pressure, velocity, contact time, and other related info to measure then frictional measurement devices shoe-floor interface may be produced desire results. Another challenging part is the characteristics of copying human gait. However, during slip, it is necessary to know the individuals foot details and it is also very condition of weather. The human posture control system is also a very important to maintain balance and protect to fall down. The balancing posture involves with biomechanics, control, and other interface with current environment which are protect not to slip. The kinematics and dynamics are very important to know about slip during gait.

1.2 Biomechanics Locomotion

The slips and falls are related with shoe or foot and floor which most complicated parameters of mechanical study. The slip is unable to avoid if the shear forces created while friction happened by shoe or floor interface. It is very important to know about foot forces and ground reaction forces when walking in normal and walking in fast with and without carrying a load. The food position is also an important point to avoid friction such as position of heel, position of foot fingers and other parts of foot. The walking speed is also required to know characteristic of slips and walking surface conditions. The slips and falls are also depending on the length of gait and step. The physical joints

(ankle, knee and hip) are also may cause of slips and falls. Especially, ankle, knee and hip are required to maintain human physical balance during walk.

Walking on inclined surface, it is high possibility to slip as shear forces increased and unable to balance that occurred slip. The slope surface increased the risk of slips and falls and it may risk by ground reaction forces, kinematics, and joint moments (Strandberg and Lanshammar 1981, Perkins and Wilson 1983, Strandberg 1983, Winter 1991, Redfern and Dipasquale 1997, Cham and Redfern 2001a, Mark et al. 2001).

1.3 Walking on Ascending and Descending Order

When the person is walking on the stair or slope surface, the body motion and muscular demands are significantly vary during walk. During walk on the stair, it is important to know to prevent slips and falls as can walk forward and backward direction (McFayden and Winter 1988, Mark et al. 2001).

During walk, carrying a load is more challenging to prevent slips and falls. The physiological activities are required to balance the walking pattern that prevents slips and falls. Kinematics of stair ambulation is very important to know when walking on the stair. It is depending on the hip and knee motion activities.

Biomechanics during slipping, the authors explained about micro-slips, macro-slips and falls briefly. Normal gait on the normal dry surface, after conducting heel on the surface very fast make a complete stop which called micro-slip. After certain distance, the complete stopped is called macro-slip. Macro-slip is take very little bit time to make a complete stopped. Another slipping name is slip-stick which not develops into falls. Slip-

stick can be divided into three groups called mini-slip, midi-slip and maxi-slip. It is very complicated to detect the mini-slip as it happened very shortly. Midi slip is about slip in certain distance and maxi-slip is about to fall but not fall on the surface. However, maxi-slip has categorized into two groups namely, heel lose contact and unbalance heel contact to make safety fall. Fig. 1.1 shows the different type of slips (Perkins 1978, Cham and Redfern 2001c, Mark et al. 2001).

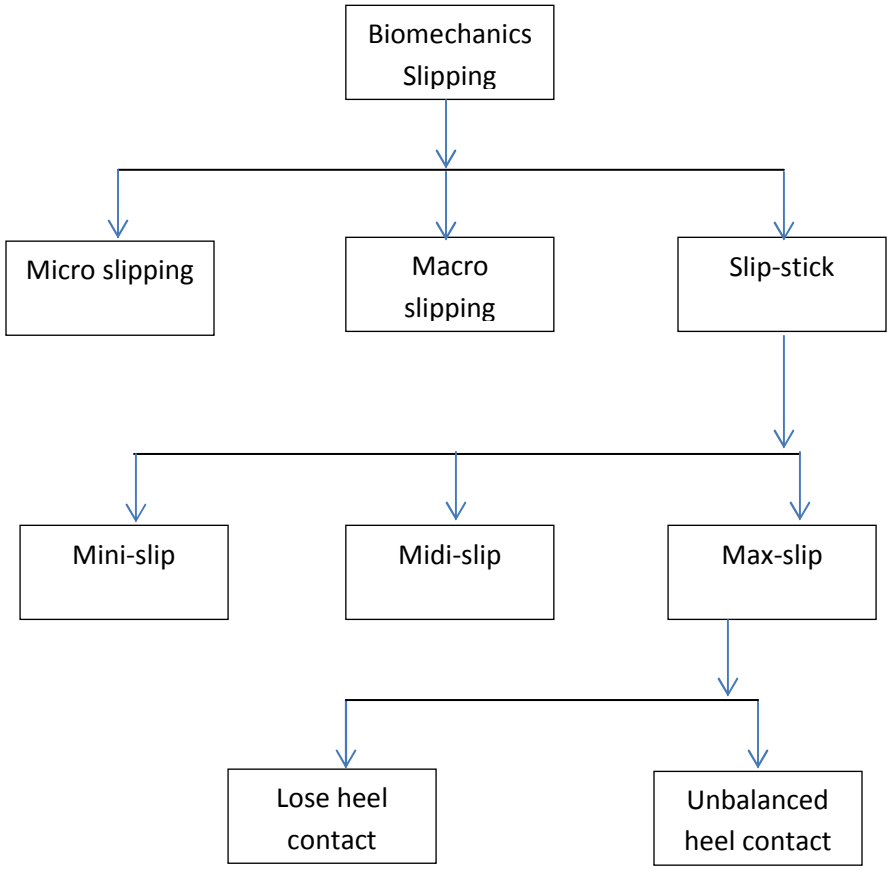

Figure 1.1: Shows the different type of slips

Souece: (Perkins 1978, Cham and Redfern 2001c, Mark *et al.* 2001)

When person is walking with carrying a load, the physical joint moments are working to control the walking speed. Mostly, hip and knee are balancing the physical load when large variations occur. The dynamic analysis will work automatically to balance body control. The human has power to control gesture during walk or during motion (Patla 1993, Woollacott and Tang 1997, Mark *et al*. 2001).

Two different direction of slips during a normal walk which are forward slip during the landing phase and backward slip during the take-off phase. Landing phase is more dangerous as need to control body weight. The slip distance significantly affected by floor conditions but not walking velocity. The friction used to apply for a measure of slipperiness. Thus, friction and slipperiness have a strong relationship for biomechanical industries. Many published paper has worked on the normal walk for research under dry, wet and complex environments. The authors have suggested taking variable parameter such as contact time, normal force build up rate, foot angle, and contact force of shoe, vertical force and sliding velocity. The authors explained about properties for safety. The static friction properties follow traditional drag-type devices and about foot slide. The steady state dynamic friction properties follow traditional of resistance to a steady state motion and it related with motion of foot and walkway.

When individuals are walking on the treadmill, it can be seen that the walking cycles are not smooth. It proves that changing the walking direction and changing the walking cycle duration. It is also changing each frame distance. It all happened cause of friction and slips. It is also necessary to balance physical conditioning not to fall down on

surface. Treadmill surface is not same as other announced surface that friction is happening while walk on the treadmill and other surface.

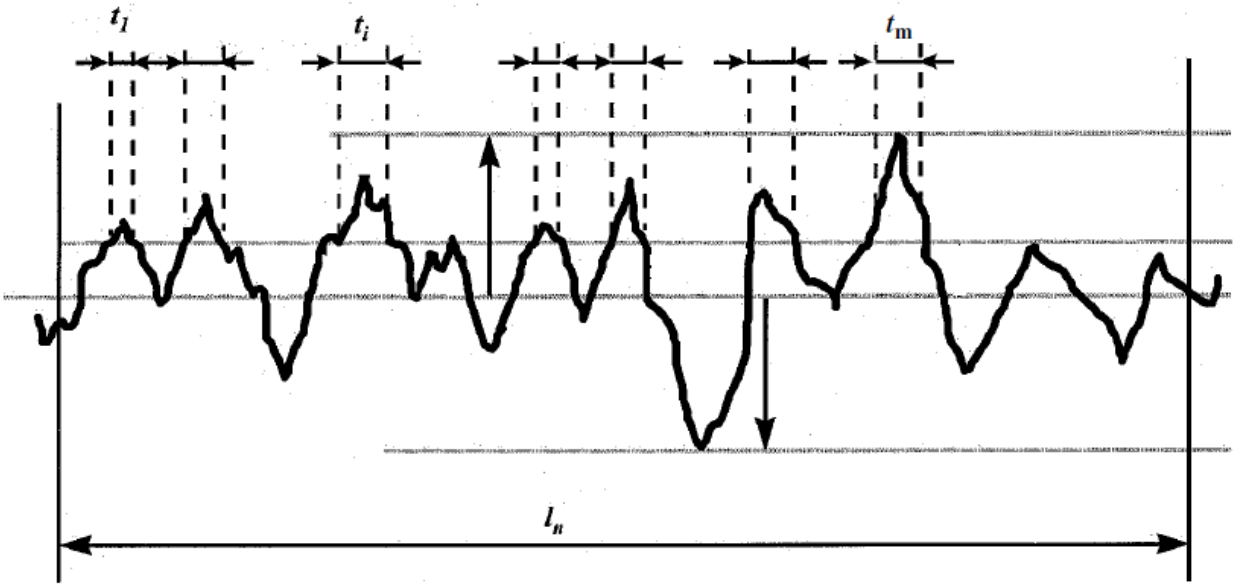

Figure 1.2: Illustration of material ratio calculation

Source: (Chang *et al*. 2010)

Chang et al. discussed about surface roughness parameters. The authors have produced typical surface roughness profile by applying some mathematical terms of the root mean square of surface heights. However, Chang et al. illustrated of material ratio calculation which calculated to measure spatial wavelengths. Figure 1.2 shows the illustration of material ratio calculation. Nevertheless, Andrew *et al*. 2011 measured irregular surface using a profilometer for gravel and larger rocks surface. They found two different shapes of gait cycle and its completely different gait cycle where individuals are walking on the treadmill.

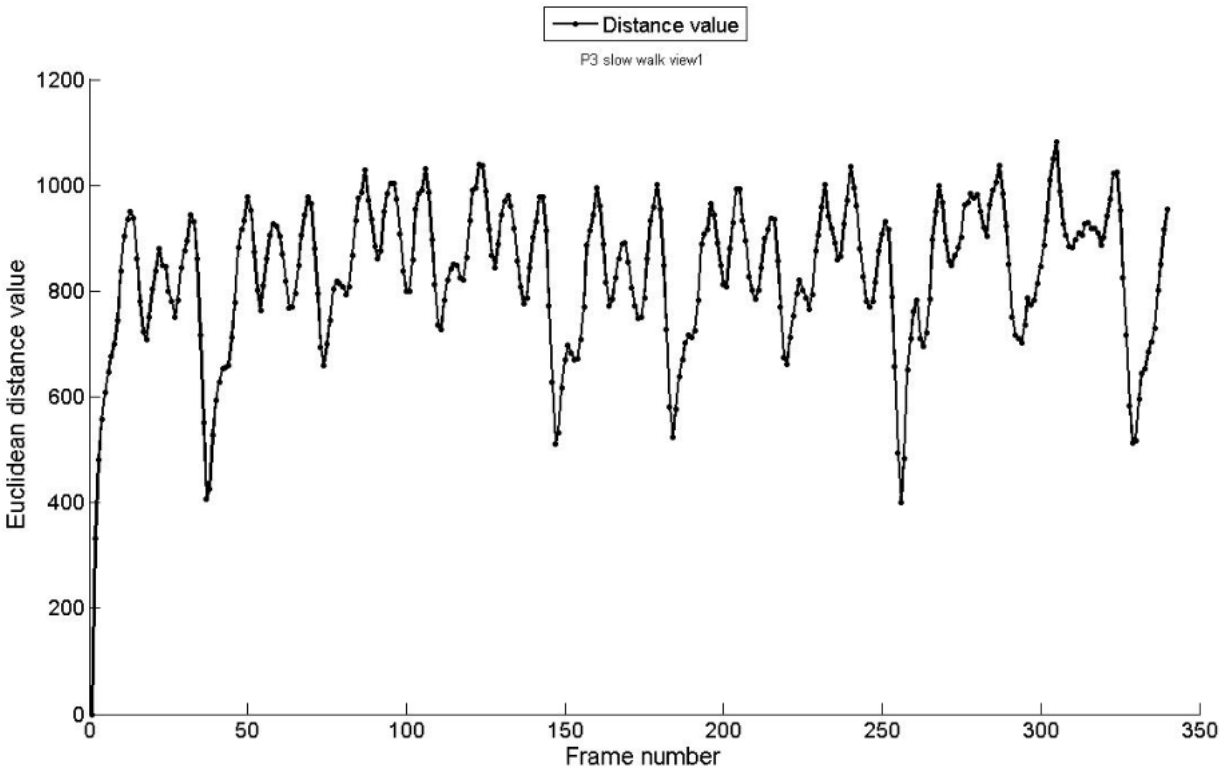

Figure 1.3: Gait cycle using Euclidean distance

Source: (Hayder *et al*. 2010, 2011)

In this case, person is walking slowly on the treadmill. The gait cycle has measured and each gait cycle has 18 to 20 frames. The Euclidean distance method has applied to get gait cycle and know how is differ from each gait frame to frame. After comparing above two figures, it can be announced that two figures are more or less look like same. Thus, gait cycle can be smooth depending on condition of walking surface and also friction of surface. Once it is not possible to get a smooth gait cycle then there is a problem created by friction or friction by irregular surface.

1.4 Comparing Slips and Falls with Three Walking Styles Slow Walk, Fast Walk and Carrying with Ball Walk

Slow Walk Vs Slips and Falls: When individuals are walking as normal speed of slow walk on the treadmill, the gait cycle will have a smooth curve. If there is no friction while individuals are walking on the normal condition surface then speed limit and well-designed cycle curve will produce. Euclidean distance method applied to get a gait cycle curve to analysis how individuals are walking and getting slips and falls. From the curve, it can be seen that there is minor change to get a smooth gait curve. It proved that when individuals are walking as normal as slow speed then it has very less possibility to get friction, slips and falls. It is safe to walk slowly on normal surface with normal environments. Figure 4 shows the slow walking style cycle.

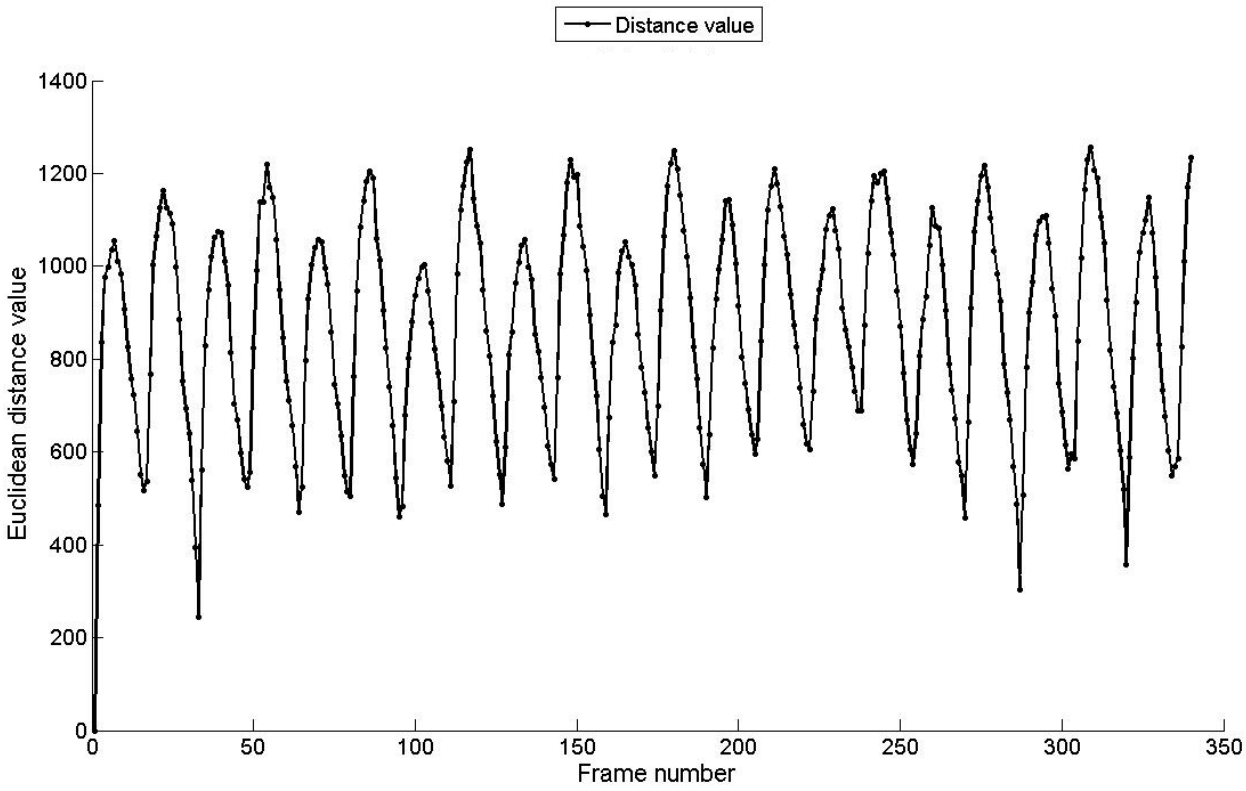

Figure 1.4: Slow walking style cycle

Source: (Hayder *et al*. 2010, 2011)

Fast Walk Vs Slips and Falls: From the fast walking style cycle curve, there is some changes of the gait cycle curve after comparing with slow walk gait cycle curve. It proved that when individuals are walking slower than fast then individuals are not in control. There is some changes of direction and very walking speed limit. There is possibility to slips and falls and it has less safety to walk fast on the normal surface in normal environments. Figure 5 shows the fast walking cycle curve.

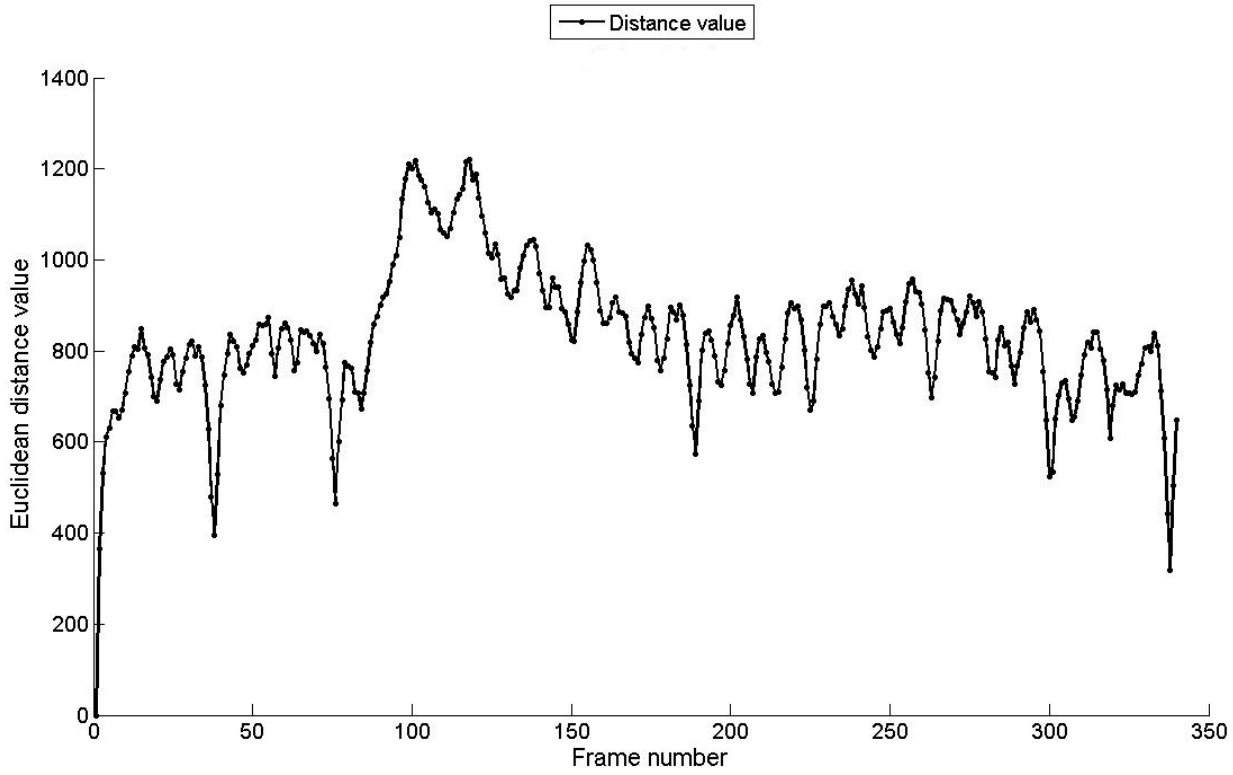

Figure 1.5: Fast walking cycle curve

Source: (Hayder *et al.* 2010, 2011)

Carrying a Ball Walk Vs Slips and Falls: when carrying a ball gait cycle has compared with slow walk and fast walk gait cycle curves, it is cleared that carrying a load during walk produced unusual gait cycles curve. It verified that it is less safety to walk with carrying a load. The main reason is to be balanced physical condition to walk

normally which is not possible after certain time. Thus, it has high possibility to slips and falls after comparing slow and fast walking styles.

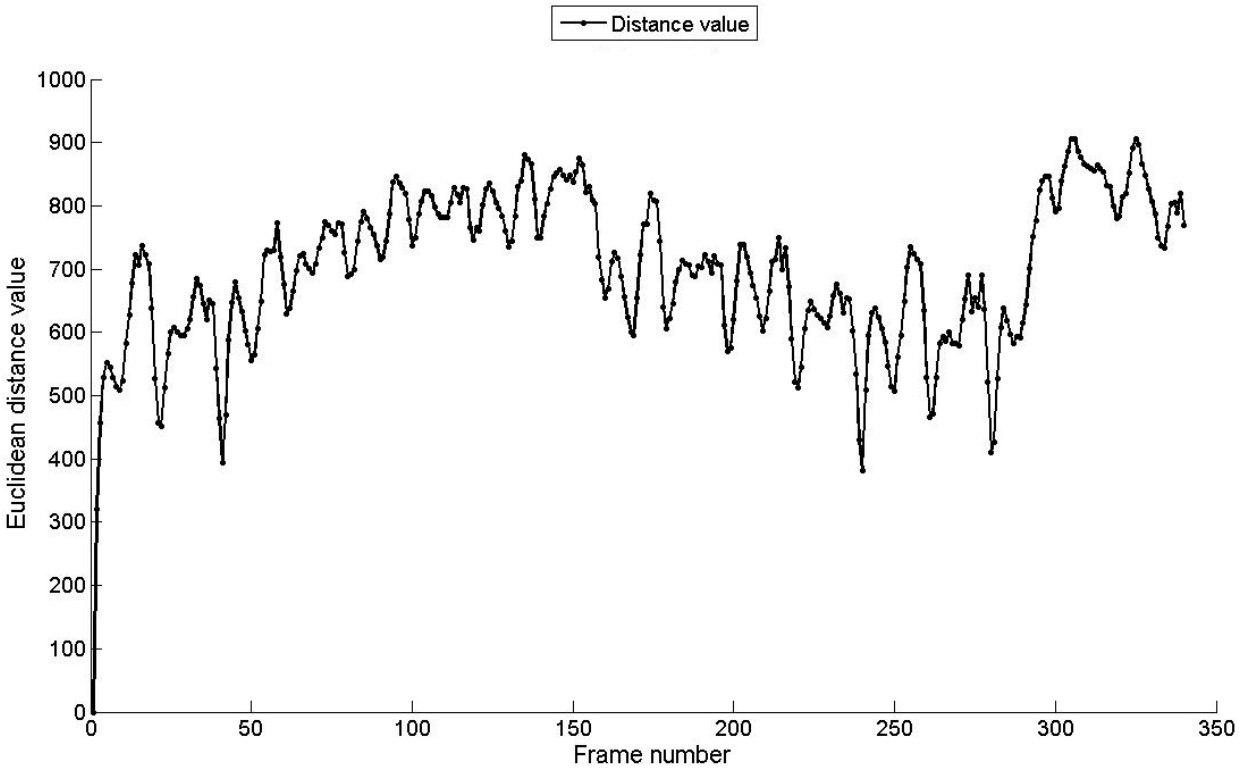

Figure 1.6: The carrying a ball gait cycles curve

Source: (Hayder *et al.* 2010, 2011)

The kind of walking styles have measured for the forward walking styles. If individuals are walking in descending order then different result may come out. As we do not have any descending order walking styles gait database that cannot be figured out to compare the ascending order gait cycles results. Figure 6 shows the carrying a ball gait cycles curve.

Finally, it can be announced that slow walk on the normal surface is giving safety walk and fast and carrying a load walk are giving less safety on normal surface under normal environment.

In this research, we will work three types of walking styles walk on treadmill surface and normal indoor environment to get the experiments results.

1.5 Conclusion

In this thesis, friction, slip and fall will study when pedestrians are working at any place under any surface conditions. The gait and locomotion analysis for tribological applications have studied to know in details about slips and falls. The different types of slip have been studied to better understanding about normal walk on the normal surface. However, biomechanics locomotion has been studied to analysis to relate the desired applications.

CHAPTER 2

OVER VIEW OF GAIT AND LOCOMOTION ANALYSIS

2.1 Overview of Gait Recognition Systems

Human gait is an effective biometric for person identification. The biometric system is mainly used to prevent unauthorised access. Biometric resources such as iris, fingerprints, palm prints and shoe prints, are a subject of extensive research work, studied and employed in many applications. Human gait is a biometric feature that can be captured from a great distance (Gafurov, 2007).

There is need for automation in applications such as surveillance, access control and smart interfaces. Today, biometrics is a powerful tool for reliable automated person identification. The motion vision's main purpose is to use surveillance when unexpected occurrences befall us. Wearable sensor systems require carrying the sensors and floor sensors system around that necessitates setting the sensors on the floor (Boulgouris *et al.*, 2005; Moeslund *et al.*, 2006).

Gait recognition can be classified into three groups, namely, motion vision-based, wearable sensor-based and floor sensor-based. The motion vision can be divided further into two groups, namely, appearance-based methods and model-based methods. The appearance-based method can also be subdivided in two types: state-space methods

and spatio-temporal methods. Most researchers used the appearance-based method compared to model-based method (Bo and Youmei 2006).

2.2 Application of Gait Recognition

The gait recognition system is capable of identifying humans from such distance beyond human interactions. This characteristic of gait recognition system is suitable for applications in large and controlled environments such as banks, military installations and even airports that is enabled to quickly detect threats.

The gait recognition system can also be used as a surveillance camera. It is able to identify an individual subject walking in the video stream as long as the individual subject's data is already stored in the database. The gait recognition system can also detect unknown subjects such as intruders walking in front of the surveillance camera by triggering an alarm. In this case, only authorised person will be allowed to pass through without setting off the alarm.

2.3 State of the Art in Gait Recognition System

Nikolaos and Zhiwei (2007) proposed Radon Transform (RT) and Linear Discriminant Analysis (LDA) techniques in gait recognition. They used silhouettes from the Gait Challenge database for the experiment. The silhouette alignment is essential to the Radon Transform as it observes the image centre as the transform centre of the feature space, and LDA is then applied to decrease its dimensionality. The Principal Component Analysis (PCA) is also applied to reduce the dimensionality. However, Hao and Zhijing (2009) also used the RT technique and followed the same experimental procedure as

Nikolaos and Zhiwei (2007) for gait recognition. They applied the USF and SOTON gait database in their experiment. On the other hand, Ju and Bir (2006) constructed the Gait Energy Image (GEI) for gait recognition purposes. They applied the PCA and Multiple Discriminant Analysis (MDA) techniques to reduce the dimension of space *(Khalid et al., 2010).* For their experiment, the USF HumanID gait database is used in order to obtain good classification results for walking styles for gait recognition system.

The research has been effectively applied in many pattern recognition problems. Thus, gait recognition systems based on silhouettes and GEI template system were used in this research. Furthermore, the Radon Transform and PCA techniques were studied to help improve the performance of the gait recognition system. Moreover, the CMU MoBo gait database was studied for use in this research. Thus, the motivation in this research lies with developing a gait recognition system and comparing it to the silhouettes- and GEI-based systems.

2.4 Challenges of Gait Recognition

The gait recognition system is a measured and challenging task due to the many variations of walking styles that exists in different environments. Ling *et al.* (2009) pointed out several challenging features. These are:

a. Object segmentation – The silhouette object segmentation exists under different conditions such as outdoor condition. The outdoor condition is continuously interrupted by various sources such as light, noise, shadow, and other conditions.
b. Abnormal walk – If the subject walks abnormally, then it becomes very difficult to identify the right person.

c. Body coverings – Most of the objects are dressed in different kinds of clothing, thus giving rise to different silhouettes sizes under different environment.
d. Gait databases – The existing gait databases are severely lacking in subject data.

2.5 Problem Statement and Proposed Gait Recognition System

Different gait databases were used in the research due to the many different databases that are available. However, some of the researchers were using the same gait database in their experiments. The size of known training and testing gait databases varies. The unknown gait dataset have not yet been set by any researcher for the experiment. Moreover, most researchers do not mention the criterion for recognition rates where only the recall capability of the system were used without any clear indication of the computational cost involved for the system.

In this research, the two techniques of PCA with and without RT are combined based on the silhouette and GEI templates explained in Chapter 3, Chapter 4 and Chapter 5 respectively. This research will focus on the different gait styles; which one is suitable to use CMU MoBo gait database in experiments described in Chapter 2. Nevertheless, most researchers did not compare between silhouettes- and GEI- based templates system using PCA with and without RT techniques. The comparison of the gait recognition results between the silhouettes- and GEI- based template systems using PCA with and without RT techniques is analysed and discussed in Chapter 5.

2.6 Objective of the Thesis

The main objective of the thesis is to survey of friction, slips and falls during a walk and to evaluate the performance of the different gait features selected for person identification.

2.7 Organization of the Thesis

This thesis contains six chapters and a brief description of each chapter is given below.

Chapter 1 briefly survey of friction, slips and falls during three different walking styles.

Chapter 2 introduces the gait recognition systems and a brief explanation of the objective of this research is provided.

Chapter 3 reviews several gait recognition methods. Since gait recognition methods are classified into three categories and for each category, a number of the most recent research papers were reviewed. The chapter ends with a proposal of the gait recognition system and an outline of the proposed plans.

The basic principles of PCA with and without RT are described in Chapter 4. The Chapter 4 gait database follows the experiment based on silhouettes and GEI templates for both proposed techniques. The proposed system of the techniques has explained in this chapter.

Chapter 5 provides data preparation techniques for the experiments. The same silhouettes- and GEI-based templates with known and unknown training datasets were shown in this chapter. However, GEI templates constructed over one complete gait cycle are presented in this chapter.

A detailed analysis and discussion on this project is explained in Chapter 6. The comparison of recognition rate between silhouettes- and GEI-based template system using PCA with and without RT is also explained in this chapter. Further, performance comparisons between PCA with and without RT techniques using silhouettes and GEI templates are stated. Lastly, the computational cost involved is presented for the system.

Finally, Chapter 7 summarises the thesis and provide some ideas for further development of the gait recognition system.

CHAPTER 3

LITERATURE REVIEW OF GAIT ANALYSIS

3.1 Introduction

The current progress of work on gait recognition done by previous researchers, which will be investigated, providing an overview of the methods. Currently being investigated and provided background information on all of the gait recognition techniques, which have been used throughout for this project. Gait recognition techniques can be broken down into two main sections, model based and motion based techniques. These different approaches are described in more detail below. Several important information, which is indirectly connected to gait recognition system that used for the development of the system, and explained details.

3.2 Purposes of Gait Recognition Systems

The gait recognition system is an intelligent system that is capable of identifying the registered person. This system is applied on many applications such as access control, surveillance and smart interference. However, it is mainly used for surveillance and in forensics. For example, robbers use masks or gloves to hide their faces or finger prints to avoid detection. However, a camera can record robbery gait on video.

3.3 Classification of Gait Recognition Systems

Gait recognition system is classified into three groups, namely, motion vision-based, wearable sensor-based and floor sensor-based. Motion vision is further divided into two groups, namely, appearance-based and model-based methods. Subsequently, the appearance-based method is further subdivided in two types: state space methods and spatio-temporal methods. Figure 3.1 shows the classification of gait recognition systems.

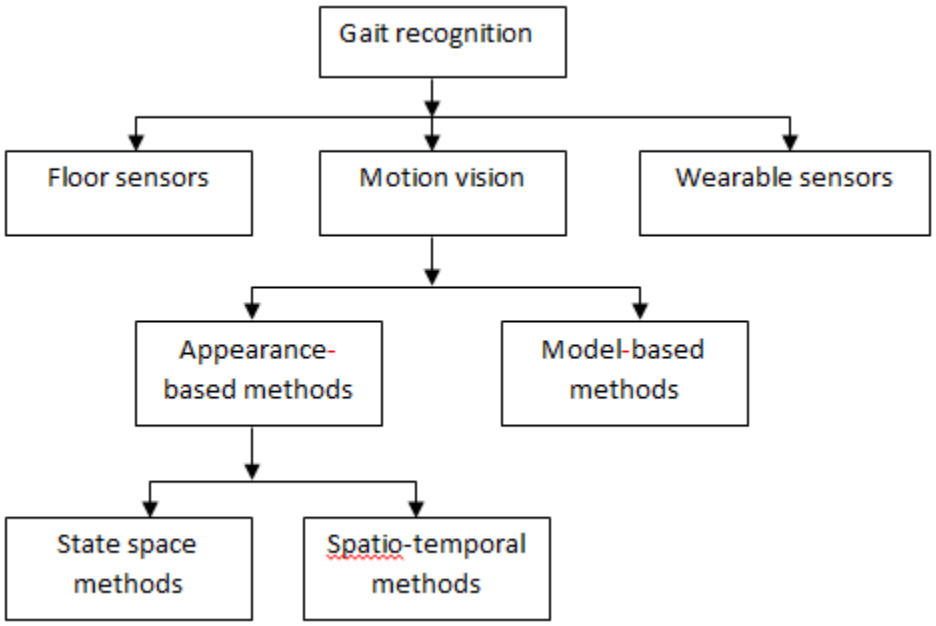

Figure 3.1: Classification of Gait Recognition Systems

Source: (Hayder *et al.* 2010)

3.3.1 Floor Sensors System

Lee *et al.* (2005) built a floor mat recognition system, which is a combination of various types of sensors. The floor mat is constructed according to the subjects foot stride. Even the length of the floor mat is calculated to accommodate two gait cycles. The system

construction shows the hardware interface details and how to apply the devices. However, the most important features chosen for the experiment are stride length, stride cadence and hill-to-hoe ratio. Figure 3.2 shows a floor sensor prototype. The researchers created their own gait database and applied it for recognition purposes. They reported that a recognition rate of above 80% is achieved by using their own small database.

On the other hand, Jaakko *et al.* (2008) proposed an array of simple binary switch floor sensors to sense footsteps. They focus mainly on analysing footsteps and walking sequences to identify the person. The selected features are then extracted and processed for recognition purposes. The discriminative Bayesian classifier is also used for recognition purposes. They match up the individual footsteps and longer walking sequences with nine different persons and presented recognition results of 64% and 84% respectively. Finally, they applied the context aware prototype to repeat the footstep location information for person identification.

Rishi *et al.* (2010) described tracking and estimating a subject's lower body parts moving on foot over the integrated floor surface. The Bayesian filter methods were applied to track the lower body pose of a walker via integrated sensors. The footsteps are generally taken for measuring purposes to calculate the accuracy of identification. Figure 3.3 shows the floor interface design. However, the footsteps alignment of the right and left feet are calculated by using sensors. Based on the database, it was reported that the experiment achieved efficient results.

Many floor sensor system techniques were successfully analysed to identify the person. These techniques are implemented with many integrated devices and other necessary materials, which are deemed reliable for the system.

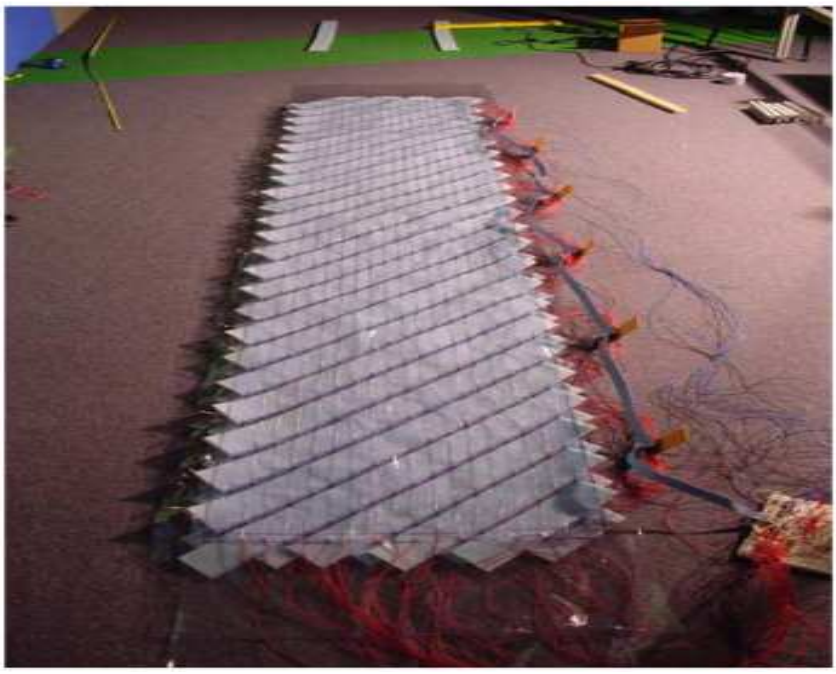

Figure 3.2: Prototype of floor sensors

Source: Lee *et al.* (2005)

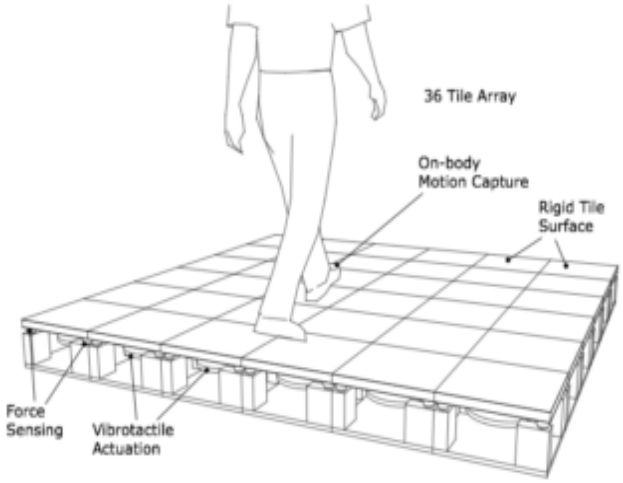

Figure 3.3: Floor sensors interface with components level

Source: Orr and Abowd (2000)

3.3.2 Wearable Sensors

Davrondzhon *et al*. (2006) proposed a wearable sensor-based technique for gait recognition. They have placed a device to the lower leg to extract the gait pattern. The three directions of vertical, forward backward and sideway motions of the lower leg were acquired to get the output from the device. The three accelerations were then applied for verification purposes. In addition, the histogram similarity and gait cycle length were used for similarity measurement. They set their own database with 21 participants. The motion record device was placed on the right leg of the participants between 20 to 40 years old. They trained on the indoor tiled surface with limited distance. Half of the walking distance signal was set for training and another half for testing. The performance results were presented as a Decision Error Trade-off curve (DET) and they reported a 5% and 9% equal error rate (EER) from the similarity and cycle length histogram respectively. Figure 3.4 shows the sensor are set to the lower leg to record the accelerations.

Figure 3.4: Wearable sensors attached to lower leg

Source: Davrondzhon and Einar (2006)

Liu *et al.* (2007) stated the characteristic problems of gait acceleration signals, which occurred during the walking process. The proposed methods are time and frequency-domain based. Besides, dynamic time warping (DTW) was used to deal with naturally occurring walking speeds. The proposed method suggested possible applications such as access control, smart interface, and other security sectors. For experiment purposes, by using their own gait database consisting of 21 subjects a 94.40% and 79.90% recognition rate was achieved for both time and frequency-domain methods respectively. The proposed method reported that it could identify persons based on gait accelerations.

Takeda *et al.* (2009) proposed a gait recognition system based on wearable sensors method. The lower part of the body was selected to measure accelerations and angular velocities during walking. The tri-axial and three gyro sensors were used for the experiment. The selected sensors were set on the abdomen and lower limb segments for measuring accelerations and angular velocities during ~~a~~ walking. The proposed method is used for measuring three-dimensional position from gravitational acceleration using wearable sensors. This method was applied on three healthy volunteers to measure acceleration data of the lower limbs. However, the Fast Fourier Transform (FFT) was applied for the characteristic frequency during walk. It was reported that the proposed method is essential for gait analysis. Figure 3.5 shows the wearable sensors set on the body.

The wearable sensors research groups are able to use wearable sensors that can be used to identify a person. Most wearable-sensor users set the sensors in different locations on the body to measure the walking patterns for identification purposes.

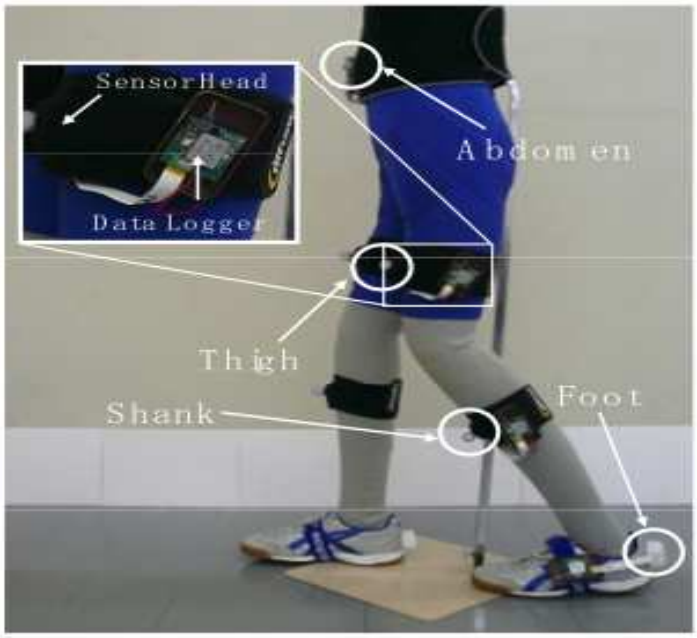

Figure 3.5: Attaching sensors in different locations

Source: Takeda *et al.* (2009)

3.3.3 Motion Vision-based System

The motion vision-based system uses video camera to capture images or video from long distances. This biometric technique is reliable for person identification in specific gait features. The main idea is to apply a combination of video and image processing techniques to extract the specific gait features. The biometric extraction technique of the motion vision-based system is shown in Figure 3.6. Figure 3.7 shows a general block diagram of the motion vision system. The advantage of the gait recognition is its biometric features that are reliably captured from a great distance. Moreover, it does not require user cooperation for gait recognition.

The various applications for the motion vision-based gait recognition system include surveillance and forensics. In robbery or criminal cases, thieves use masks to cover their faces and use hand gloves so that it is not possible to capture their faces or fingerprints for identification of the persons involved. However, by using the motion vision system, a camera can record the users gait on video for match-up analysis.

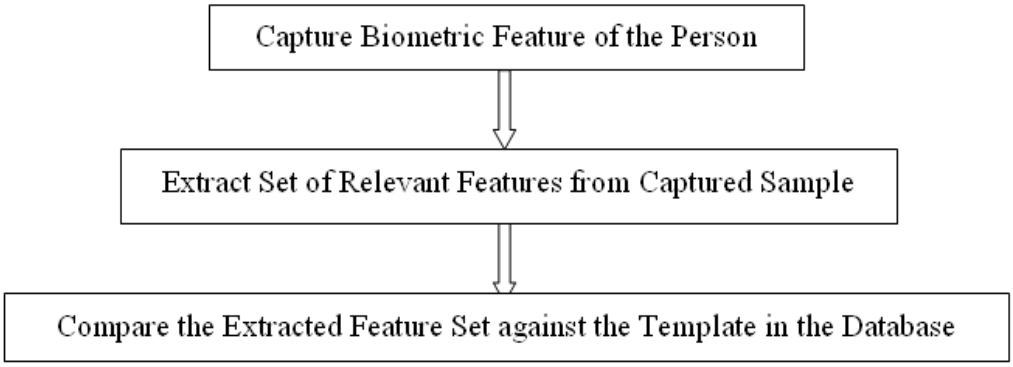

Figure 3.6: Extraction technique flow chart for motion vision-based system

Source: Nikolaos *et al.* (2005)

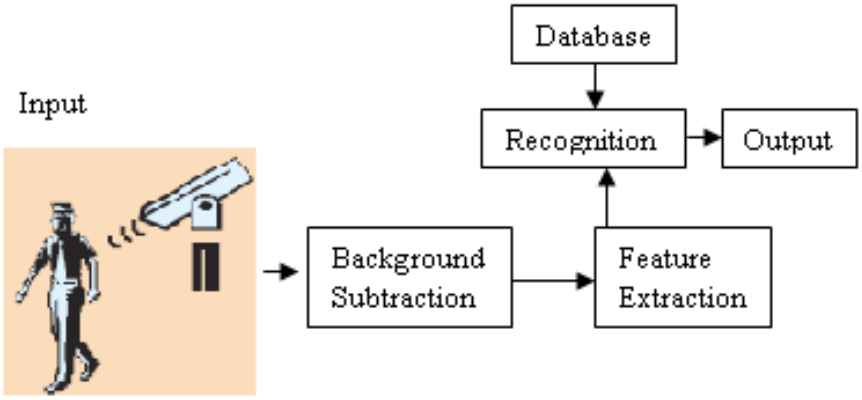

Figure 3.7: General block diagram of a gait recognition/authentication system

Source: Nikolaos *et al.* (2005)

Khalid *et al.* (2009) proposed a novel gait representation based on optical flow fields computed from normalised and centred-person images over a complete gait cycle. The

Gait Energy Image (GEI) and Motion Silhouette Image (MSI) were constructed from gait silhouettes. The GEI and MSI templates were also applied in the experiment. However, they represented various covariances such as clothings, carry-ons, shoes and speed for comparing the recognition rates. For templates matching, the Euclidean distance was applied to measure the similarity between two subjects. For the experiment, SOTON and CASIA gait databases were used that yielded different results. However, the indoor and outdoor datasets were applied and yielded different results. Furthermore, the fusion technique was applied to obtain efficient recognition results for improved recognition rates.

Xiaochao *et al.* (2008) proposed an effective gait recognition approach based on the Gait Energy Image (GEI). GEI is the average silhouettes over one gait cycle. GEI templates were constructed individually for each person. The Gabor filter was selected to improve gait features, while the discriminative common vector (DCV) was used for reducing space dimensions. The three types of gait templates presented by the researchers are called simple of GEI, three regions of a GEI and dynamics weight mask (DWM). However, the marked and selected three regions contained walking information to identify the person. In this experiment, the USF HumanID gait database was selected for recognition purposes. The experimental result of the GEI and non-GEI -based templates methods were compared between them and with other similar research methods. It was reported that the proposed system achieved better result.

Heesung *et al.* (2009) proposed the backpack removal method for efficient and robust gait recognition. Initially, the GEI templates were constructed over one gait cycle from

the provided gait database. Then, the simple recursive principal component analysis (RPCA) technique was applied to remove the backpack from GEI templates. It was reported that the backpack was successfully removed from the gait representation templates while the subject is carrying a backpack during a walk. Three different walking styles were selected: slow, quick and walking-with-backpack, and the experimental results were compared. The results were also compared to other similar research-methods and it reported efficient results.

a. Appearance-based Approach

The gait appearance model is defined as a combination of histograms of individual silhouettes and contextual silhouettes. It is represented to be invariant to translation, rotation and scale by means of a shape description and gait images plane. In other words, appearance-based approaches employ a compact representation to characterise the motion patterns of the human body without taking into consideration of the underlying model structure. In this approach, several advantages and disadvantages are available with different features. Some examples of motion vision silhouettes are shown in Figure 3.8.

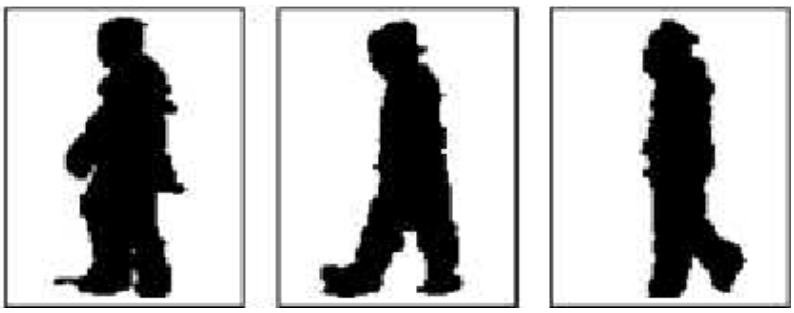

Figure 3.8: Examples of motion vision silhouettes

Source: Philips *et al.* (2002)

I. State Space Method

This method represents human movements as a sequence of static configurations. Each configuration is recognised by analysing the appearance of the body in the corresponding pose. In other words, the state space method consider that gait motion is composed of a sequence of static body poses, and recognise it by considering temporal variation observations with respect to those static poses.

Shi and Youxing (2007) approached the appearance-based methods for gait recognition system. Individual silhouettes and contextual silhouettes were taken and 2D polar plane used at the centre of the silhouette. They analysed how subjects' walking appearance changed during a walk. The definition of appearance model is presented as a combination of histograms of individual silhouettes and contextual silhouettes. However, the Jefferey divergence criterion and dynamic time wrapping technique was applied to calculate the similarity between test and reference sequences. In the experiment, the CASIA database was used, which contained 20 subjects and 12 sequences per subject for different viewing angles. The planned technique reported recognition rates of 92.5%, 98.75%, and 100% when k=1, k=2 and k=3 respectively.

Han *et al.* (2005) represented the feature extraction process based on static and dynamic knowledge methods. First, the basic gait features were selected for analysis. Second, the gait cycle was detected based on successive peak values of the width and height. Discrete Cosine analysis was applied to get the periodical sequences. The silhouettes were marked into three sections, namely, upper body part, middle body part, and lower body part. Here the lower body part was selected to measure the walking

distance over one gait cycle time. However, joint angles were measured from lower dynamic body part. To classify the gait features, the Support Vector Machine (SVM) was used for testing and training dataset. The three gait databases, namely, Little and Boyd, CMU (slow walk) and NLPR achieved three different recognition rates of 100%, 90.2%, and 90.6% respectively.

Xu *et al.* (2006) proposed a gait recognition system based on walking direction for human identification purposes. They proposed a novel approach to calculate the walking direction and extracting features by utilising a human model. They investigated and evaluated the recognition rates in any walking directions by applying Support Machine Vector (SMV). However, the real walking video data was applied to the experiment and a high recognition rate was obtained. The proposed method mainly investigated the effect of changes of walking directions on recognition performance. Finally, they reported that the proposed method is robust with respect to different walking directions and types of clothing.

Sungjun *et al.* (2006) proposed a new approach based on the appearance model method for gait recognition. A new feature vector called sample point vector was proposed. The purpose of using sample point vector is to calculate the mean and the variance values of each pixel that reflects the dynamic and static information for gait recognition. At the outset, the background subtraction process was applied for individual image sequences to obtain silhouettes. The sampled point vector was extracted along the central axis of the silhouette image. Moreover, to classify individual gait recognition,

the reduced multivariate polynomial model technique was applied. For the experiment, the CASIA database was used.

Jun *et al.* (2006) approached a novel technique for gait recognition that is applied to different viewing angles. At first, moving objects contained in the difference motion slices were extracted. Two body shape appearances were expressed, which are static information appearance shape and dynamic information ~~of~~ habitual motion. The extraction of different motion slices and gait images were performed for the experiment. For similarity measurement and classifier, three different samples of classifier were used, namely, nearest neighbour (NN), KNN and exemplar nearest neighbour (ENN). To perform the experiment, the NLPR database which contained 15 different subjects of four gait sequences each was used. The length of each sequence is 26 frames. Based on the result, the proposed method reported an efficient person recognition capability.

Bo and Yumei (2006) proposed two techniques, which are the PCA with and without LDA for gait recognition. At first, background subtraction was performed to construct the silhouettes. The produced silhouettes contained noise due to lighting variations. To remove lighting noise in the silhouettes, the Otsu method and morphological operations were applied to produce good quality silhouettes. The images were captured in frontal, lateral and oblique orientations of walking person contour for sequence classification. The silhouettes were then normalised. Next, the PCA with and without LDA techniques were applied to perform the experiments. The Normalised Euclidean Distance (NED) was applied for silhouettes matching purposes. Mixed gait databases were arranged containing 30 subjects and 4 sequences per subject. The recognition rates achieved was

87% on PCA with LDA technique. Homologous and CMU gait databases were also applied for comparison purposes. The CMU database has different walking styles, which represented different results. On the CMU MoBo gait database, 96% recognition rate was obtained on the same walking styles of training and testing dataset.

Xiaochao *et al.* (2008) presented the 2D Gait Energy Image (GEI). The GEI templates were constructed to get a robust gait feature. The Discriminative Common Vectors (DCV) was applied to reduce the dimensionality of the feature space. The DCV also improved class separability. Furthermore, the Gabor-based method was used to improve the recognition rates. The proposed method was performed on the USF HumanID gait database. The recognition rate was then compared to other similar research techniques. Ultimately, the proposed technique achieved an average recognition rate of 53.86%.

Michela *et al.* (2008) proposed the front view approach for gait recognition system. First, standard background subtraction was done from video sequences where gait cycles is obtained using the periodic function. Then, gait volume descriptor was described to normalise the 3D gait volume. Three different types of walking directions were selected and performed for the experiment. In addition, three different gait databases, namely, University of Southampton, CASIA-A and B were applied. It was reported that the proposed method achieved a recognition rate of 96.50%. It was also compared to other similar research methods.

II. Spatio-Temporal Method

In this method, motion is characterised by the entire 3D spatio-temporal data (i.e., x, y and time) such as a sequence of grey-scale images. This data is treated as a large vector and recognition is done by mapping this vector to lower dimension feature vector and applying pattern recognition to it. Therefore, the gait representation is a sequence of feature that must be compared with another sequence when the fundamental walking periods T1 and T2 of the two sequences are not equal.

Sungjun *et al.* (2007) proposed the Mass Vector method for gait recognition. They used the Dynamic Time Wrapping (DTW) method to deal with naturally changing walking speeds to match nonlinear time normalisation walking speed. They have extracted the silhouettes using normal subtraction method and normalised it to get accurate recognition rates. For the experiment, they applied NLRP database, which contained 20 subjects and 4 sequences per subject. They compared the proposed system with other researchers' system. The proposed system achieved a recognition rate above 80%.

Tao Ding (2008) proposed a robust technique for gait recognition. The proposed system is based on modelling silhouette variation information, which is extracted by Locale Linear Embedding (LLE). The LLE was used to map the reduced dimensionality from higher dimension to lower dimension images and extracted spatio-temporal information. However, gait sequence is important to evaluate the difference between the models representing different gait cycles to verify that spatio-temporal information extraction is not affected. On the other hand, gait cycle localisation and time scaling were described to get robust silhouettes information. Mainly, the proposed spatio-temporal gait

information based on LLE is to extract modelling shape variations information. For the experiment, the CMU MoBo database was applied on different gait styles training and testing dataset. It was reported that the proposed algorithm is a robust identification-based algorithm for recognition system.

Yangming and Guangjian (2008) proposed anatomical knowledge for gait recognition. At first, they extracted the human silhouettes from gait video sequences. Then, the anatomical knowledge was used to describe the silhouettes. For gait periodic analysis, the height and width periodic ratio was analysed based on local minimum and maximum gait period variations. The Hidden Markov Model (HMM) was applied to get a smooth gait periodic cycle for accurate results. The CMU MoBo database was selected for the experiment with high recognition rate achieved.

Arun *et al.* (2005) proposed a combination technique (isoluminance stereo vision technique with 3D template matching method) to improve the gait recognition rates. The Visual Hull (VH), isoluminance lines for stereo vision and 3D template matching techniques was applied to the proposed gait method. The VH was used for the human modelling system and it is classified into two bases, namely, volume-based and surface-based. Stereo vision was used to measure an object in 3D position with cameras placed in different directions to observe it. The 3D template matching technique was used to find the precise position and orientation of the object. However, the Hidden Markov Model (HMM) was employed to model a signal with variability in space and time parameters. The proposed method achieved better result with HMM.

Saeid *et al.* (2008) proposed the wavelet transform approach for gait recognition. The wavelet descriptors were used to describe the model of object's boundary and spatio-temporal boundary. At first, background subtraction was performed on each image and it produced perfect silhouettes. The USF gait challenge database was used for recognition purposes. For the experiment, 16 subjects were used with 10,400 frames. The training data comprising 7,000 frames and testing data with 3,400 frames were set for the experiment. To compare the proposed method's result, the Fourier descriptors and wavelet were used. The wavelet outperformed the Fourier descriptors method.

Guoying *et al.* (2006) proposed the fractal scale and wavelet moment for gait recognition. Fractal scale method is better for one dimensional signal classification and it can describe the self-similarity of signals. Here, wavelet analysis was applied to translate and scale a function. The fractal scale has two types, namely, computational of global fractal scale and local fractal scale, and it has also two different meanings. Moreover, a combination of fractal scale and wavelet moments improved the recognition rates. For the experiment, the slow walking styles for training and testing datasets were arranged to perform and achieve 100% recognition rates. The combined method of fractal scale and wavelet moments improved recognition rates on slow walking style of training and testing datasets. However, slow walking styles training and fast walking styles testing datasets were performed and it obtained better results than other researchers.

Song *et al.* (2008) proposed to extract gait feature for gait recognition. The proposed method focuses on the features of shape variations information. They mainly applied the shape differences information between successive frames to indicate gait information

called interframe variation vector (IVV). At first, moving subject was detected by applying normal background subtraction methods, then they extracted the human silhouettes and unwrap it to 1D distance. Moreover, the PCA technique was used to reduce the dimensionality of the silhouettes and extract the IVV. For the classification, the KNN was used to identify humans. For the experiment and performance evaluation, CASIA database was applied. The experimental results were then compared to other similar methods and it was reported that the proposed method achieved a 100% recognition rate.

Dong *et al.* (2007) proposed the Marginal Fisher Analysis (MFA) and Content Based Image Retrieval (CBIR) system to reduce the dimension of the images. The MFA technique was used to reduce dimension of the individual silhouette. They have constructed an average gait cycle from gait video for the experiment. For the CBIR, another technique called Marginal Biased Analysis (MBA was adapted to the significance feedback problem. CBIR was used to get relevant feedback problems from positive sample as well as its neighbour's positive samples. The KNN was used as classifier to measure the distance between galley and probe images. For the experiment, the USF HumanID and Corel Images Retrieval gait databases were used. They compared their recognition results with different similar techniques and reported that the proposed technique achieved better recognition rates.

b. Model-Based Methods

Model-based approaches explicitly modelled human body or motion. Model-based approaches usually perform model matching in each walking sequences frame so that parameters such as trajectories are measured according to the model. Model-based approaches study static and dynamic body parameters of human locomotion. Although model-based approach is view-invariant and scale-invariant, it reflects the kinematic characteristics of walking manner. The specific gait parameters were used only for model-based approaches that usually require high quality gait sequences to be useful. This method has several merits and demerits that depend on features. The static parameters feature is view-invariant and compact. The main problem is the difficulty in capturing the images. Other gait features such as ellipse parameters, hip angle, and combination of shape parameters are compact representation, but it is low in robustness. The model-based approach is shown in Figure 3.9. Figure 3.9(a) shows distance static parameters which are measurements taken from static gait frames. Figure 3.9(b) shows ellipse fittings. In silhouettes, seven regions are divided to measure each region for recognition. Figure 3.9(c) shows hip rotation model. It calculates hip angles as a way to identify person. Figure 3.9(d) shows combination of body shapes. It measures combination of static parameters, ellipses, rotation angles to recognise person.

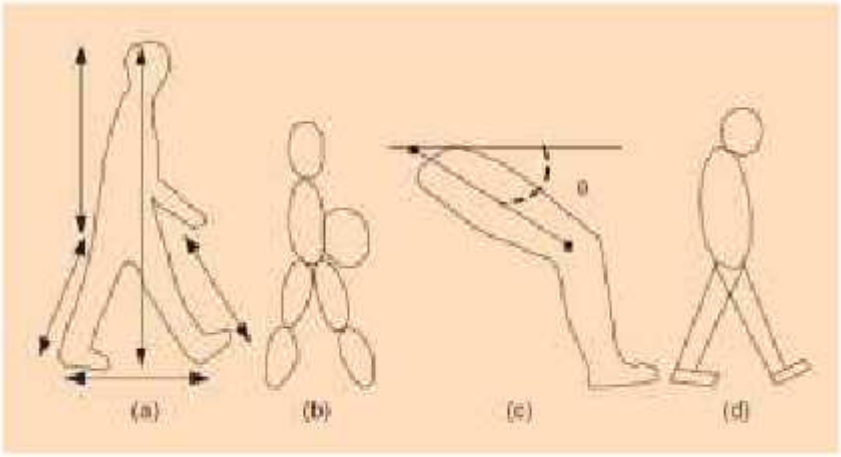

Figure 3.9: Model-based approach

Source: Boulgouris, N.V. (2005)

Xiaxi *et al.* (2008) proposed the multiple views style for gait recognition. They argued that multiple views have unequal discrimination power and therefore, unequal contribution of recognition process. At first, they tested and evaluated all the views individually, and then combined all the results. They set a weight for each view based on its importance. For the test, at first, they selected fast walk and slow walk sequences. Six cameras were located in six different positions to capture the walking images. They then took bounding boxes of silhouettes from the original images for the subject, then align and normalise all the silhouettes into uniform dimensions. The most suitable views were found to be frontal and side views. The best result were obtained by using the product and the min combination rules. Using the CMU (MoBo) database, they achieved 92% recognition rate.

Junqiu *et al.* (2008) proposed an integrated algorithm for tracking and segmenting silhouettes supported by gait recognition. The three modular approaches are tracking,

segmentation and gait recognition modules. The tracking module gives beginning input to the gait recognition module. The proposed tracking module is prepared based on the mean-shift algorithm. However, they created bounding box by tracking module. Furthermore, the tracking module outcome contained some inaccuracies due to background differences. Dynamic Time Warping (DTW) was described to get smooth gait sequences curve for recognition purposes. Nevertheless, they presented good quality gait silhouettes using Standard Gait Model (SGM). The Min-Cut algorithm was used for the interactive segmentation and improved the performance of subject segmentation. The experimental results reported that the proposed method improved initial tracking and segmentation results.

Ai and Ji (2007) proposed an approach based on positioning of the human body joints for gait recognition system. At first, silhouettes extraction was done using normal background subtraction and morphological operations to get good quality silhouettes. Then, 12 positions of body joints coordinates during walk were selected and calculated according to geometrical characteristics. The discrete Fourier transform was applied to compute angle features. Finally, the KNN classifier was used for subject matching. To evaluate the performance, the Soton gait database was used for experiment. The experimental results were also compared with other researcher results and the proposed results were reported to have achieved 78% recognition rates.

Table 3.1: Classification of gait recognition methods

Technique	Representative Works	Database Used	Performance	Feature	Advantage	Disadvantage
Appearance-Based	Nikolaos And Zhiwei (2007)	Gait Challenge	96% Correct Recognition	Whole Body	Sensitive to structural difference	High complexity and low robustness
	Dimosthenis *et al.* (2007)	USF	85% Correct Recognition	Projections	Robustness , low complexity	common structural representation
	Xu *et al.* (2006)	Real Human Walking Sequences	80% Correct Recognition	Walking Direction	?	
	Han *et al.* (2005)	CMU MoBo	90.2 % Correct Recognition	Position Of Angle	Robustness	common structural representation
	Hong *et al.* (2006)	CASIA	92.5% Correct Recognition	Person Walking	Sensitive to structural difference	High complexity and low robustness
Model-Based	Liang *et al.* (2004)	Own Database	87.50%	Dynamic Feature	Compact representation	Difficult capturing
	Junqiu *et al.* (2008)	Own Database	Not Given	5D Space	Compact representation	Low robustness

	Chew *et al.* (2002)	Not Given	85% Correct Recognition	Hip Angle	Compact representation	Low robustness
	Haiping *et al.* (2006)	10005 Frames and 285 Sequences	93%	Body Pose	Compact representation	Low robustness
	Rong *et al.*	CMU MoBo, USF	96%, 61%	Individual Body Parts	Compact representation	Low robustness

Table 3.1 presents the classification of gait recognition methods. It includes representative works, database used, performance, features, advantages and disadvantages. This table shows only appearance-based methods and model-based methods.

3.4 Existing Gait Databases

Gait recognition has been an active research topic in recent years. To perform experiments and evaluation of gait recognition systems, several gait databases are available for research purposes. The existing gait databases are CMU MoBo, USF, NLPR, CASIA, USF HumanID, and Soton. These gait databases are described briefly in the following section.

3.4.1 CMU MoBo Gait Database

Carnegie Mellon University (CMU) Motion of Body (MoBo) gait database is one of the most well-known gait database used in gait research. The gait data collection was started in March 2001 and it contained 25 subjects (23 males and 2 females) of individuals walking on a treadmill in the CMU 3D room. Ralph and Jiabo (2001) performed the four different walking styles: slow walk, fast walk, incline walk, and walking-with-a-ball. The CMU 3D room was adapted to capture multi-view walking sequences six video cameras were set and placed around the treadmill sufficient to record gait video. High quality 3 CCD cameras were employed (Figure 2.11) and captured with images size of 640*480 with 24-bit colour resolutions. All the cameras were calibrated.

The selected participants had spent few minutes to familiarise their walk on the treadmill before video capturing. The subjects' walking styles were recorded in the flowing order: for slow walk, the speed of the treadmill was comfortably adjusted to walking speed of the subjects. For fast walk, the subject was asked to walk comfortably fast. For incline walk, the treadmill was set at a 15 degrees incline angle with speed adjusted for a

comfortable walk. Finally, for walking-with-a-ball, the subjects were asked to hold a ball in front of his/her body while walking on the treadmill at comfortable speed. It is assumed that carrying a ball at walking pace is normal walking style. When the number of frames over one gait cycle for slow walk is compared, a similar frame number was noticed in carrying-a-ball walking styles, though it differs from person to person. The aim is to analyse and observe the effects of gait style while using the arms during a walk.

Each subject had spent 15 minutes on the treadmill to complete the gait video recording. The length of each sequence is 340 frames recorded at a speed of 30 frames per second. There were 8,160 images recorded for each subject while observing 10 full gait cycles in an 11-second period. A background image was also captured with each camera to facilitate background subtraction. Table 3.2 shows an overview of the MoBo gait database. Figure 3.10 shows the setting of the cameras around the treadmill. Figure 3.11 shows sample of all six walking styles.

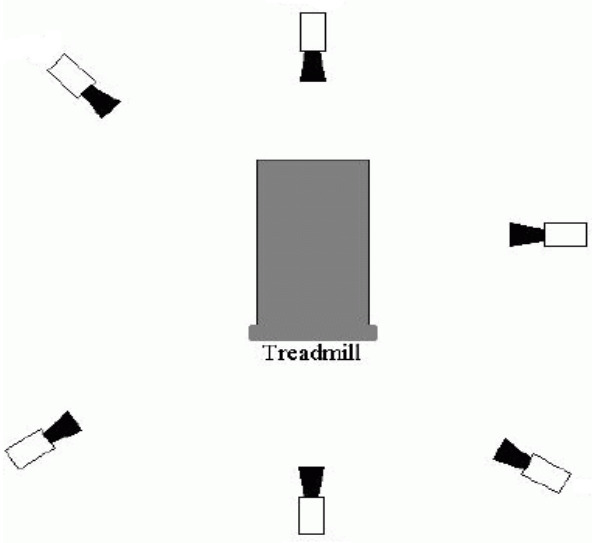

Figure 3.10: Setting of cameras around the treadmill

Source: Ralph and Gross (2001)

Figure 3.11: Sample of all six walking views

Source: Ralph and Gross (2001)

Table 3.2: Overview of the MoBo gait database

Walking location	Indoor treadmill
Subjects	25
Views	6
Synchronized	Y
Walk styles	4
Sequence length [sec]	11
Pixel height	500

Source: Ralph and Gross (2001)

For each subject, basic information were recorded including sex, age, weight, and the treadmill speed for the different walking sequences.

3.4.2 CASIA Gait Database

The Institute of Automation, Chinese Academy of Science (CASIA) is providing the CASIA gait database freely to gait recognition researchers in order to promote research in this field. In the CASIA gait database, there are three datasets, namely, DatasetA (former NLPR gait database), DatasetB (multi-view dataset), and DatasetC (infrared dataset).

DatasetA was created with 20 persons on 10 December 2001 with three directions: parallel, 45 degrees and 90 degrees to the image plane. Twelve image sequences per

person and four sequences for each of the three directions were taken. The database has 19,139 images.

DatasetB (multi-views dataset) was created in January 2005 with 124 subjects. The gait data was captured from 11 views and were made in three variations, namely, view angle, clothing and carrying condition changes.

An infrared (thermal) camera collected DatasetC between July and August 2005 containing 153 subjects in four walking conditions: slow walking, fast walking, incline walking and normal walking-with-a-bag. The videos were captured at night.

3.4.3 USF Gait Database

The University of South Florida (USF) collected gait data over four days, from 20-21 May 2001 and 15-16 November 2001 at their facility involving 33 subjects. The data set consists of persons walking in elliptical paths in front of the cameras with multiple circuits. The USF database for each person has up to five covariates: two different shoe types (A and B), two different carrying conditions (with or without briefcase), on two different surface types (grass and concrete), from two different viewpoints (left and right) and some at two different time instants.

Thus, the person's gait images were taken in 32 possible conditions as shown in Figure 3.12. However, not all the subjects were imaged in all conditions. The full data set is partitioned as depicted in the following grid.

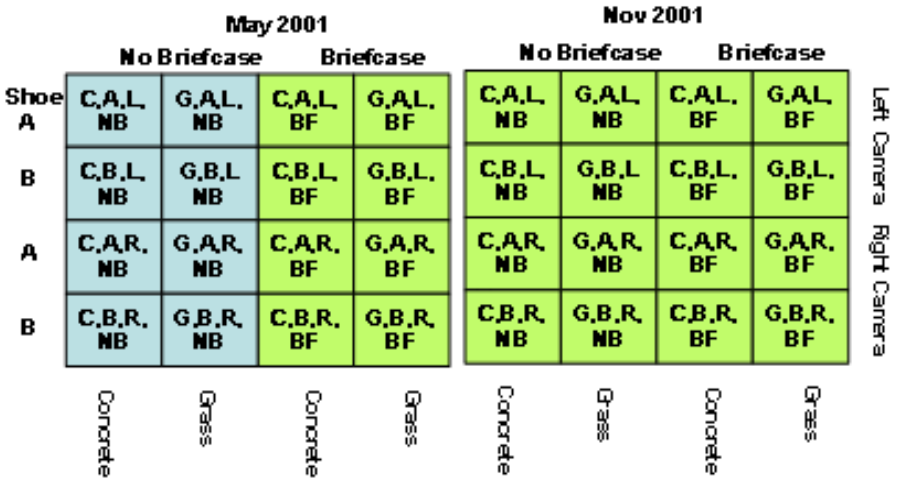

Figure 3.12: 32 possible conditions of USF gait database

The full version of the data sets were provided consisting of 1,870 sequences from 122 subjects.

3.4.4 Challenge Experiments and Base Line Performance

A set of challenge experiment of different difficulty levels based on the collected data were provided. The challenge tasks were constructed in terms of gallery and probe sets. The gallery sets are subsets of the "enrolled" data and the probe sets are subsets of the query data.

The largest subset were selected and the right camera sequences were arbitrarily chosen as the gallery set (G, A, R, NB, t_1), i.e., (Grass, Shoe type A, Right Camera, No Briefcase and time t_1). The rest of the subsets formed the probes, testing the effects of various covariates.

3.4.5 NLPR Gait Database

The NLPR gait database includes 20 subjects and four sequences for each viewing angle per subject, two sequences for one direction of walking, the other two sequences for the reverse direction of walking. For instance, when the subject is walking lateral to the camera, the direction of walking is from right to left for two of the four sequences, and from left t to right for the remaining sequences. All the gait sequences were captured outdoors twice on two different days. The subjects walk along a straight-line path at free cadences in three different views with respect to the image plane.

3.4.6 Soton Gait Database

The Soton gait data recorded the subjects outdoors and indoors. In indoor environment, the subjects walked along a defined track, under controlled lighting and on a treadmill. On the other hand, in outdoor environment, the subjects walked along the track with raincoat, if necessary. Two forms of data were collected, i.e., indoors and one outdoors.

The first form of indoor image is that of a subject walking on a treadmill. The second records subjects walking along a specially designed track with designed background.

The last data was recorded outside the background control area along the trajectory where the subjects walked. The background was intentionally made with cars and people.

The large database was created in summer 2001. Each subject has six different views with two views (frontal-parallel and oblique) per scenario. It was taken outside, inside the track and inside the treadmill environment.

The small database obtained at least 10 subjects walking around the inside track with a green background. Each subject wears various footwear, clothes and carrying various bags and focused their at different speeds. The small database did not use the treadmill or outside data.

3.5 Selected Gait Databases

To evaluate and perform the experiment, a public gait database was selected. For this research, the CMU MoBo gait database was selected as it is popular among the researchers. Several projects have achieved high recognition rates with different techniques after using the CMU MoBo database. It recorded various walking styles to evaluate the different walking style recognition rates and has set standard techniques to evaluate gait test. This database is freely available from Ralph and Jiabo (2001). However, the most important advantage for selecting this database is that it has sufficient gait cycles for each subject. In addition, it has six types of gait styles, which is applied in this research.

Table 3.3: Existing gait databases

Database Name	Num. of Subjects	Num. Of Sequences	Environment	Type	Variations	Url
CMU Database	25	600	Indoor, Treadmill	By request	Viewpoints, Speed, Carrying Conditions, Incline Surface	www.hid.ri.cmu.edu
CASIA Database set A	20	240	Outdoor	By request	Viewpoint	www.sinobiometrics.com
CASIA Database set B	124	13640	Indoor	By request	Viewpoints, Clothing, Carrying, Condition	
CASIA Database set C	153	1530	Outdoor, At Night, Thermal Camera	By request	Speed, Carrying, Condition	
Gait Challenge Database	122	1870	Outdoor	By request	Viewpoints, Surface, Shoe, Carrying, Condition, Time	www.gaitchallenge.org
Soton Small	12	Not Given	Indoor, Green Chrome-Key Backdrop	By request	Carrying Condition, Clothing, Shoe, View	www.gait.ecs.soton.ac.uk

3.6 Conclusion

Table 3.3 summarises the chapter based on literature survey. The model-based and appearance-based methods were reviewed. In addition, wearable sensors-based and floor sensors-based methods were briefly explained. The appearance-based method is divided into two groups, namely, spatio-temporal method and static state method. There

are several articles that briefly described the use of both methods. Moreover, the selected gait database (CMU MoBo) was briefly described along with other available gait databases.

3.7 The Proposed Gait Recognition System

The main interest in this research is to investigate gait recognition performance using two different techniques for gait recognition systems. To build the gait recognition system, the first step involves choosing a suitable gait database for the experiments. The selection of gait database was described in this chapter. Next step involves developing the gait recognition systems by applying PCA with and without RT techniques explained in Chapter 4. For the gait recognition system, two gait features selected, namely, silhouettes-based and GEI-based features used for the proposed techniques for gait recognition system.

Two types of techniques were proposed. The first technique reduces the dimension of space and performs the experiments. The second technique combines PCA with RT to verify the effects of recognition rates.

CHAPTER 4

PROPOSED SYSTEM

4.1 Introduction

Figure 4.1 shows the block diagram for gait recognition based on PCA method used in this research. A 2-D gait images were concatenated to form 1-D image vectors. A zero mean 1-D training images set were computed. PCA was then applied on the collection of 1-D zero-mean images set vector to produce a low-dimensional features vector.

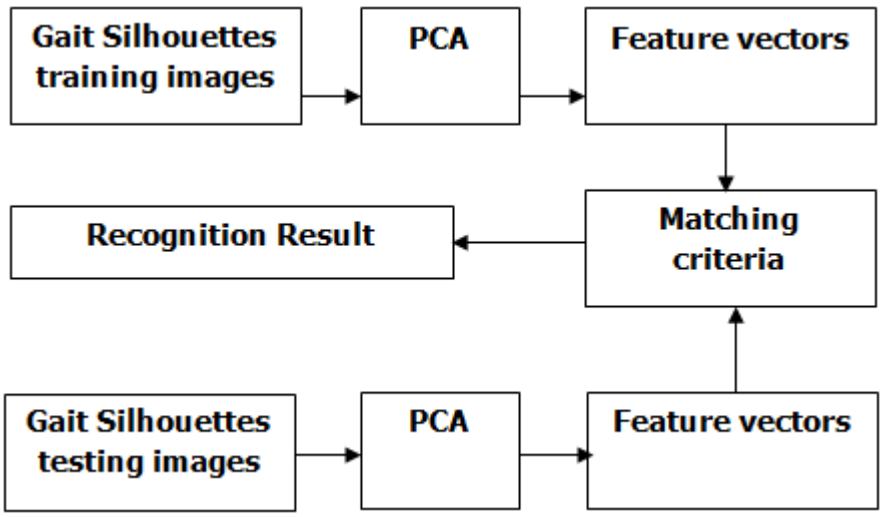

Figure 4.1: Block diagram for gait recognition using PCA

Source: Hayder *et al.*, 2010, 2011

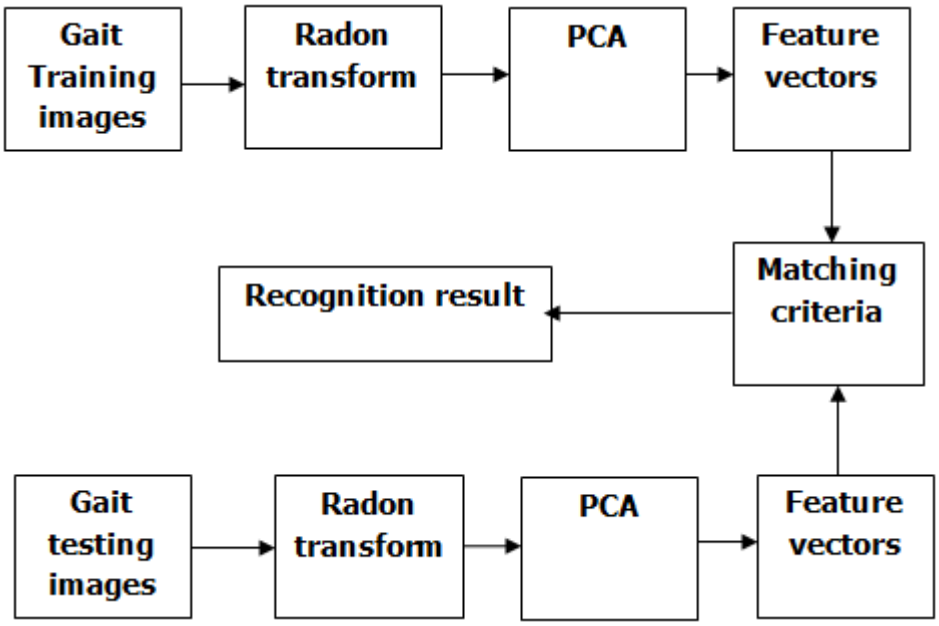

Figure 4.2: Block diagram for gait recognition using PCA with RT techniques

Source: Hayder *et al.*, 2010, 2011

Figure 4.2 shows the block diagram of PCA with Radon Transform. Radon Transform was applied on the image to compute its 2-D projection image along angles varying from 0^0 to 180^0. The result of the projection is the sum of the intensities of the pixels in each direction. All the projections of the image were concatenated to form 1-D Radon Transform vector. The 1-D Radon Transform vectors for all training images were computed and PCA applied on the collection to produce a low dimensional feature vector.

4.2 Principal Component Analysis (PCA)

Principal component analysis technique is also known as dimensional reduction technique which transform a vector X with size n to a unit vector Y with size k, where n is always smaller than k (Moghaddan, 2002 and Miroslaw, 2010). The advantage of

using PCA technique is to reduce the feature space dimension by considering the variance of the input data.

The preferred projections ways are that the maximum amount of information is obtained in the smallest number of feature space dimensions. In order to obtain the best variance in the data, the data is projected to a subspace, which is capability, by the eigenvectors from the data. In that sense, the eigenvalue corresponding to an eigenvector match the amount of difference that eigenvector handles.

In different applications, PCA technique is used broadly in image processing, gait detection and recognition, performance, in large databases and video. These applications are briefly explained.

For image processing, the image is compressed from larger dimension into smaller dimension. The PCA method is widely used to recognise person by comparing the characteristics of the gait with known database. It can be applied to the freely available databases and useful for video stream coding and compression of talking heads.

PCA is an important tool for data analysis and able to calculate eigenvalue decomposition of a data covariance matrix or singular value decomposition of a data matrix.

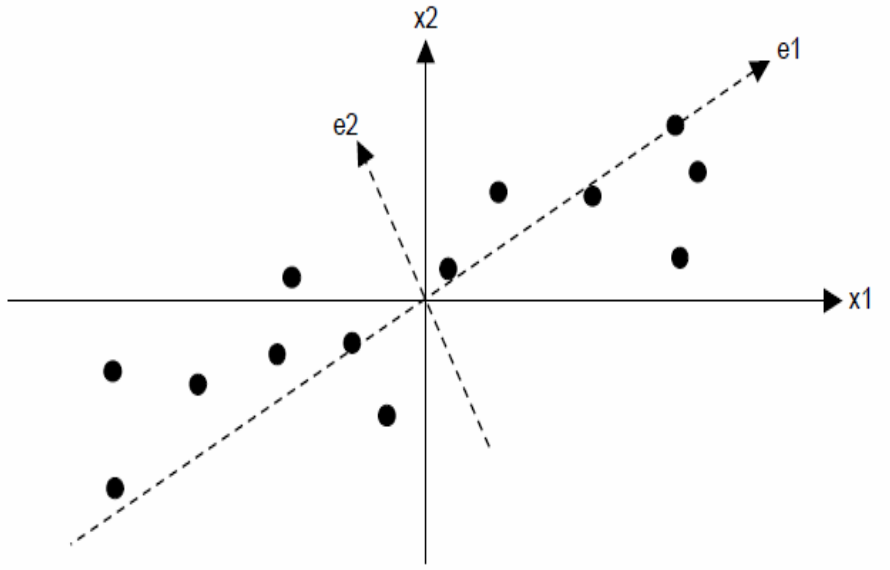

Figure 4.3: Principal Component Analysis on a 2-D data resulting in two eigenvectors, e1 and e2

Source: Mark *et al.*, 2002

For example, for an image with a 250x250 resolution, the feature vector will be (250x250) = 62,500. For a feature vector with 62,500 features points, it is not feasible to be used for recognition purposes. PCA extracts the major difference in the feature vector and accept a perfect reform of the data to be shaped from only a few of the extracted feature values, hence reducing the amount of essential calculation. Figure 4.3 shows Principal Component Analysis on a 2-D data resulting in two eigenvectors, e1 and e2.

4.3 Radon Transform (RT) Technique

The Radon Transform is one of the most powerful technique used to identify features within an image. Radon transform is well known in a wide range of image applications.

It is an integral transform function over straight line. One common form of RT is expressed among different forms in Equation (4.1).

$$F(\rho,\theta)=\int_{-\infty}^{\infty}\int_{-\infty}^{\infty}(x,y)\partial(\rho-x\cos\theta-y\sin\theta)dxdy \tag{4.1}$$

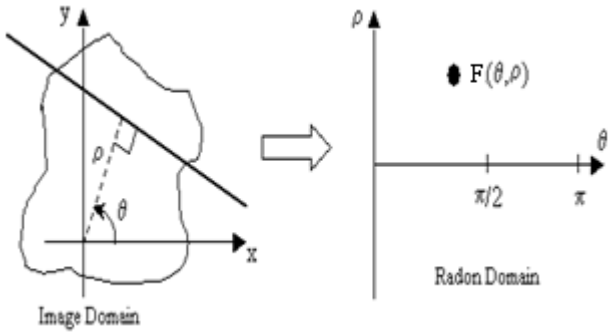

Figure 4.4: Image domain and radon domain

Source: idlastro.gsfc.nasa.gov/ idl_html_help/RADON.html

where, X is defined as integral along a line through the image, θ is the angle and ρ is the distance of the line from the source of the coordinate system as shown in Figure 4.4. F(ρ, θ) is the integral line of a 2D function f(x, y) along a line from -∞ to +∞. The point and direction of the line is determined by two parameters ρ and θ as shown in Figure 3.4. F(ρ, θ) is the integral of f(x, y) over the line $\rho = x\cos\theta + y\sin\theta$. In this gait analysis project, the two dimensional function is the binary silhouettes as it is the discrete form of pixel intensities along lines of different directions. The reference point has set centre of the silhouette as given in Figure 4.5. This figure shows the fundamental procedure of Radon Transform on binary silhouettes. Figure 4.5(a) is two parameters (ρ, θ) to verify the location of the integral line; Figure 4.5(b) is computation of Radon coefficients.

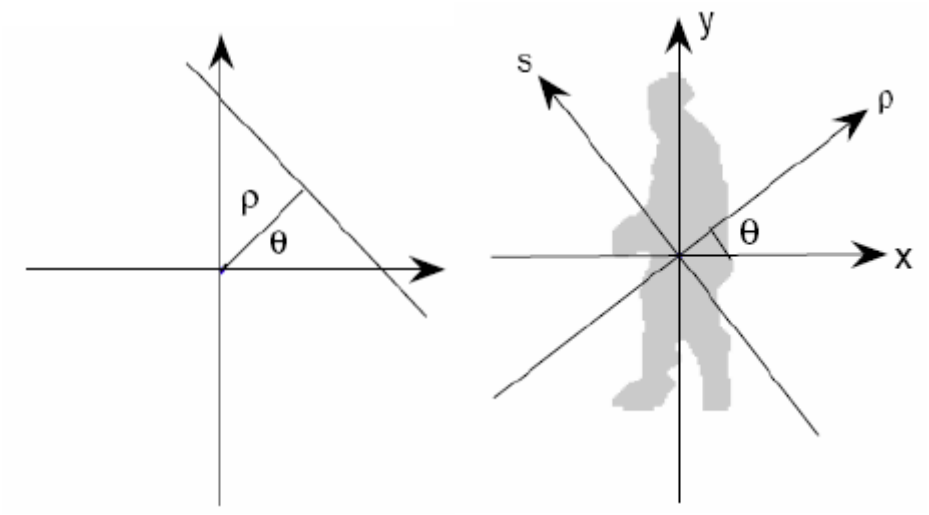

(a) **(b)**

Figure 4.5: The fundamental procedure of Radon Transform on binary silhouettes: (a) Two parameters (ρ, θ) determine the location of the integral line; (b) Computation of Radon coefficients

Source: Lei *et al.*, (2009)

The Radon Transform was used for silhouettes to establish mapping between domains determined by the coordinate system (x, y) and (ρ, θ). The radon domain is also determined by visualising Figure 4.5 that computes the radon co-efficient method. This figure shows an exact silhouettes direction projected onto the ρ axis. Otherwise, pixels along a set of lines parallel to the s axis are added together. A coefficient (ρ_i, θ_i) in the radon domain correspond to the sum of pixels along a line parallel to the s axis in the original silhouettes. The position and way of the summation line is determined by ρ and θ.

The Radon Transform is very appropriate for gait representation and recognition because during human walking, the large angular differences of the legs and arms axes are formed with respect to horizontal axis. In conclusion, the individual forms and walking patterns can be drawn by identifying and studying these radon coefficients.

4.4 Matching Criteria

The most important work in the experiment is to estimate periodicity of walking in a gait cycle. When a person is walking, the wide of the foreground silhouettes changes due to frequently changing lower body parts. The maximum and minimum widths of the subjects' foreground difference is found by applying the Euclidean distance method.

A fundamental idea of the recognition system is the pattern matching plan based on measures of space between pattern vectors. These various ways can be measured by two vectors. Generally, for the recognition purposes, the Euclidean space is used to measure between two pattern vectors. This space method is very famous in the pattern recognition research field.

To examine the Euclidean space, simply study root of square differences between coordinates of a pair of objects. The square of difference between two scalars of each feature point in two feature vectors is added up and the square root of the addition is then calculated.

The Euclidean distance between two points A and B is the length of the line segment connecting them $\underline{AB}$, where two points, $A = (a_1, a_2, a_3 \ldots, a_n)$ and $B = (b_1, b_2, b_3 \ldots., b_n)$ are in Euclidean n space, then the distance from A to B or from B to A is known as:

$$d(A,B) = \sqrt{(a_1 - b_1)^2 + (a_2 - b_2)^2 + ...+ (a_n - b_n)^2} \quad (4.1)$$

$$d(A,B) = \sqrt{\sum_{i=1}^{n} (a_i - b_i)^2} \quad (4.2)$$

The location of a point in a Euclidean n space is a Euclidean vector. Hence, A and B are Euclidean vectors, begging from the source of the space. The magnitude of a vector measures the length of the vector. From this expression, the Euclidean space is the norm of the difference between two vectors.

The Euclidean distance method is one of the most commonly used algorithms in human recognition systems (Kanak and Pratibha, 2011; Xiang *et al.,* 2010; Jyori and Gupta, 2011; Yi *et al.,* 2010). This method is very similar to the correlation algorithm and in cases where submitted data has no negative values, it produces equivalent results. The main advantage of the Euclidean distance method over the correlation method is that it is reportedly slightly faster (Hayder *et al.*, 2010). Other similarity measurements are available such as cosine distance (Schneider *et al.,* 2007), Mahanalobis distance (Gedikli and Ekinci, 2005; Daoliang *et al.,* 2007; Ekinci, 2006) and nearest neighbours (Liang *et al.,* 2003). For this project, the Euclidean distance was selected for similarity measure.

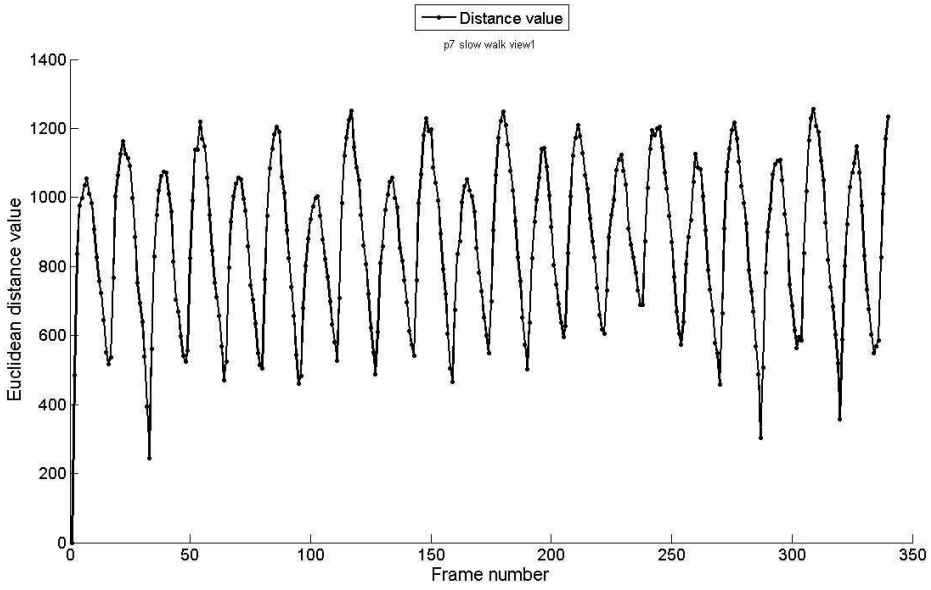

Figure 4.6: Sample of the Euclidean distance result for one subject Source: Source: Hayder *et al.*, 2010, 2011

The Euclidean distance is used for measurement purposes. If Euclidean distance between frame A and frame B in the train database is smaller than a fixed threshold value T, then frames A and B are considered to be the same subject. Threshold T is the largest Euclidean distance between any two images in the training database divided by a threshold tuning value (Tcpara) as given in Equation (4.3) (Hayder *et al.*, 2010). The threshold is defined as:

$$T = \frac{[\max(\| \Omega j - \Omega k \|)]}{Tcpara} \tag{4.3}$$

Where, Tcpara is a tuning value; j, k = 1, 2, 3. . . , N. N is the total number of training images and Ω is the reduced dimension images for a given frame subject. A sample of

the Euclidean distance is shown in Figure 4.10 to verify the frame to frame matching for one subject. It can be seen from Figure 4.10 that each frame displays different magnitudes on one complete cycle. It is easy to select a gait cycle by applying the Euclidean distance method. The gait cycle can also be obtained manually.

In the algorithm, two performance matrices were measured, namely, recall and reject. For recall, if a test image is correctly identified to an image of the same person from the training database, it is called Correct Classification (CC) as shown in Equation 4.4. However, if the test image is incorrectly matched with another subject images, it is called False Acceptance (FA) as shown in Equation 4.5. If an image from the training database is rejected by the system, then it is called False Rejection (FR) as in Equation 4.6. For reject, if any test frame from the unknown set cannot be identified by the system, then it is called Correct Classification. If the test image can be detected by the system, then it is called False Acceptance (Hayder *et al.*, 2010).

$$\text{CCR} = \frac{\text{the correct matching frames}}{\text{total test frames}} \text{x100} \tag{4.4}$$

$$\text{FAR} = \frac{\text{the number of false acceptance frames}}{\text{the number of total test frames}} \text{x100} \tag{4.5}$$

$$\text{FRR} = \frac{\text{the number of false rejection frames}}{\text{The total number of test frames}} \text{x100} \tag{4.6}$$

4.5 Conclusion

In this chapter, two techniques of gait recognition have discussed details with block diagram. However, matching criteria has explained in details that how produced recognition rates.

CHAPTER 5

DATA PREPARATION

5.1 Introduction

Data preparation is concerned with creating datasets for application in the experiments. Two types of datasets are needed to be generated, namely silhouettes-based and GEI template-based. The known and unknown datasets also necessitate production of the silhouettes- and GEI template-based system. The following section describes the data preparation.

5.2 Gait Databases

Based on available literatures, there are many ways to subtract human body from video sequences to obtain foreground images. The normal subtraction technique produced imperfect silhouettes. It is therefore necessary to investigate further ways to receive quality silhouettes. It is believed the best way is to apply the normal subtraction method and use morphological filters to construct quality silhouettes. However, updating the background is also required to deal with colour space. Based on the environment, generation of background from video sequences is essential while updating the silhouettes background. More importantly, the human body's silhouettes must be in perfect shape to obtain high recognition rate accuracy.

However, better quality silhouettes reception during silhouette extraction process can be obtained by applying fixed threshold value separately for every single person for each walking styles and each view.

Most researchers agreed that the foreground must be at centre of the frame. This technique produced smooth gait cycle curve for matching purposes and might acquire high recognition rates. Bo and Yumei (2006) aligned the foreground by applying diagonal, horizontal and vertical scanning projection for the experiment. Lei *et al.* (2009) used different existing gait databases and normalised the foreground at the centre for the experiment. Sungjun *et al.* (2007) reported that the extracted silhouettes normalised the foreground at the centre.

In addition, Vili *et al.* (2009) used existing CMU MoBo gait database for the experiment achieving better gait cycle curve. However, the foreground silhouettes were not aligned at the centre. Guoying *et al.* (2007) used similar database for experimental purposes. Changhong *et al.*, (2009) also applied the database without changing the silhouettes data.

In this project, the provided silhouettes data is assumed to be set accordingly that is normalised at the same position for all subjects and each view. Figure 5.1 shows sample of complete gait cycles using CMU MoBo gait database. Smooth gait cycles pattern were received which proved silhouettes are aligned.

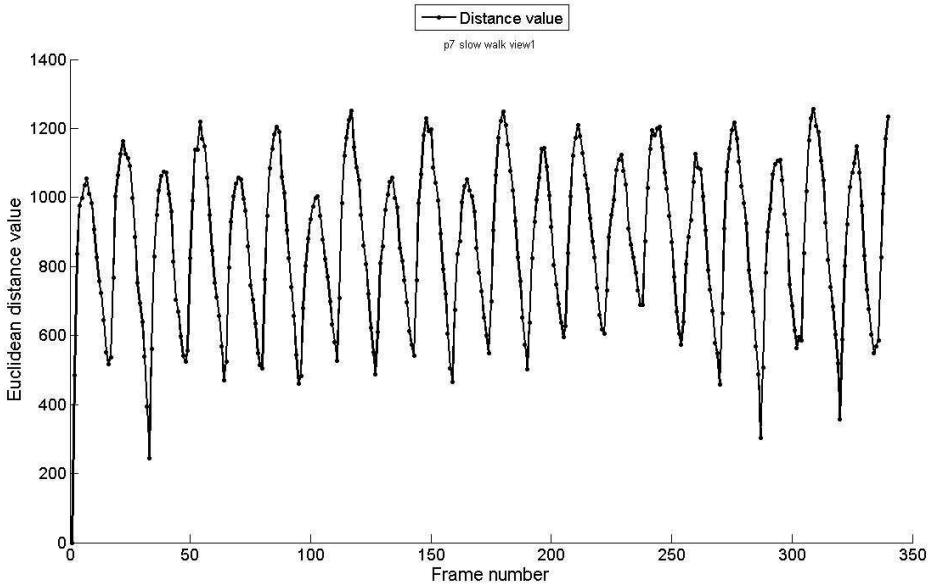

Figure 5.1: Sample of complete gait cycles for one subject

Source: Hayder *et al.*, 2010, 2011

5.3 silhouette data sets

5.3.1 Silhouettes Extraction

In the gait recognition system, silhouette is defined as a region of pixels of the walking person. It is the simplest form of line art and is used specifically in cartoon animations, technical designs. In this aspect, silhouettes extraction is the most important part to determine the recognition rate accuracy for the gait recognition system. In this system, silhouettes extraction generally involves the operation of segmenting the human body from a background. This process will be deal with in more details in the next section.

Background subtraction is a method to detect a movement or important variations within a video frame with respect to a reference. If the pixel value and background value is not the same, then the processed pixel is marked as a silhouettes region. The

silhouettes are then obtained by subtracting the reference image frame from the current image frame (Rosalyn *et al.*, 2009; Hansung *et al.*, 2005). For example, let the current image frame be denoted as I_c, the reference image frame as I_r, and the output of the image frame as I_b. The general background subtraction operation is expressed by Equation 5.1. In addition, Figure 5.2 illustrates the background subtraction process. The current image, I_c, the reference image, I_r, and the output image, I_b, are shown in Figures 5.2(a), 5.2(b) and 5.2(c) respectively.

$$I_b = | I_c - I_r | \tag{5.1}$$

(a) Current image (I_c) **(b) Reference image (I_r)** **(c) Output image (I_b)**

Figure 5.2: Illustration of background subtraction

Silhouettes extraction from gait video sequences in any environment does not usually produce perfect silhouettes. Therefore, in most practical cases, there is a need to apply an efficient algorithm for the gait recognition system. The simplest way to produce

silhouettes is by morphological operations using the normal background subtraction method.

Xi *et al.* (2006) proposed an algorithm for updating background information. They combined two features, namely, high level and low level knowledge features to update the background information in order to extract silhouettes. Moreover, they also applied fuzzy logic inference system to combine spatio-temporal information to remove moving things and process the human body silhouettes.

Yi and Mehmet (2005) applied the Least Median of Squares (LMeDS) background modelling method to detect the image from video sequences and extract the background. However, they also applied threshold value via the histogram technique to compare the resultant difference of the current image and background image. Furthermore, Gaussian filters are used to eliminate noise from the extracted silhouettes.

5.3.2 Training and testing data sets

In this project, 25 individual subjects were selected and each individual subject has four kinds of walking styles. Each walking styles has six different walking views and each different walking views has 340 silhouettes. The gait database was divided into two groups, namely, known database and unknown database for experiment where 13 subjects are for known and 12 subjects are for unknown selected randomly for all three walking styles. The known gait database was further divided in two sets, namely, training dataset and testing dataset. Each view has 340 silhouettes, and from this 340

silhouettes, a minimum of 14 walking cycles are available. Each cycle has approximately 18–20 frames (Hayder *et al.*, 2010).

In this project, out of 14 cycles, 10 gait cycles were selected for training and four for testing based on 13 known subjects. Only one cycle is selected for unknown from the 12 unknown subjects. For the experiment, the total number of images used for the three walking styles are 6,713 training, 2,691 testing, and 672 unknown testing for PCA-only technique. The known test database is used to test the recall capability of the gait recognition system. In contrast, the unknown test database is used to test the rejection capability of the system. The size of all the provided silhouettes frame is 486*600. The classification of the rearranged database structure is shown in Figure 5.3.

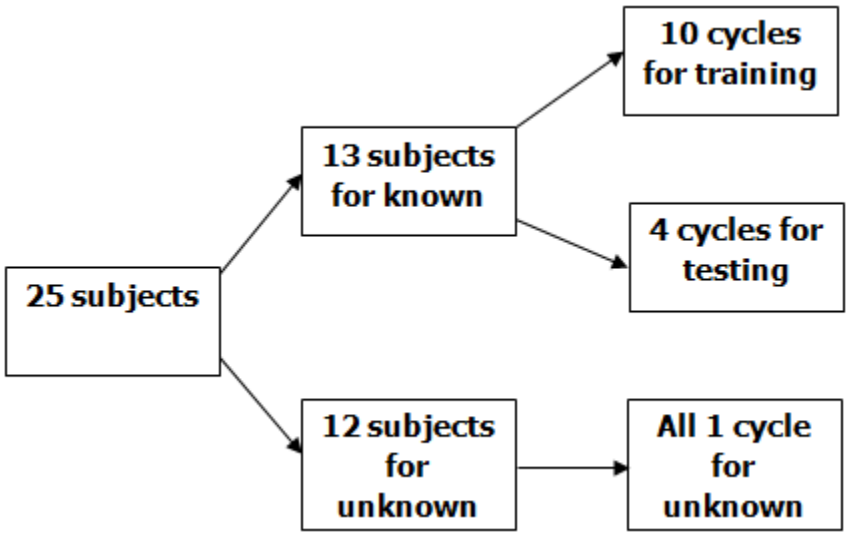

Figure 5.3: Silhouettes training and testing data sets

Source: Hayder *et al.*, 2010, 2011

Figure 5.4 shows a sample of a complete gait cycle for one subject. Figure 5.4 6o 5.7 shows the samples of known training, known testing and unknown testing for slow, fast, and carrying-a-ball walking styles for silhouettes based-systems respectively.

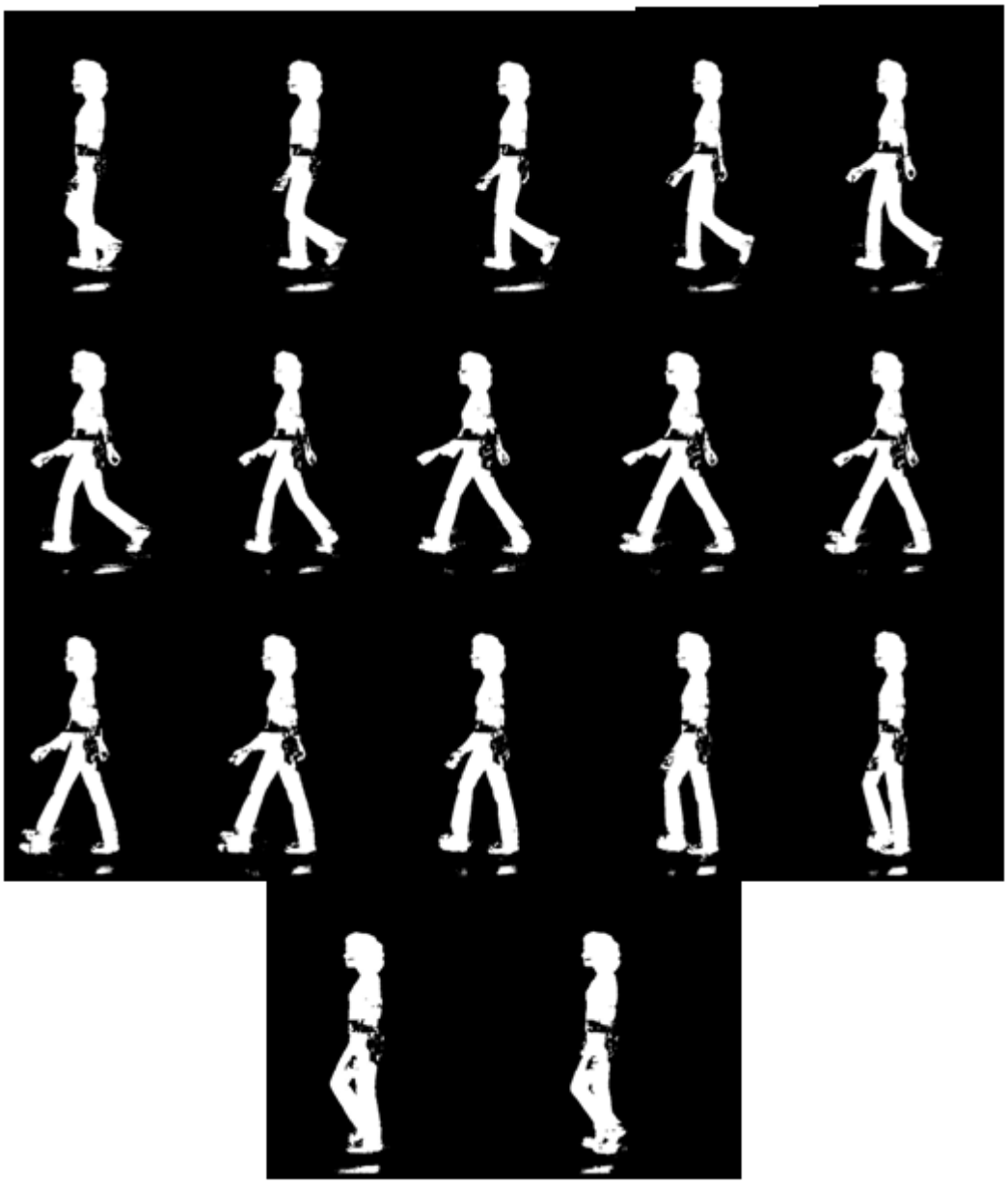

Figure 5.4: A complete gait cycle for one subject for fast walking style

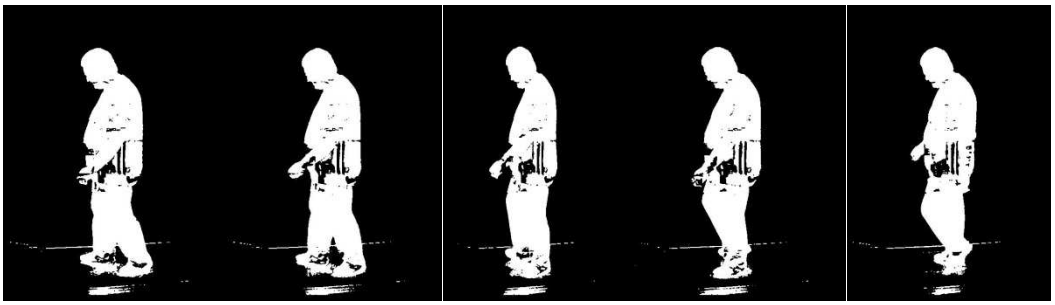

(a) Slow walking style training frames

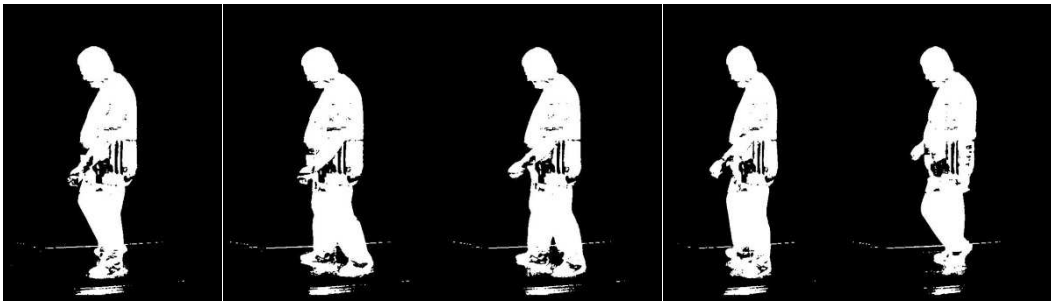

(b) Slow walking style testing frames

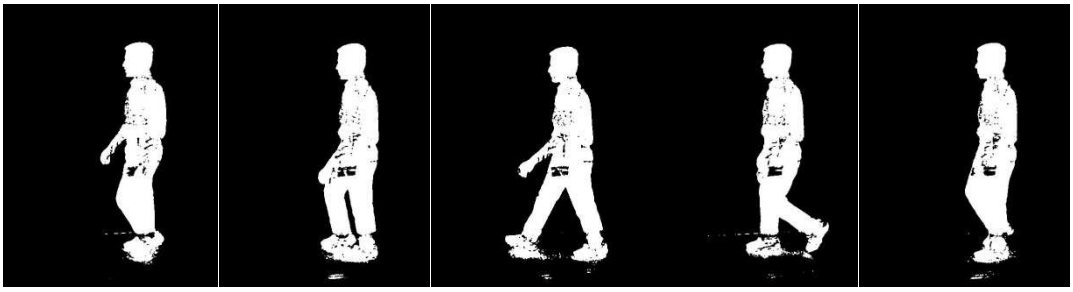

(c) Slow walking style unknown testing frames

Figure 5.5: Samples of slow walking style for known and unknown datasets

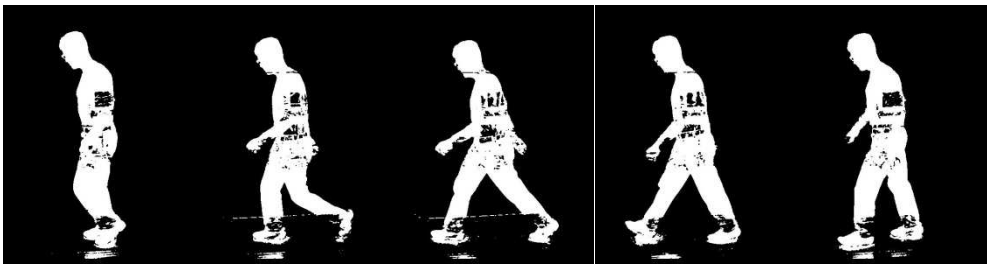

(a) Fast walking style training frames

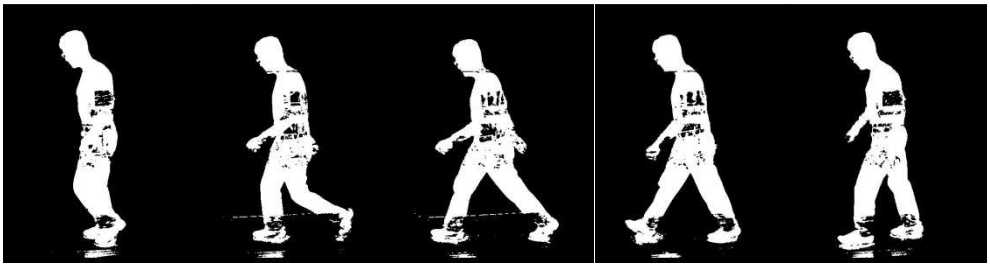

(b) Fast walking style testing frames

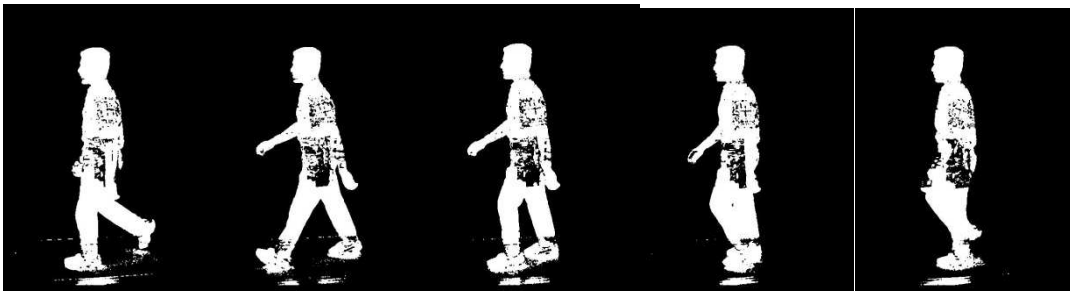

(c) Fast walking style unknown frames

Figure 5.6: Samples of fast walking style for known and unknown datasets

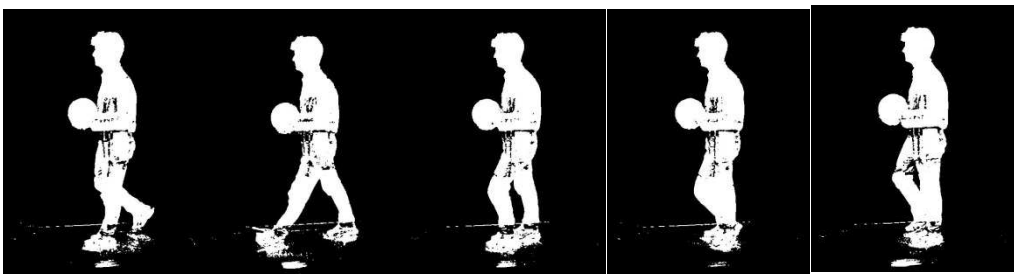

(a) Carrying-a-ball walking style training frames

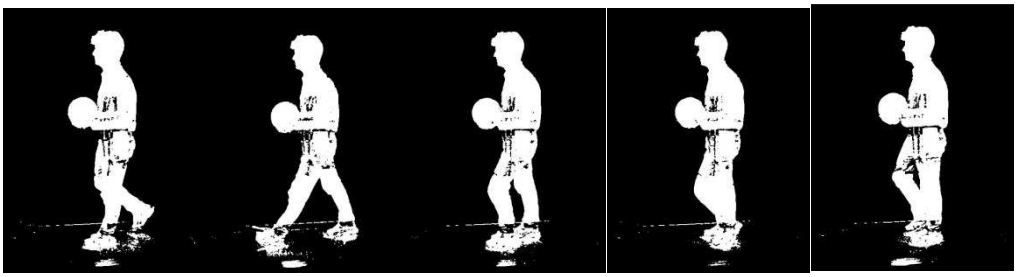

(b) Carrying-a-ball walking style training frames

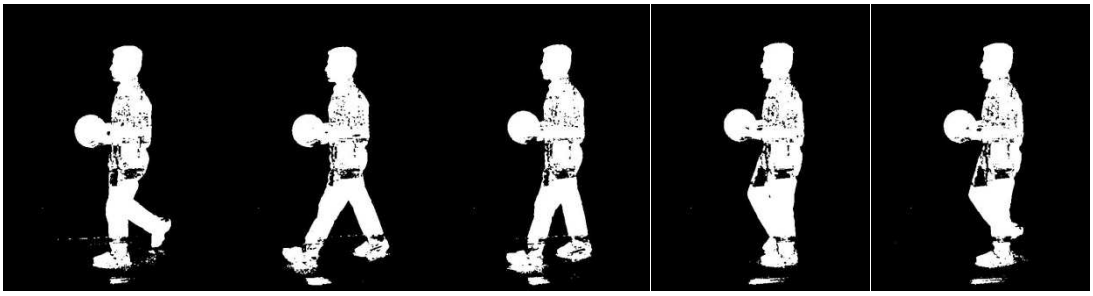

(c) Carrying-a-ball walking style training frames

Figure 5.7: Samples of carrying-a-ball walking style known and unknown datasets

5.4 Gait Energy Image (GEI) data sets

Nini *et al.* (2009) explained the construction of GEI templates and compares the performance with other research. The proposed techniques were reported to have improved recognition rates compared to other research using GEI templates. Heesung *et al.* (2009) also performed GEI templates experiments. Mayu *et al.* (2010) described GEI templates methods for application in human age applications for different experiment. In the final analysis, the GEI templates-based method is found efficient for application in person identification. In this section, the silhouette sequences arrangement to build GEI templates were made to enhance the experiment.

Gait Energy Image (GEI) is the sum of images of the walking silhouettes divided by the number of images. GEI is a useful representation with superior selective power and strength against segmental errors (Heesung *et al.*, 2009; Khalid *et al.*, 2010). Given the pre-processed binary gait silhouette images $B_t(x, y)$ at time t in a sequence, GEI is expressed as Equation 5.2.

$$G(x,y) = \frac{1}{N}\sum_{t-1}^{N} B_t(x,y) \qquad (5.2)$$

Where, N is the number of frames in one complete gait cycle and x and y are values in the image coordinates (Nini *et al.*, 2009; Khalid *et al.*, 2010; Ju and Bir, 2006; Heesung *et al.*, 2009). To make GEI templates, the silhouettes were selected from the provided CMU MoBo gait database. Figure 5.9 shows the constructed sample of GEI templates over one gait cycle seen at the far right images. Figure 5.10 to 5.12 shows the samples

of known training, known testing and unknown testing for slow, fast, and carrying-a-ball walking styles for GEI templates-based systems respectively.

The provided CMU MoBo database has four kinds of walking patterns, namely, slow, fast, incline and carrying-a-ball walk. Each walking pattern has six types of views from different angles. Each view captures 340 frames that can be calculated with a minimum of 14 cycles, and each cycle has approximately 18 to 20 frames. One gait cycle frame constructs a GEI template. Thus, one subject has a minimum of 14 GEI templates. For the training and testing datasets, 10 GEI templates were selected for training and four for testing in order to perform the experiment. The total number of GEI training and GEI testing templates are 13*10=130 and 13*4=52 respectively. For the unknown subject, one cycle has been selected to construct GEI unknown templates indicating each person has one GEI unknown template. Figure 5.7 shows sets of training and testing GEI databases. The previous silhouettes gait database section that arranged and prepared the GEI templates for this section were realistically followed to compare results. The total numbers of GEI testing templates were compared with GEI training templates for recognition purposes. The GEI testing templates were used to test the recall capability of the gait recognition system. Another 12 subjects called GEI unknown templates with one cycle for three walking styles were prepared for reject capability of the system. The technique of PCA-only was applied in this chapter for recognition purposes. The 130 GEI images were used for training dataset while 52 GEI images were used for testing dataset.

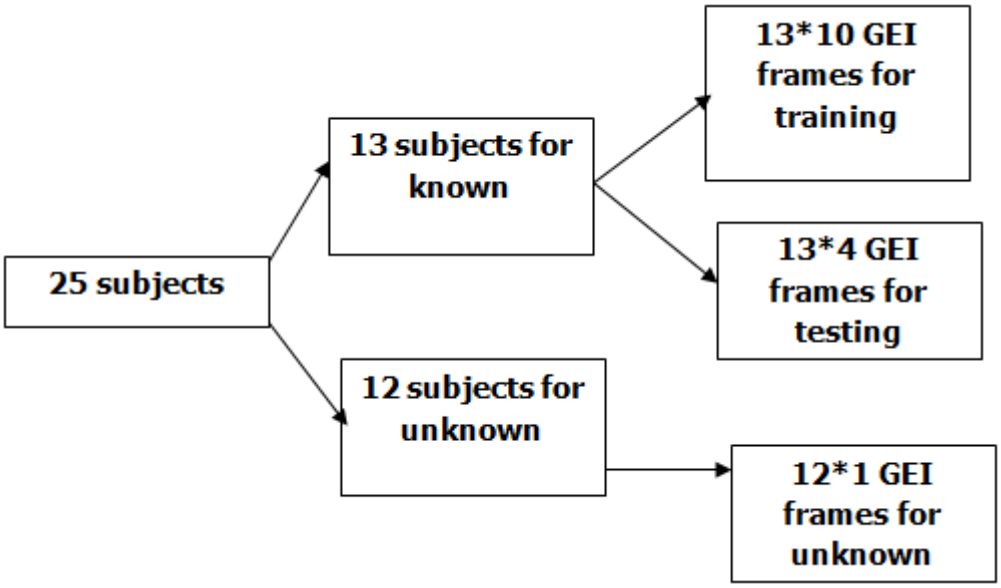

Figure 5.8: Design of testing and training gait datasets

Source: Hayder *et al.*, 2010, 2011

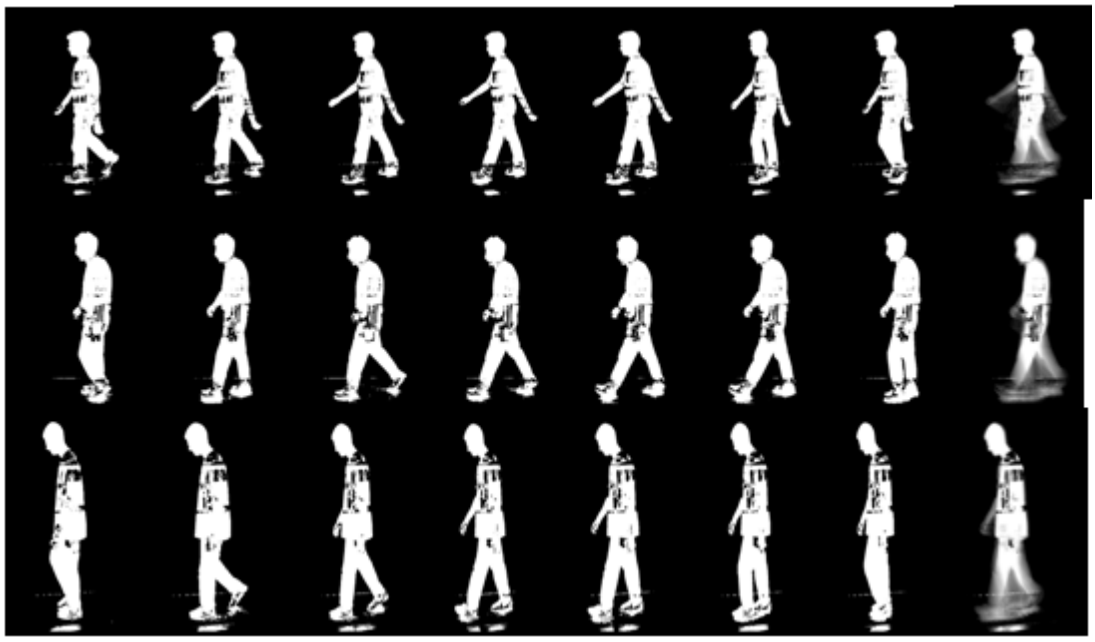

Figure 5.9: The constructed sample of GEI templates from a sequence of Silhouettes for fast walking style

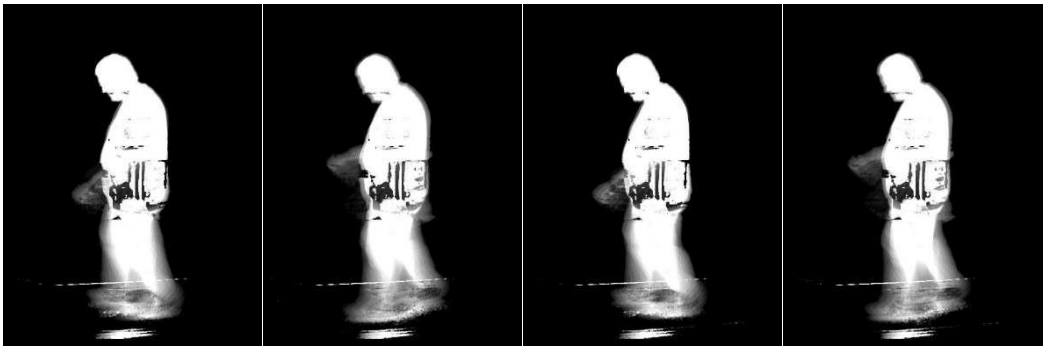

(a): Sample of slow walking styles of GEI training input

(b): Sample of slow walking styles of GEI training input

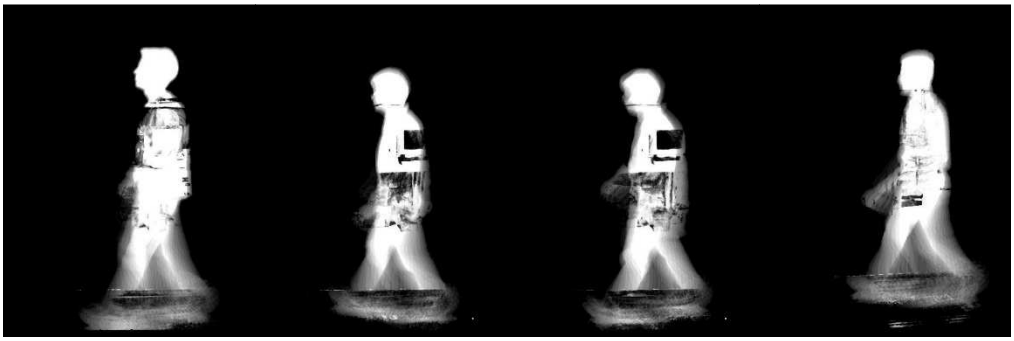

(c): Sample of slow walking styles of GEI training input

Figure 5.10: Samples of slow walking styles known and unknown datasets for GEI templates systems

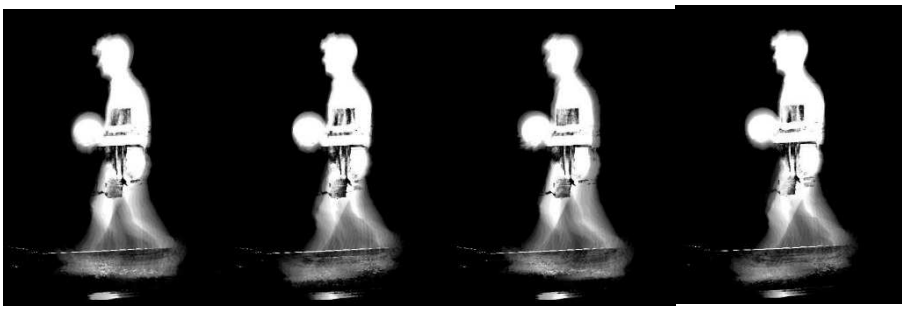

(a): Sample of fast walking styles of GEI training input

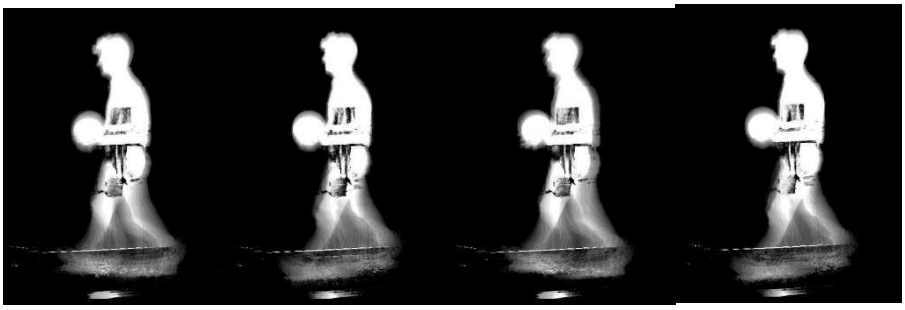

(b): Sample of fast walking styles of GEI training input

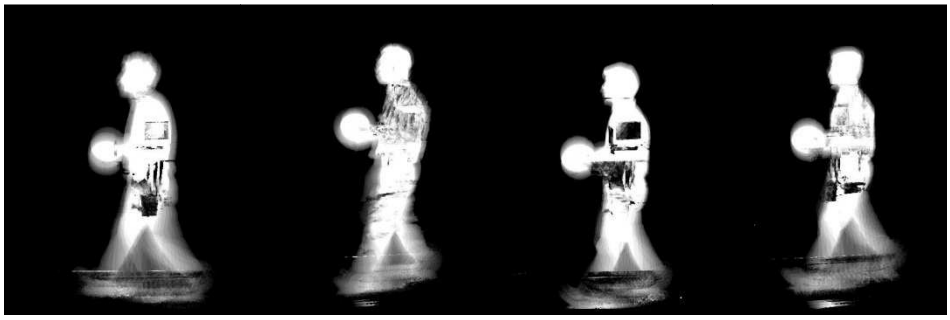

(c): Sample of fast walking styles of GEI training input

Figure 5.11: Samples of fast walking styles for known and unknown datasets for GEI templates systems

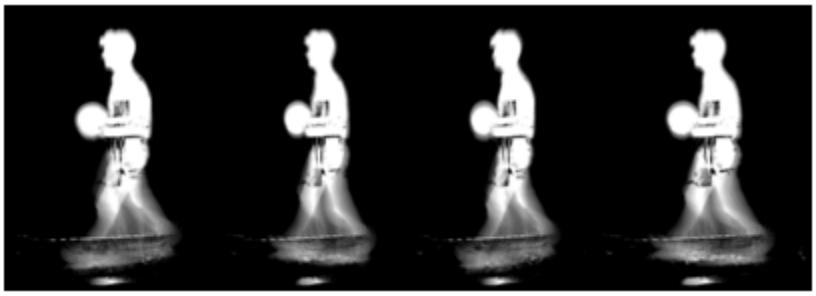

(a): Sample of carrying-a-ball walking styles of GEI training input

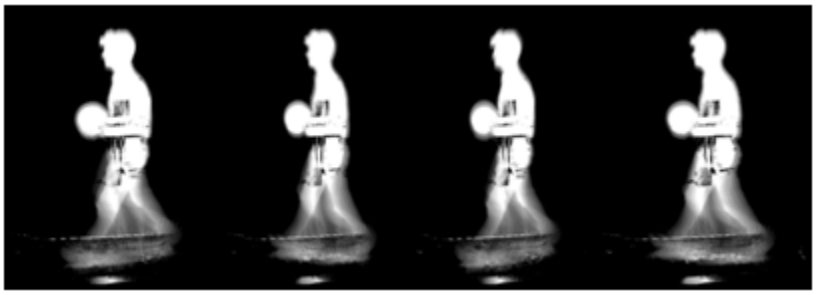

(b): Sample of carrying-a-ball walking styles of GEI testing input

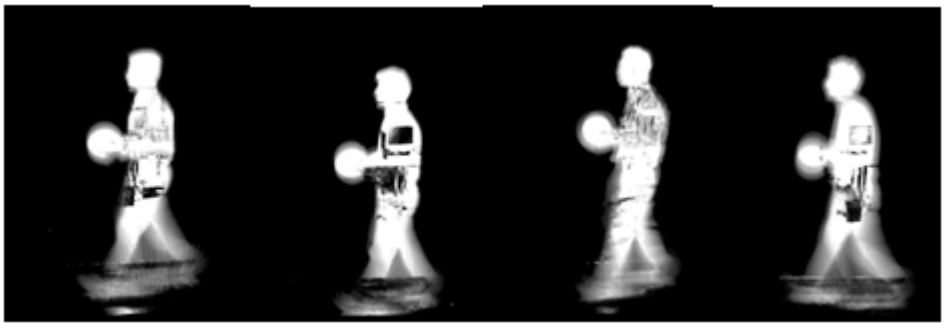

(c): Carrying-a-ball walking styles of unknown GEI templates gait dataset input

Figure 5.12: Samples of carrying-a-ball walking styles for known and unknown datasets for GEI templates systems

5.5 Conclusion

In this chapter, data preparation were described. The known and unknown datasets were briefly explained for silhouettes-based system. However, the known and unknown datasets were processed for the GEI-based system.

CHAPTER 6

RESULTS AND DISCUSSION

6.1 Introduction

The main objective of this thesis is to compare the recognition rates between silhouettes- and GEI template-based system using Principal Component Analysis (PCA) with and without Radon Transform (RT) techniques. Section 6.2 describes the PCA technique for silhouettes as gait features and also setting threshold parameter using PCA technique only. Section 6.3 describes PCA with RT technique with setting threshold parameter. Section 6.4 explains the comparison of recognition rates between silhouettes and GEI templates. Section 6.5 provides performance comparison between PCA with and without RT using silhouettes and GEI templates, and finally, Section 6.6 summarises the chapter.

6.2 using PCA only

6.2.1 Silhouettes as gait features

6.2.1.1 Setting Threshold Parameter using PCA Technique Only

The threshold value is a place or position to begging to obtain system result. The value of the threshold tuning parameters can be used to tune the performance of the system to have either high correct recall with high false acceptance rate for application such as boarder monitoring, or high correct rejection rate for unknown persons for application

such as access control. For this work, the threshold tuning parameters were set so that the system has equal correct recall rates and correct rejection rates. The TCPARA (threshold) value mentioned that was chosen for each system is shown in Figure 6.1 to 6.3, and each walking system has different TCPARA values. The recognition rate varies according to set TCPARA value. If the system sets TCPARA value to 1, then it will have high recognition rate percentage. Thus, the recognition rate is dependent on the TCPARA values of the system (Hayder *et al.*, 2010).

An acceptance (the frames match) or rejection (the frames do not match) is determined by using a threshold value. To collect results for the false rejection rates, all the frames for a single subject is compared with every other frames of other subjects. No frame is compared with itself and each frame is only compared once, giving testing frame for comparisons to test false rejection for method. Using test images, every person is compared with every other subject. This gives comparisons of subject with no person compared to himself, and each frame only compared once. For every threshold value, we might compute a FAR and a FRR (Figure 6.1 to 6.3) by the system.

Figure 6.4 shows experimental performance using PCA-only technique for three walking styles. It also shows the Equal Recognition Rate (ERR) for PCA techniques for three walking styles. When the recall correct classification is equal to reject correct classification, it is called ERR. For this work, the ERR achieved 90.78%, 90.26% and 87.75% for PCA-only method for the three walking styles: slow walk, fast walk, and carrying-a-ball walk respectively. The fixed threshold values are 6.42, 6.34, and 4.90 for slow walk, fast walk and carrying-a-ball walk respectively. If the TCPARA value is set to

1, then the best correct classification rate attained is above 95% for PCA-only methods for all three walking styles when reject correct classification rate is 0%.

Figure 6.1, Figure 6.2 and Figure 6.3 shows the recall correct classification rate is decreasing as TCPARA value increases, while the reject correct classification rate is increasing as TCPARA value increases. However, the FAR for both recall and reject decreases as TCPARA value increases. However, each walking styles FAR and FRR may be calculated from both systems according to the recognition rates. The FAR for both recall and reject decreases as TCPARA value increases. Therefore, different walking styles have different threshold values for the system and it is similar for all three walking styles for PCA with and without RT techniques based on silhouettes- and GEI-based templates.

Based on the three walking styles, the researcher observed that slow walking styles represented better ERR compared to carry-a-ball walking styles and fast walking styles. The fast walking styles achieved slightly better ERR than carrying-a-ball walking styles. The carrying-a-ball walking styles attained low ERR than slow walking styles and fast walking styles.

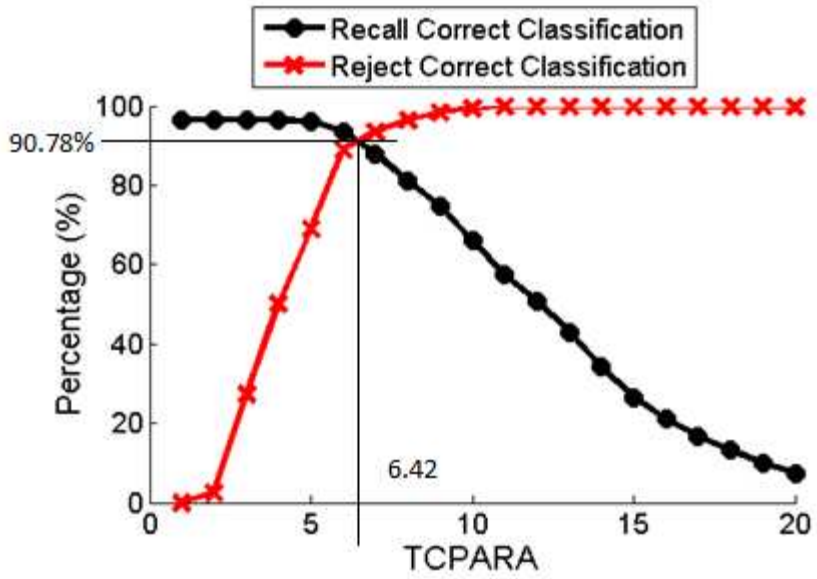

Figure 6.1: Recognition result using PCA for slow walk

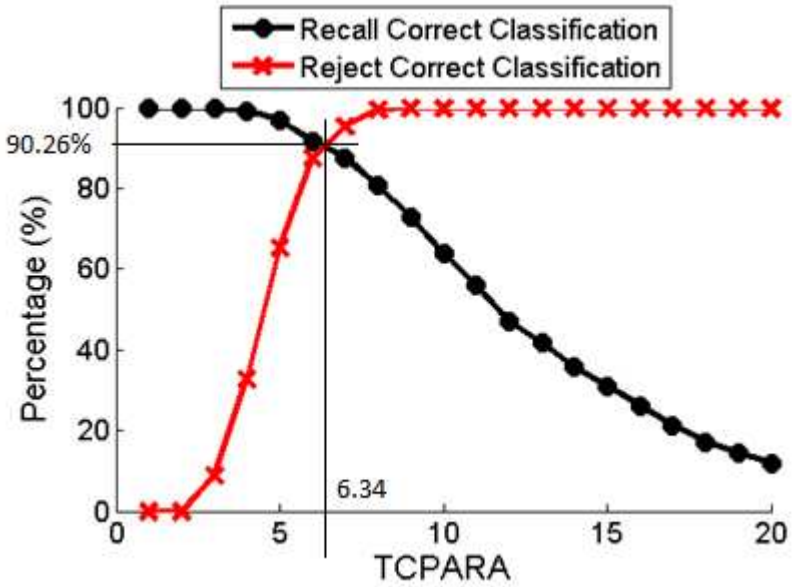

Figure 6.2: Recognition result using PCA for fast walk

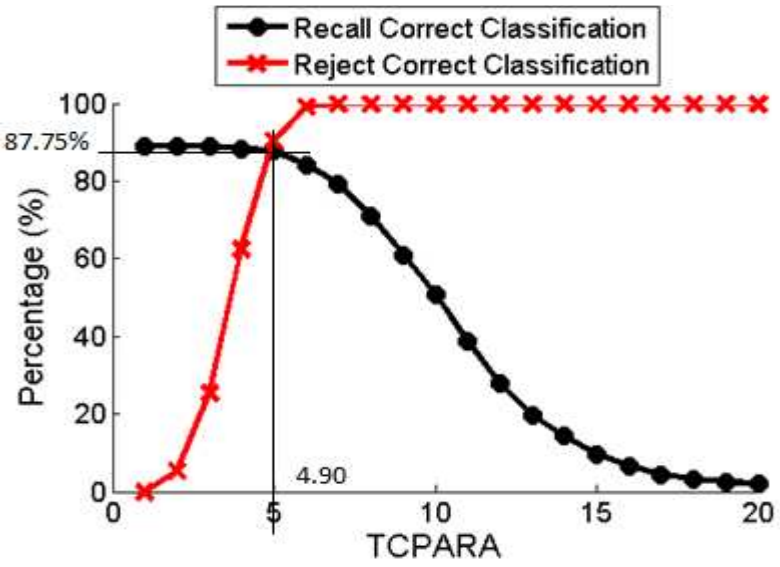

Figure 6.3: Recognition result using PCA for carrying a ball

6.2.1.2 Results and discussion

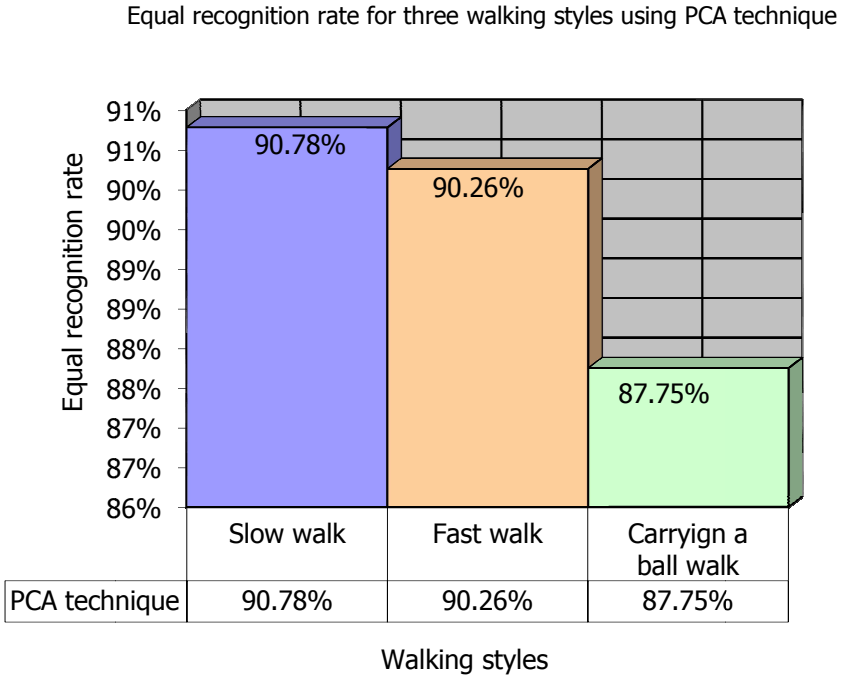

Figure 6.4: Equal Recognition Rate for three walking styles using PCA techniques

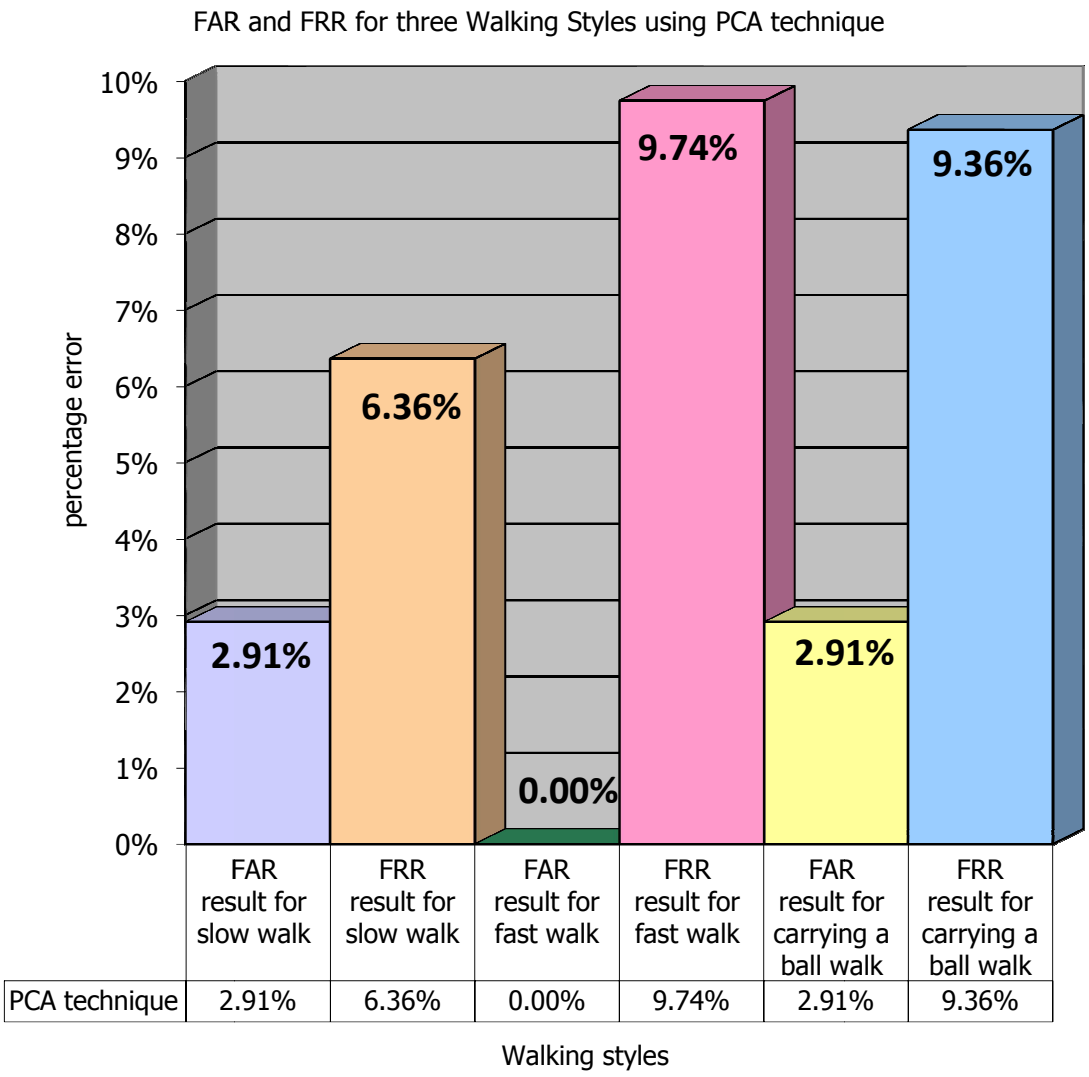

Figure 6.5: FAR and FRR for three walking styles using PCA techniques

Figure 6.5 shows the FAR and FRR results using PCA-only method. The FAR and FRR are dependent on the achieved recognition results and fixed threshold values. According to the slow walk, fast walk, and carrying-a-ball walk of ERR (shown in Figure 6.1 to 6.3), the slow walking styles attained 2.91% FAR and 6.36% FRR, while recognition rate attained was 90.78%. The fast walking styles obtained 0.00% FAR and 9.74% FRR, when recognition rate was 90.26%. Finally, carrying-a-ball walking styles acquired

2.91% FAR and 9.36% FRR, whereas recognition rate attained was 87.75%. By summing up all three, namely, equal recognition rates, FAR, and FRR, then a 100% match up with the system rates is obtained. Figure 6.6 shows output of the correct matching displaying the matching frames "Test[158]-Train[459]" correctly matching the training dataset frame in same subject. However, the correct frame matching was computed manually.

(a) Slow walking styles

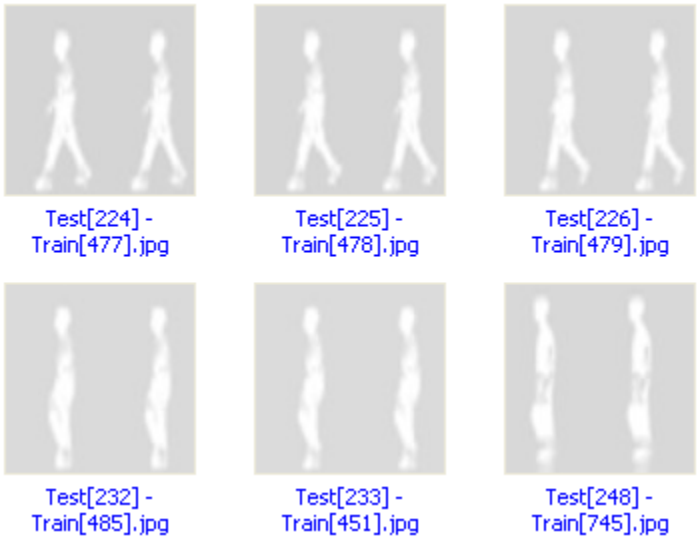

(b) Fast walking styles

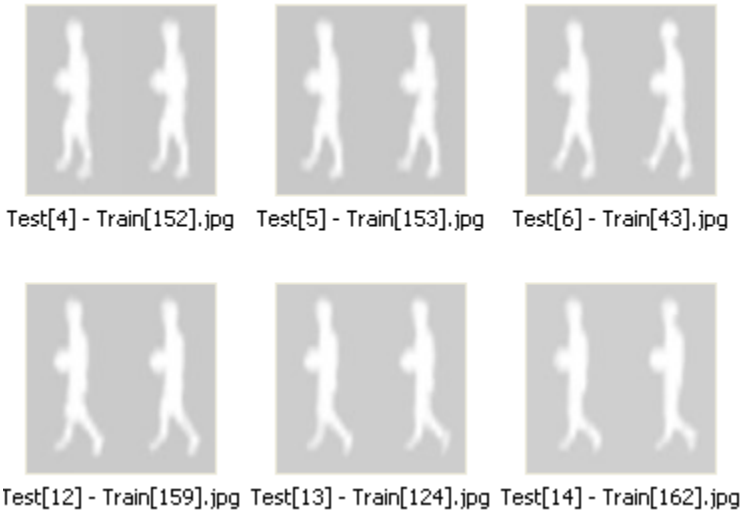

(c) Carrying-a-ball walking styles

Figure 6.6: Sample of output of correct matching frames

6.2.2 GEI as Gait Features

6.2.2.1 Setting the Threshold Tuning Parameter for GEI-based template system

Section 6.5.1 mentioned the purpose of applying tune parameters to the system. The different templates-based system has different threshold values for recall and reject. In this GEI-based templates system using PCA-only technique, different TCPARA values for each walking system were obtained as shown in Figure 6.7 to Figure 6.9.

After applying the PCA-only method on GEI templates for the three walking styles, three different ERR, namely, 91.62%, 90.90% and 92.34% were achieved as shown in Figure 6.10. The fixed threshold values obtained were 6.31, 6.60 and 10.12. It was mentioned earlier that if TCPARA value is decreasing, then recognition rate increases, with 95% of

recognition rates achieved from slow and fast walk. However, above 90% recognition rate is achieved for carrying-a-ball walk.

The carrying-a-ball walking styles represented better recognition rates compared to slow and fast walking styles. Moreover, each walking styles rejection rates may be calculated according to equal recognition rates. From the three walking styles, it was observed that carrying-a-ball walking styles represented better ERR compared to slow and fast walking styles. However, the slow walking styles achieved slightly better ERR than fast walking styles. The fast walking style attained lower ERR than slow walking style and carrying-a-ball walking styles. Therefore, the three walking styles presented three different results.

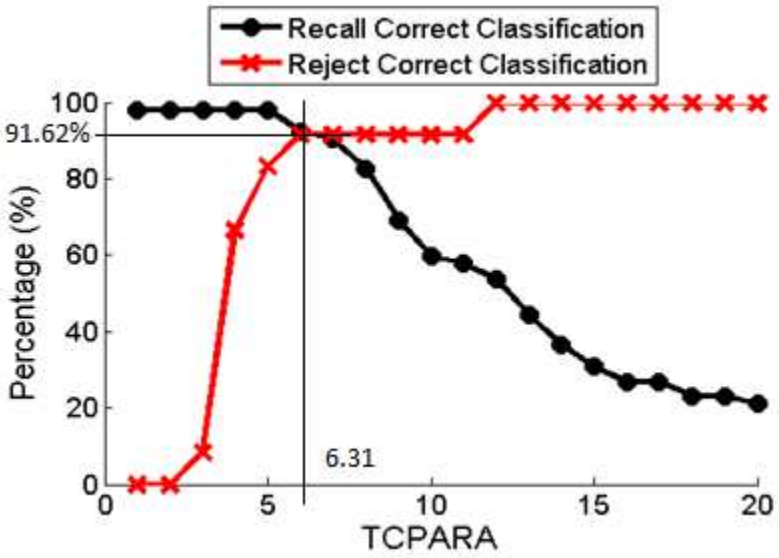

Figure 6.7: Recognition result using PCA-only for slow walk

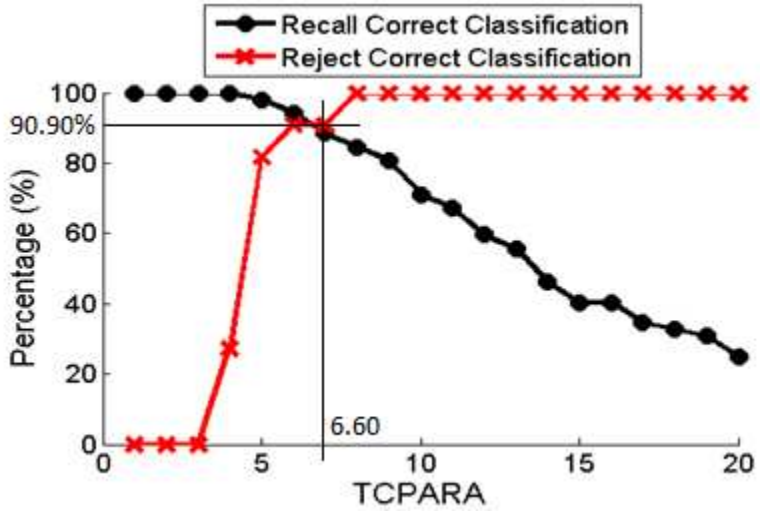

Figure 6.8: Recognition result using PCA-only for fast walk

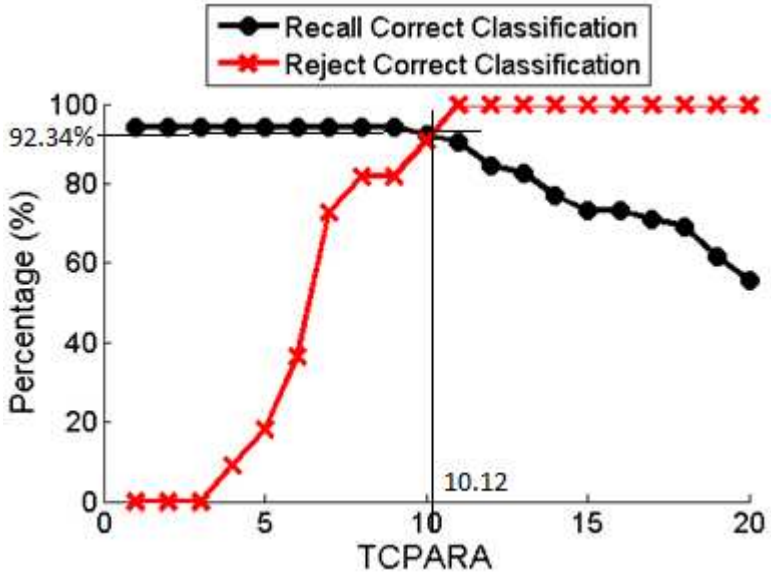

Figure 6.9: Recognition result using PCA-only for carrying-a-ball walk

6.2.2.2 Results and discussion

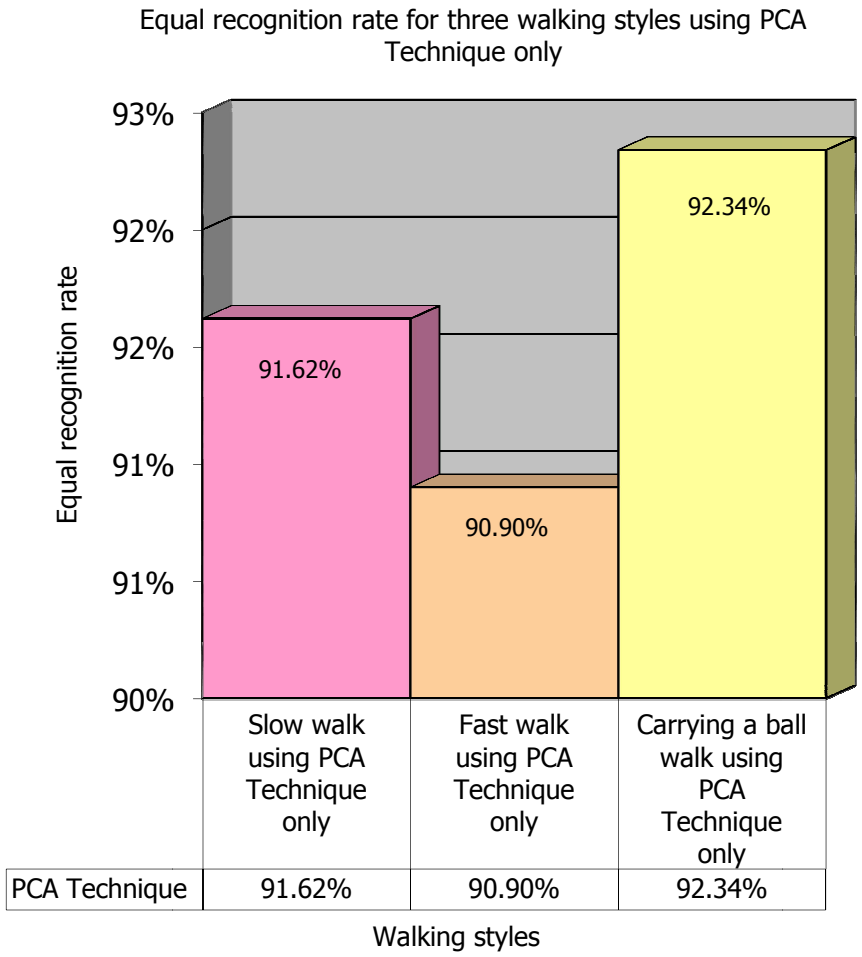

Figure 6.10: Equal recognition rates for three walking styles using PCA-only

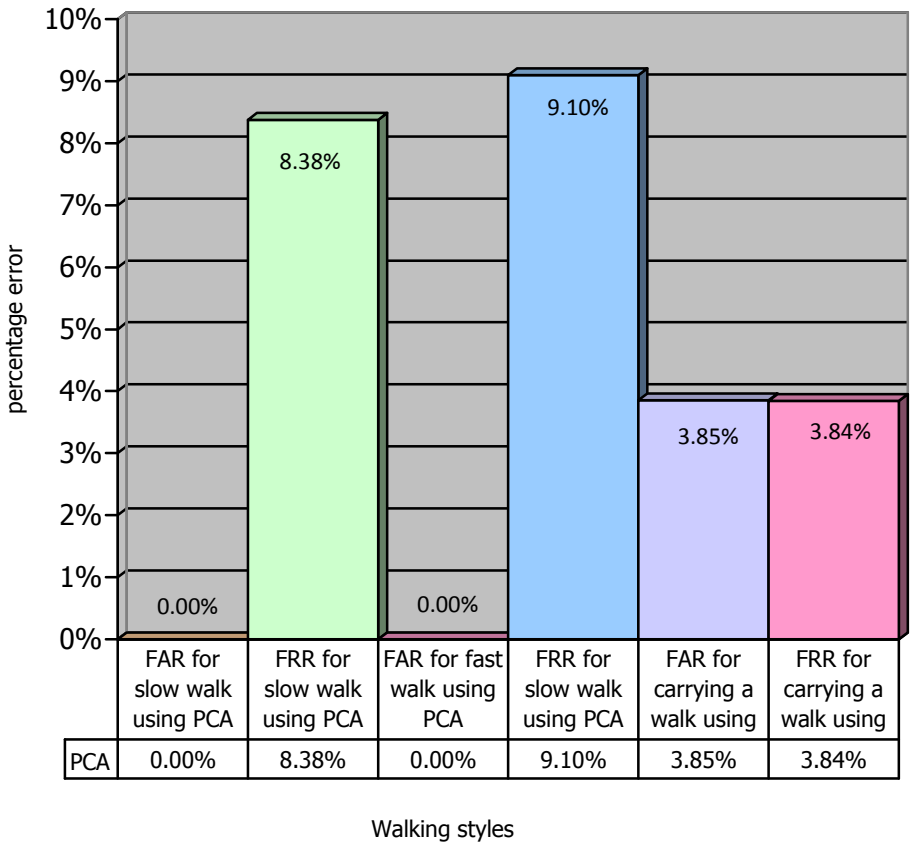

Figure 6.11: FAR and FRR for three walking styles using PCA-only

Figure 6.11 shows the FAR and FRR results using PCA method. The FAR and FRR are dependent on the achieved recognition result and fixed threshold values. According to the slow walk, fast walk, and carrying-a-ball walk of ERR (Figure 6.7 to Figure 6.9), the slow walk attained 0% FAR and 8.38% FRR, while recognition rate was 91.62%. The fast walk obtained 0.00% FAR and 9.10% FRR, when recognition rates were 90.90%. Lastly, carrying-a-ball walk acquired 1.92% FAR and 13.46% FRR, whereas recognition rate attained was 90.38%. When all three equal recognition rates, FAR and FRR were summed up, then a 100% match up with the system recognition rates are obtained.

Figure 6.12 shows output of the correct matching frames. It displays the matching frames "Test[9]-Train[29]" correctly matching training dataset frames.

(a) Slow walking styles

(b) Fast walking styles

(c) Carrying-a-ball walking styles

Figure 6.12: Sample of GEI output of the correct matching frames using PCA-only; (a) slow walking styles, (b) fast walking styles, and (c) carrying-a-ball walking styles

6.3 A Comparison of Recognition Rates between Silhouettes and GEI Templates

6.3.1 Using PCA with Radon Transform

For this project, the CMU MoBo gait database was selected from various available databases. This database is suitable for application in the experiment because it contains different types of walking styles database. The existing gait databases also have different available gait styles. The main reason CMU MoBo database was selected is because it can be downloaded from the website provided freely by Ralphs and Gross (2001). The selected database provides silhouettes and video sequences extracts used in this project.

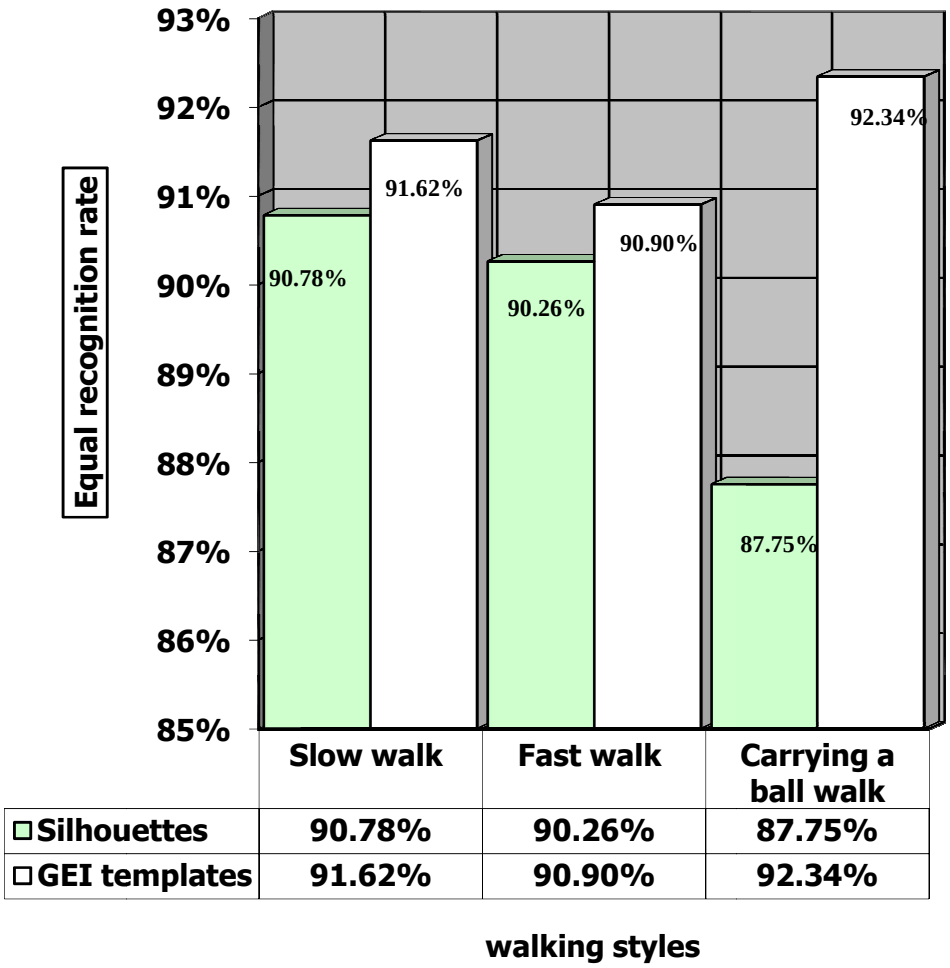

Figure 6.13: A comparison of recognition rates between silhouettes- and GEI template-based system using PCA only technique

Figure 6.13 shows the comparison between silhouettes- and GEI template-based systems using PCA-only technique. For slow walking styles, GEI template-based system obtained ERR that is slightly better than silhouettes-based system using PCA-only technique. For fast walking styles, GEI template-based system achieved approximately 0.5% more ERR than silhouettes-based system using PCA-only technique. However, for carrying-a-ball walking styles, GEI template system yield higher ERR than silhouettes-

based system using PCA-only technique. The GEI-based system achieved approximately 4.54% better result for carrying-a-ball walking styles compared to silhouettes-based system using PCA-only technique. In this PCA-only technique, carrying-a-ball walking styles presented better equal recognition result based on GEI template-based system, and fast walking styles presented slightly lower ERR based on GEI templates systems. The most significant ERR difference was achieved from carrying-a-ball walking styles based on GEI templates using PCA-only technique.

For the silhouettes-based system, slow walking styles presented slightly better result than fast walking style, but significantly different than carrying-a-ball walking styles. However, it was reported that slow and fast walking styles gave almost identical results. The low ERR is obtained from carrying-a-ball walking styles. Thus, slow walking styles ~~is~~ provide better result compared to fast and carrying-a-ball walking styles on silhouettes-based system using PCA-only technique. It can be concluded that GEI template-based systems gave better results on all three walking styles compared to silhouettes-based system using PCA-only technique.

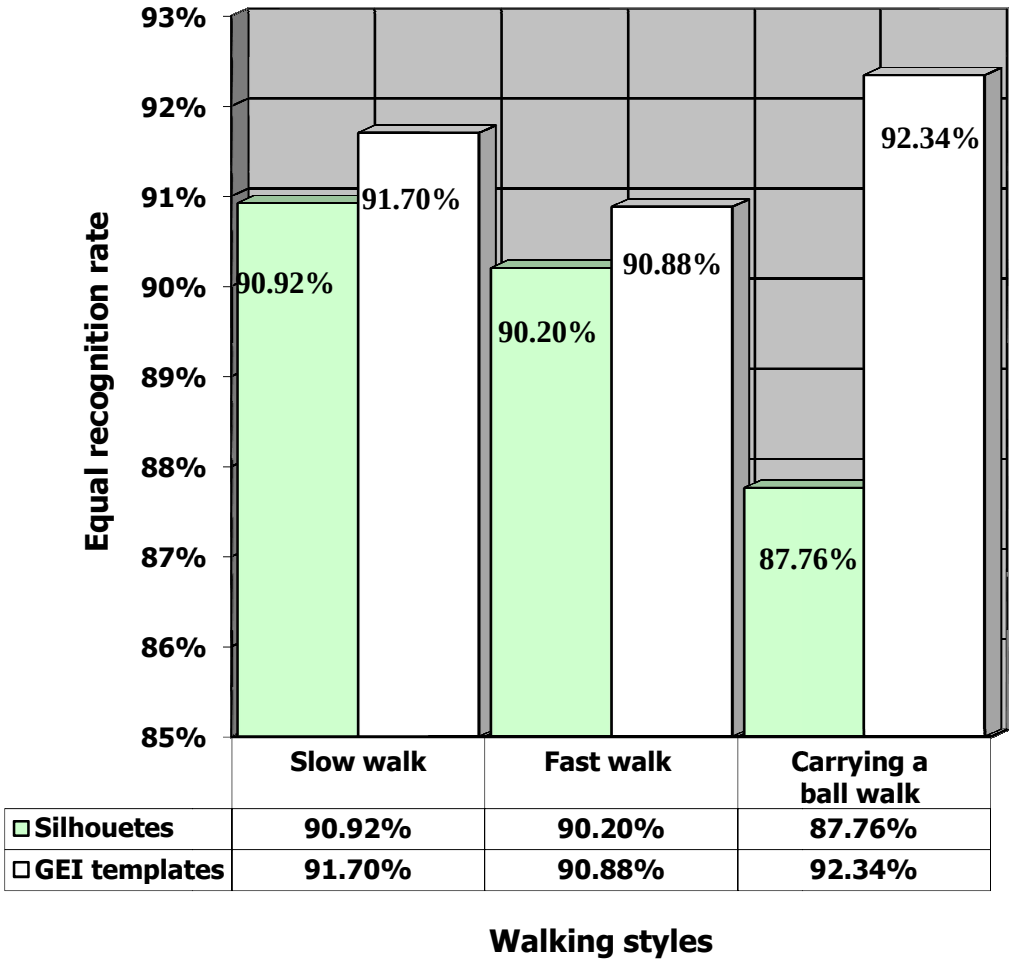

Figure 6.14: A comparison of recognition rate between silhouettes and GEI templates using PCA with RT technique

Figure 6.14 shows a comparison of recognition rates between silhouettes- and GEI template-based systems using PCA with RT technique. For slow and fast walking styles, the GEI template-based system presented significantly better ERR than silhouettes-based system using PCA with RT technique. However, for carrying-a-ball walking styles, GEI template-based system obtained significantly better ERR compared to silhouettes-

based system using PCA with RT technique. In addition, it was reported that slow walking styles presented better recognition rate for both template-based systems using PCA with RT technique. The slightly lower ERR were obtained from fast walking styles based on both template systems using PCA with RT technique. In conclusion, the GEI template-based system obtained better result than silhouettes-based system using PCA with RT technique. The silhouettes-based systems always yield lower ERR for PCA with RT technique on all three walking styles: slow walk, fast walk, and carrying-a-ball walk respectively.

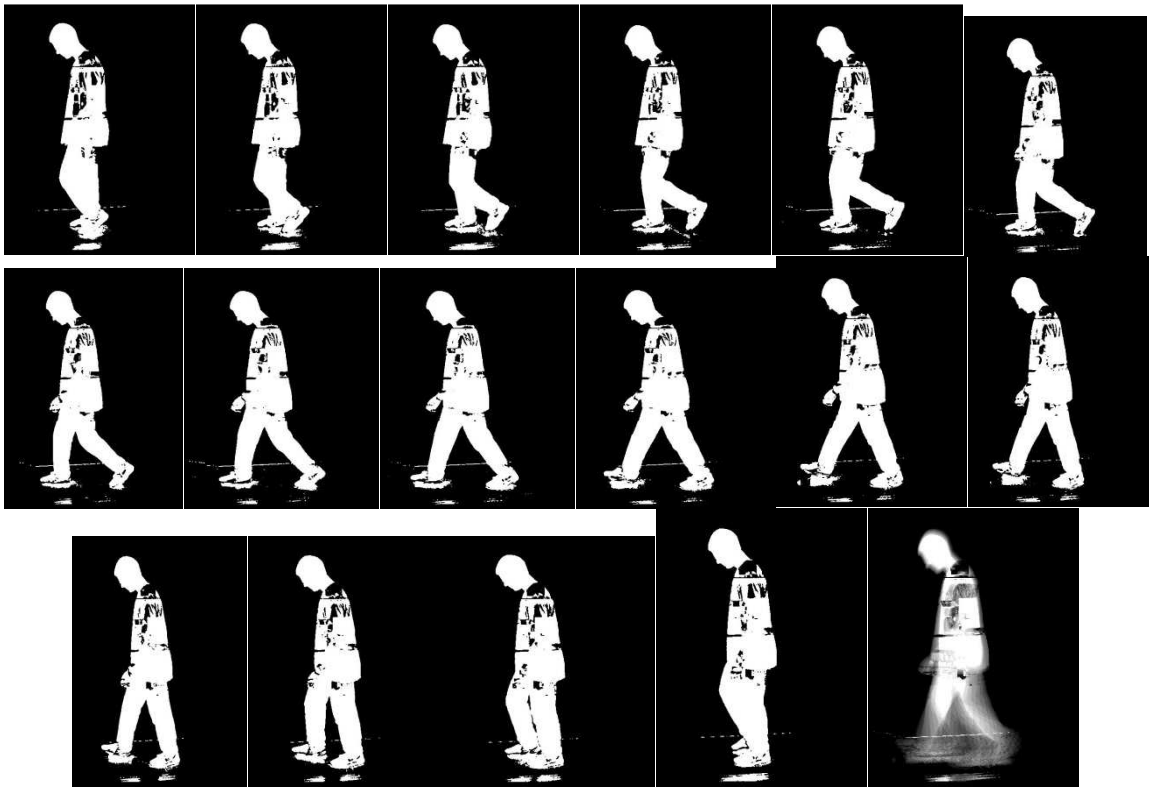

Figure 6.15: Sample of one gait cycle and a GEI template

The GEI templates were prepared to compare the experimental results with silhouettes-based system. GEI is defined as the average frame over one gait cycle. Figure 6.15 shows the sample of one gait cycle which were used to construct GEI templates as shown at the last row right-most frame. Figure 6.16 shows two different conditions of GEI templates where the head, torso and other upper body parts moved very little during walking. It can be verified that the pixels with high intensity values in a GEI template mean indicate that the body parts moved little, while the lower body parts of legs, hands and other lower body parts moved frequently with low intensity values. In addition, GEI template contains information of lower body parts on how people move during walking. Therefore the covariance conditions can be detected and analysed from GEI templates according to body shape changes.

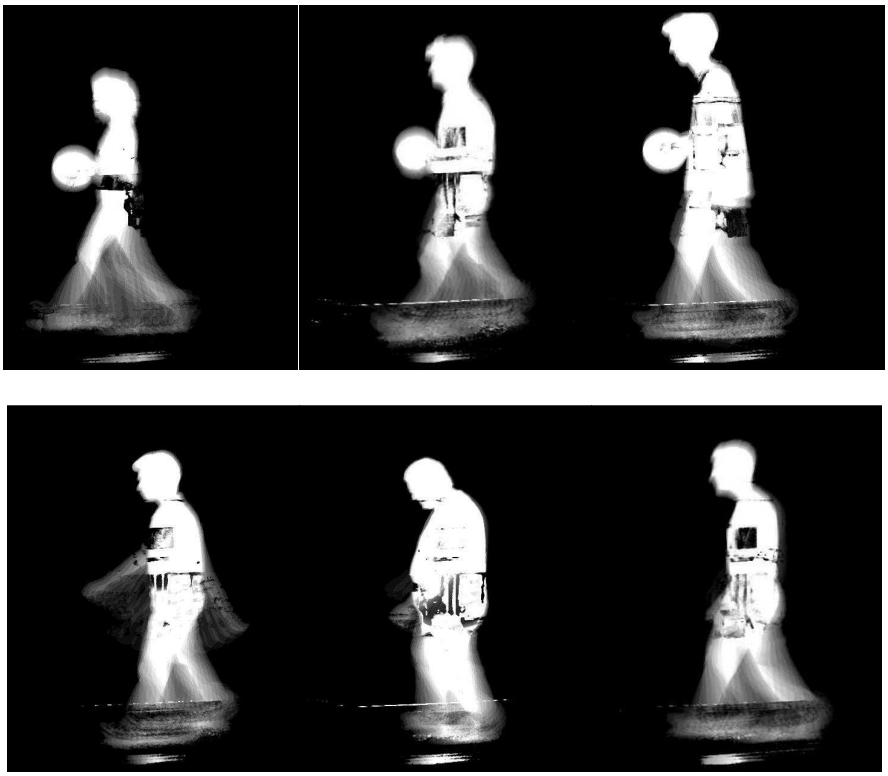

Figure 6.16: Sample of two different conditions of GEI templates

The most informative part of the GEI is the dynamic areas that caused the common covariance conditions during a walk. The common covariance conditions, such as carrying tools and clothings, of human appearance changes during a walk. The static areas also retained valuable information for classification, but are sensitive to changes in various covariance conditions. Basically, it contains body shape information, thus allowing person identification from dynamic areas of the GEI template.

Investigations revealed that the GEI template-based system obtained the best ERR because every single frame has different number of pixel values over a complete gait cycle. The next gait cycle also yield another GEI template and so on. The researchers noticed that each GEI template has approximately the same number of pixels. However, each particular frame pixel over one gait cycle may not have the same particular numbers of frame and pixel values as the next gait cycle and so on. Nevertheless, the average pixels over one gait cycle may have approximately the same number of pixel values as the next GEI pixel values. Thus, this is the main advantage for applying GEI template-based system to obtain the highest accuracy recognition rate. In conclusion, the GEI template-based system achieved better result than silhouettes-based system using PCA with RT technique.

6.4 Performance Comparison between PCA With and Without RT using Silhouettes and GEI Templates

6.4.1 Principal Component Analysis (PCA)

Ling *et al.* (2009) presented spatio-temporal for gait recognition. At first Hough Transformed templates were constructed over one gait cycle for the experiment. The Laplacian of Gaussian technique was applied to detect edges of silhouettes gait intensity and then mapped it between the image space and accumulator space. Secondly, the commonly-used PCA technique was applied to reduce the dimension of the images without much loss of information. The obtained results were compared with other proposed results, and the proposed system achieved efficient result. For the experiment, CASIA gait database was used for recognition purposes.

Qiong *et al.* (2009) proposed PCA and LDA methods for recognition systems. The PCA technique was used to reduce the dimension of the image, while the LDA technique was used to perform optimisation of the pattern class. The Euclidean distance and correlation were applied for measuring purposes. For the experiment, FERET database was applied for evaluation, and reported that PCA with LDA techniques obtained more efficient result than PCA-only technique.

Su and Qian (2010) proposed Fuzzy PCA (FPCA) algorithms to GEI templates. At first gait video sequences over gait cycle were processed and GEI images constructed. GEI produced one image with an average of one gait cycle. However, eigenvalues and eigenvectors were constructed using FPCA and the obtained eigenvectors were expected

into lower aspect space. For the feature classifier, the NN classifier was used for the experiment. CASIA gait database was applied and stated that FPCA achieved more efficient result compared to using PCA with RT technique, KPCA and PCA-only techniques.

Murat (2006) analysed multiple projection systems for gait recognition using common PCA technique. At first, the distance vector was produced. It is defined as the difference between bounding box and outer contour of silhouettes. The four projections presented four 1-D signals which is the value of distant vector. The normalised gait cycle performed auto correlation to obtain smooth gait cycle. Secondly, eigenspace conversion based on PCA technique is useful to time various distant vectors, and the statistical distance-based supervised model categorisation is then completed in the lower dimensional eigenspace for person detection. Lastly, the final decision was produced by fusion strategy and achieved an efficient result.

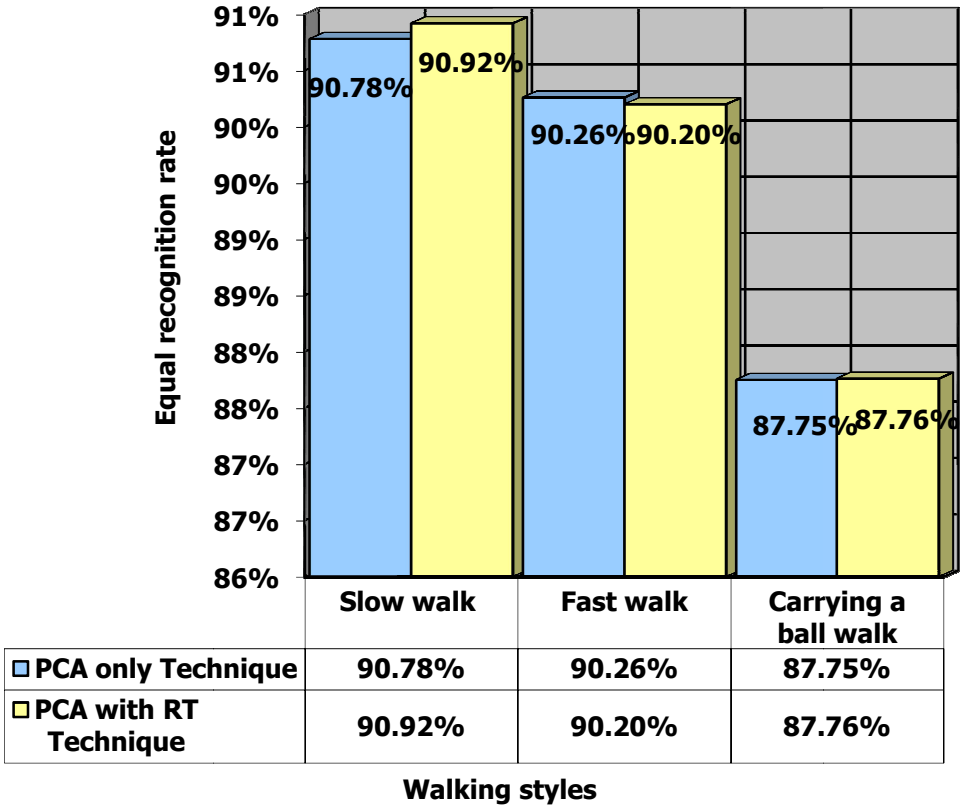

Figure 6.17: Performance comparison between PCA technique and PCA with RT technique using silhouettes

Figure 6.17 shows the performance comparison between PCA with and without RT techniques using silhouettes-based system. For all three walking styles based on silhouettes, PCA with and without RT techniques were applied for experimentation. When applying silhouettes-based system, PCA with and without RT techniques presented identical ERR. The reason for obtaining identical ERR is that the testing frame is compared to large number of training frames to match up similar frame. However, variations of each frame pixels are not significant over a complete gait cycle. When the first frame of one gait cycle is compared to first frame of next gait cycle, then it is clear

that pixel variations is negligible. Moreover, if a testing frame does not find similar amount of pixels frame from next gait cycle, then it continue searching the next gait cycle to find similar match up frames. Each testing frame is compared with all training dataset only once. Moreover, the silhouettes normalisation is also an important point to achieve high accuracy results.

On silhouettes-based system, the slow walking style presented the best identical ERR compared to fast and carrying-a-ball walking styles using PCA with and without RT techniques. More number of frames were obtained from a complete gait cycle based on slow walking styles. Thus, the difference for each frame size to each other is very small compared to fast walking styles. There is a very high possibility of getting similar match up frames and achieve high ERR.

Fast walking styles has the second highest ERR. When the subject's walking speed is fast, then it is possible to change the initial walking direction and speed. The walking direction may change on each gait cycle. In this case, the fast walking styles has provided a slightly lower ERR than slow walking styles.

Carrying-a-ball walking styles presented worse ERR than slow and fast walking styles. When a person is carrying a ball during walking, then the walking direction will change rapidly. It is necessary to adjust the body balance while the subject is carrying some things on the hand or on the body. The walking direction may change quickly on each gait cycle. This is the case for obtaining low ERR. It was also proven that when a subject

is carrying extra belongings during walking, then gait recognition will vary depending on each person.

However, some of the frame pixel values are excessive, and therefore similar match up frames cannot be obtained. Thus, when a subject's walking direction changed even very slightly, then recognition rates will also change accordingly.

In this case, efficient ERR was achieved from these experiments. Many researchers obtained high correct classification of recognition rates in different arrangements of gait database and features. In this silhouettes-based system, the computational time is longer and required higher memory space to run the system.

Performing recognition in a high dimensional space can significantly diminish the efficiency of system performance. Principal Component Analysis (PCA) is widely utilised to reduce the dimensionality of the data. The goal of PCA is to reduce the dimensionality of the data while retaining as much as possible of the variations present in the original dataset. PCA allows us to compute a linear transformation that maps data from a high dimensional space to a lower dimensional space.

6.4.2 Principal Component Analysis (PCA) with Radon Transform (RT)

Tanaya and Rabab (2010) proposed the use of Different Radon Transform (DiffRT) in gait feature extractions for gait recognition purposes. They were applied to differential RT (DiffRT) to extract high frequency features information. At first, the average silhouettes made and applied DiffRT to extract average silhouettes features. For the

experiment, USF gait database was applied and achieved efficient result. The proposed method was also compared with other methods and it performed better.

Nikolaos and Zhiwei (2007) and Hao and Zhijing (2007) proposed to analyse gait feature extraction using Radon Transform (RT) and Linear Discriminant Analysis (LDA). The silhouettes were aligned at the centre using Radon Transform technique. The silhouette alignment is important as transform image information from centre of the silhouettes. For the experiment, USF gait database was used. A few other gait databases were used for the experiment, but the proposed method greatly improved recognition rates compared to other databases. The Radon Transform was also applied for gender recognition and achieved a resourceful result (Lei *et al.*, 2009).

Jia *et al.* (2009) analysed and described human shape features. The connected chips linking (CCPL) and mean-shift estimation were used to extract contour pixels of the targets. The contour features were transformed into normalised Radon matrixes. The main target is to identify whether that input frames are normal human motion or aggressive human motion. The AdaBoost algorithm was applied to classify normal or aggressive motion. The proposed method was efficient for analysing gait motion. Chatana *et al.* (2010) used RT for human identification based on Electrocardiogram (ECG) and achieved best accuracy result.

GEI-based gait recognition system is one of the most powerful system for obtaining high recognition rates. GEI template is the average template over one gait cycle. After performing GEI templates to the experiment, high recognition rates were achieved

compared to silhouettes-based system as shown in Figure 6.18. Different recognition rates were obtained in different walking styles using PCA with and without RT techniques based on GEI templates system. For the slow walking styles, PCA with RT technique presents considerably better result than PCA-only technique. The fast walking styles shows identical recognition rates for both techniques. For carrying-a-ball walking styles, PCA with RT technique also shows identical results.

In addition, slow walking styles presented better result compared to fast walking styles for both techniques. The slightly low recognition rate was obtained from fast waking styles than slow walking styles for both techniques, and carrying-a-ball walking styles presented appreciably better results compared to fast and slow walking styles. Slow walking styles and carrying-a-ball walking styles yield significantly higher recognition rates than fast walking styles.

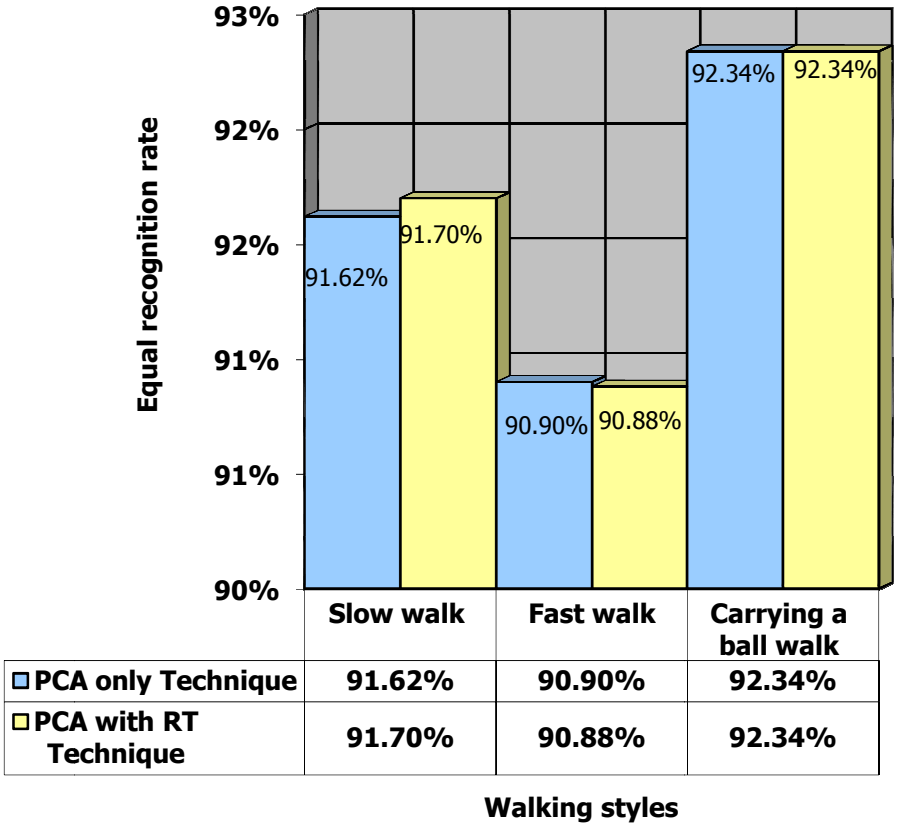

Figure 6.18: Performance comparison between PCA with and without RT techniques using GEI templates

GEI template-based system achieved better recognition rate compared to silhouettes-based system using PCA with and without RT techniques. The purpose of using GEI-based system is that it contains average information over one gait cycle. However, the specific frame-value may not be the same as the next-cycle-similar-frame-value over one gait cycle, but in the end, the average-cycle-frame-value is approximately the same. This is the most important advantage for applying GEI templates to obtain best accuracy recognition rate. Thus, the ERR achieved a little better on GEI templates than silhouettes-based system. The fast walking styles on GEI-based system also obtained

slightly better result than silhouettes-based system. However, the carrying-a-ball walking styles attained significantly better results compared to silhouettes-based system. The silhouettes-based frames were excessive causing low recognition rate acquisition, but when silhouettes were converted to GEI templates, then it achieved high recognition rate. Here, GEI templates training and testing dataset is limited in numbers to match up the testing frame from training dataset. However, a small number of the frame changes made significant difference the recognition rate percentage.

The GEI templates shape is different from silhouettes shape, which means that pixel values in ~~the~~ silhouettes and GEI templates are different. In addition, GEI template presents variable covariance conditions to identify how person moves during walking.

The Radon Transform is especially appropriate for gait representation and recognition. When people walk, naturally the large angular variations occur in legs and arms with respect to the horizontal axis. It means that the Radon Transform is measured from the centre of the silhouettes. Each angle energy of the original silhouettes will come out in precise coefficients that vary considerably through time. Thus, Radon coefficients are very important for identifying the subject's shape and walking styles. However, Radon calculates with respect to the silhouettes translating invariance and easy to calculate. Moreover, each Radon coefficient comprises contributions from several pixels, thus it is less risky to variations due to false noisy pixels on the original silhouettes.

The projection of the image intensified along a radial line oriented at a specific angle. The RT mapping is from the Cartesian coordinates (x, y) to Polar coordinates (distance

and angel). Although PCA with and without RT techniques gave almost identical recognition rates, the matched frames are different for both silhouettes- and GEI-based systems. Thus, PCA applied on Radon Transform feature does not increase recognition rates. Radon transform is not helping significantly on normalise-frontal image. It was applied to verify improvement gains when applied on normalised frontal image. The RT probably has some small rotational effects on the image that is unseen to the naked eyes.

6.4.3 Comparison of Recognition Results with other Researchers Results

In order to test flexibility of walking styles, the researchers displayed the proposed algorithm on CMU database to compare with other researchers algorithms based on silhouettes systems. Table 6.1 shows the comparison of gait recognition rate with other researchers. It can also be seen from Table 6.1 that the recognition performances of proposed methods are superior to Amit, Zhang and Bo and Youmei algorithms in different walking styles conditions. For the slow walking styles, the proposed methods recognition rate is worse than Zhang and Daoliang's algorithms, but superior than Amit's algorithms. However, the proposed method's result is slightly better than Bo and Youmei's algorithms. For fast walking styles, the result achieved is superior than Amit, Zhang, and Bo and Youmei algorithms, but equal results were obtained with Daoliang's algorithms. Finally, for carrying-a-ball walking styles, the obtained recognition result is slightly lower than Amit's algorithm, but Zhang's algorithms achieved superior results. However, Bo and Youmei and Daoliang achieved better results than the proposed method in carrying-a-ball walking styles.

Amit *et al.* (2003) used half of the gait cycles for testing and another half for training. However, the Hidden Markov Model (HMM) technique was applied to the experiment. The highest result displayed was 91% on ball walking styles. The cumulative match score system was applied to display the experimental result and achieved 91% correct classification rate (CRR) in the top three matches on same walking styles (ball vs ball). Zhang *et al.* (2004) also followed Amit's technique, but different gait dataset were set. Four gait cycles for training and one for testing were applied. However, the experimental result displayed ~~of~~ cumulative match score system and achieved 100% (CCR) recognition rate on slow walking styles and carrying-a-ball walking styles, which is better than Amit and Bo and Youmei's technique. Bo and Yumei (2006) applied PCA with and without LDA for recognition purposes. They followed Amit *et al.* (2003) and Zhang *et al*. (2004) database settings and adapted the walking speed for comparison. A 96% recognition rate was found which is very close to Zhang's algorithm, but superior to Amit's algorithm. Daoliang *et al*. (2007) applied PCA technique based on GEI gait templates, which is the same as one of the proposed techniques, but gait database was set differently from Daoliang's algorithm. They set half of the gait cycles for training and another half for testing. Daoliang *et al.*(2007) obtained better result than the proposed system under different conditions.

A low recognition rate was received from carrying-a-ball walking styles. The first ten gait cycles for training and next four for testing were taken. However, the last four cycles may not be the same as first ten cycle's walking styles directions, walking speed or body movement to adjust balance for carrying additional stuffs. This may cause low recognition acquisition rate for carrying-a-ball walking styles.

The recognition rate depends on the size of the database. Thus, the proposed gait dataset is different from others and obtained different results. The above-mentioned authors used known gait dataset only, but did not compare it with unknown dataset. If known and unknown gait database is set, then it may change the percentage of the recognition rate. This rate will reduce if the system has found similar matching frame from any one unknown dataset. The researcher tested with unknown dataset and found similar frames from unknown dataset by proposed system. This is the cause of low recognition acquisition rate. When the recalls correct classification is equal to reject correct classification, it is called ERR. Therefore, the average recognition rate achieved comparatively low recognition rate than other researchers (Table 2). The proposed methods focused on ERR to compare with other systems.

From Table 6.1, the proposed technique showed that slow and fast walking styles obtained different recognition results than each other, but carrying-a-ball walking styles obtained low recognition rates than slow and fast walking styles. The fast walking styles gave 100% recognition rate only. This suggests that for reasons of low recognition, certain parts of the body may not be efficient than others. In particular~~ly~~, the motion of the legs and hands may not adjust in the same manner as slow or fast walking styles in every gait stride. It may rapidly change from frame to frame. Thus, the walking directions may change to adjust the control of the body for carrying-a-ball. Therefore, walking conditions are not stable while carrying-a-ball during a walk. It can be reported that the proposed algorithm demonstrated good recognition rates for slow and fast

walking styles. The carrying-a-ball walking styles achieved slightly low recognition rates compared to other results.

TABLE 6.1: Comparison based on CMU database

Train vs Test	Amit *et al.* (2003)	Zhang *et al.* (2004)	Bo and Youmei (2006)	Daoliang *et al.* (2007)	Proposed method (silhouette based system)	Proposed method (silhouette based system)	Proposed method (GEI based system)
Slow vs slow	72% (CCR)	100% (CCR)	96% (CCR)	**100% (CCR)**	**96.37% (CCR)**	**90.78% (ERR)**	**98.07% (CCR)**
Fast vs fast	68% (CCR)	96% (CCR)	96% (CCR)	**100% (CCR)**	**100% (CCR)**	**90.26% (ERR)**	**100% (CCR)**
Ball vs ball	91% (CCR)	100% (CCR)	96% (CCR)	**96% (CCR)**	**89.62% (CCR)**	**87.75% (ERR)**	**94.23% (CCR)**

6.4.4 Computational Cost

Both PCA with and without RT techniques require longer system time to compute using silhouettes-based system. Since silhouettes take up more space as it contains larger number of training and testing frames, thus silhouettes-based system require larger memory to read the system for PCA with and without RT techniques. However, if GEI template-based systems were used for PCA with and without RT techniques, then the system will run very fast as it takes up low space and low memory to read the system. The computation time is very limited and efficient for GEI template-based system. Thus,

the system's computational time is dependent on the size of the known and unknown datasets.

The approximate computational time is designated in Table 6.2 for slow walking styles recognition system. GEI template-based system is much more computationally efficient than silhouettes-based system using PCA with and without RT techniques. The results were obtained by using a platform with an Intel Dual Core 1.98 GHz CPU and 3.24 GB memory.

Table 6.2: Comparison of the computational time of silhouettes and GEI template-based system for recognising based on proposed gait dataset

Computational cost	**Silhouette-based system (sec)**	**GEI-based system (sec)**
PCA with RT technique	20226	52
PCA only technique	19620	50

It was suggested that this project use GEI template-based system using PCA-only technique to get the desired output from the system.

The advantage of the gait recognition is its biometric features. These biometric features can be reliably captured from a great distance. Moreover, it does not require user cooperation for gait recognition. It is very difficult to recognise a subject if the subjects are almost the same size (width and height). If subject's body figure is changed from big size to slim size, or slim size to big size, then it becomes complicated to recognise

the subject. Abnormal walking styles also give rise to complexities in identifying person. If we are able to make 100% reliable gait recognition system in any situations or environments, then the subject need not ~~to~~ carry any materials to identify subjects and research will go on.

6.5 Conclusion

The comparison of recognition rates between PCA with and without RT techniques based on silhouettes and GEI templates system were described. The comparison between silhouettes and GEI templates system were also described in detail. The reasons of using both PCA with and without RT techniques based on silhouettes and GEI templates comparisons were also stated, even though it has been reported that the PCA-only method based on GEI template is the best for the system. The best equal recognition result was 92.30% using PCA with and without RT techniques based on GEI templates for carrying-a-ball walking styles. Finally, PCA-only technique presented efficient result based on GEI templates.

CHAPTER 7

CONCLUSION

7.1 Overview of Friction, Slips and Falls

Friction slips and falls survey describes briefly. The three walking styles have compared with slips and fall during walk on treadmill. The survey found that under normal surface condition, slow walk is safer compared to fast and carrying a load walk.

7.2 Gait Features

The CMU MoBo gait database was selected for this research. The selected gait database contains 25 subjects with four types of walking styles. The silhouettes extraction methods were briefly explained in Chapter 2. The provided silhouettes were selected for the research. After that, the database was rearranged to suit the experiment.

Two datasets were prepared, namely, known dataset and unknown dataset. The known dataset (13 subjects) was divided into two sets, namely, training dataset and testing dataset. Twelve subjects were selected for unknown dataset. Fourteen cycles were selected for the experiments where 10 cycles were used for training and four cycles for testing. Each gait cycle contains approximately 18-20 frames. The training dataset consists of 6,729 frames, which were selected from CMU MoBo database. Similarly, the 2,714 frames for the test dataset were selected from same database. These frames were selected based on subjects walking styles.

Next, the Gait Energy Image (GEI) was constructed to compare recognition rates with silhouettes-based system. GEI was made by average of one complete gait cycle. The GEI template dataset was rearranged from silhouettes dataset. The training dataset consist of 130 templates, which were selected from subject gait cycles. The 52 GEI templates in the test dataset were also chosen from the same subject gait cycles. The 12 GEI templates dataset were preferred for unknown dataset.

7.3 Principal Component Analysis (PCA) Techniques

The basic concept of PCA method was described briefly to be used for the experiment. The PCA technique was proposed to obtain the recognition rates. The proposed method was used to reduce the dimension of the images for experiment. The PCA method was applied for two features that are silhouettes- and GEI template-based systems. Both feature techniques presented acceptable recognition rates. The GEI template-based system was found with better recognition rates than silhouettes-based system.

7.4 Principal Component Analysis (PCA) with Radon Transform (RT) Technique

The fundamental concept of PCA-only and PCA with RT methods were briefly explained for use in the research. The Radon Transform was applied to verify if there is any improvement when applied on normalised frontal image, since the RT probably has some small rotational effects on the image that are hard to see with the naked eyes. Although PCA with and without RT gave almost the same recognition rates, the matched frames are different for both silhouettes- and GEI-based systems. Thus, PCA applied on

Radon Transform features does not increase recognition rates. Radon Transform is not contributing significantly on normalise-frontal images. The PCA with RT technique was also proposed for this research which was applied to calculate each angle of silhouettes and transform to formulate feature vector. The RT output was passed through PCA to reduce the dimension of the frames for conducting test. This technique was applied to silhouettes- and GEI template-based systems to compare the recognition rates. The recognition results were presented in that section.

7.5 Analysis and Discussion

Two methods were proposed and investigated. The first technique proposed to reduce the dimension of the frames and performed the experiment. The second technique proposed to transform data to lie on co-efficient template and passed through PCA to reduce the dimension for the experiment. Both proposed techniques were applied for recognition purposes. A comparison of recognition rates was presented between silhouettes and GEI templates using PCA with and without RT techniques. However, performance comparison were presented between PCA with and without RT techniques, based on silhouettes and GEI templates. The advantages of GEI template-based system were briefly described. In addition, the computational cost was also explained. The obtained recognition rates were compared with other researchers. As a result, the PCA with RT technique achieved 92.34% recognition rate using GEI template-based system in this research.

The experiments were tested with known and unknown datasets, and threshold tuning parameters can be used to tune the system performance to suite an application. GEI

template-based system presented more efficient result than silhouettes-based system using PCA with and without RT techniques. Although PCA with and without RT gave almost identical recognition rates, the matched frames are different for both silhouettes- and GEI-based systems. The GEI template-based system on PCA-only technique is better for the system because of shorter system run time and low memory. Thus, the three walking styles gave more efficient results based on the proposed techniques.

7.6 Future Works

Although the PCA with and without RT techniques output has shown an improvement for gait recognition systems, it is necessary to perform the experiment with different walking styles under different conditions (slow vs fast, fast vs ball, and so on) for comparison. It is also important to verify the recognition rates using different gait databases under the proposed methods.

The proposed gait recognition techniques necessitate performing with similar sized subjects such as height, width, size of the body and verifying the recognition rate accuracy with known and unknown datasets. However, the current techniques can be tested with different walking styles on training and testing dataset to find the percentage of matching frames using CMU MoBo gait database.

References

Ai-Hua, W. and Ji-Wei, L. 2007. A Gait Recognition Method Based on Positioning Human Body Joints. Wavelet Analysis and Pattern Recognition, ICWAPR, International Conference on, pp: 1067 – 1071.

Amit, K., Aravind, S., Rajagopalan, A. N., Naresh, P. C., Amit K. R., and Rama, C. 2004. Identification of Humans Using Gait. IEEE Transactions on Image Processing, Vol. 13, No. 9, September 2004, pp: 1163-1173.

Andrzej, D. 2007. Biometrics-lecture-part1-2007-09-24". Speech Processing and Biometrics Group Signal Processing Institute, Ecole Polytechnique Federale De Lausanne (EPFL), http://scgwww.epfl.ch/courses

Arun, N., Mandayam, G. and Sreela, S. 2005. Gait Recognition Based on Isoluminance Line and 3D Template Matching. Intelligent Sensing and Information Processing, Proceedings of International Conference on, pp: 156-160.

Bashir, K., Tao, X. and Shaogang, G. 2007. Human Identification Based on Gait Analysis. Proceeding of the IEEE Conference on Control, Automation and Systems, pp: 2234-2237.

Bashir, K., Tao, X. and Shaogang, G. 2008. Feature Selection on Gait Energy for Human Identification. Proceeding of IEEE International Conference on Acoustics, Speech, and Signal Processing, pp: 985-988.

Bo, Y. and Yumei, W. 2006. A New Gait Recognition Method Based on Body Contour. Control, Automation, Robotics and Vision, ICARCV International conference on, pp: 1-6.

Bouchrika, I. and Nixon, M. 2008. Gait Recognition by Dynamic Cues. 19th IEEE International Conference on Pattern Recognition, 2008, Tampa, FLorida, USA, pp: 1-4.

Boulgouris, N.V., Hatzinakos, D. and Plataniotis, K. N. 2005. Gait Recognition: A Challenging Signal Processing Technology for Biometric Identification. Signal Processing Magazine, IEEE, pp: 78-90.

CASIA gait database, online, 2006. Centre for Biometrics and Security Research, CASIA. www.cbsr.ia.ac.cn

Cham, R. and Redfern, M. S. 2001a, Changes in gait biomechanics when anticipating slippery¯oors, Gait and Posture, in press.

Cham, R. and Redfern, M. S. 2001c, Heel contact dynamics during slip events on level and inclined surfaces, Safety Science, in press.

Changhong, C., Jimin, L., Heng, Z., Haibong, H. and Jie, T. 2009. Factorial HMM and Parallel HMM for Gait Recognition. IEEE Transactions on systems, man, and cybernetics -pat c, Applications and reviews, Vol. 39, no.1, pp: 114-123.

Changhong, C., Jimin, L., Heng, Z., Haihong, H. and Jie T. 2009. Frame difference energy image for gait recognition with incomplete silhouettes. Pattern Recognition Letters, Volume 30, Issue 11, 1 August 2009, pp: 977-984.

Changhong, C., Jimin, L., Heng, Z., Haihong, H. and Jie, T. 2009. Frame difference energy image for gait recognition with incomplete silhouettes, Pattern Recognition Letters 30 (2009), pp: 977–984.

Changhong, C., Jimin, L., Heng, Z., Haihong, H. and Jie, T. 2009. Frame difference energy image for gait recognition with incomplete silhouettes, Pattern Recognition Letters 30 (2009), Volume 30, Issue 11, 1 August 2009, pp: 977–984.

Chetana, H., H. Rahul, P., Sagar, D.S., Deepa, S. P., Venugopal, K.R. and Patnaik, L. M. 2010. Human Authentication Based on ECG Waves Using Radon Transform. Security Technology, Disaster Recovery and Business Continuity Communications in Computer and Information Science, 2010, Volume 122, pp: 197-206.

Chien-Wen, C., Wen-Hung, C., Sheng-Huang, L. and You-Yin, C. 2009. A Vision Based Analysis System for Gait Recognition in Patients with Parkinson's Disease. Expert systems with application at Science Direction, pp: 7033-7039.

Chin-Chuan, H., Hsu-Liang, C., Chih-Lung, L. and Kuo-Chin, F. 2003. Personal authentication using palm-print features, Pattern Recognition, 36, pp: 371-381.

Cuntoor, N. K. and Chellappa, A. R. 2003. Combining Multiple Evidences for Gait Recognition. Proceedings, International Conference on Multimedia and Expo, pp: 111- 113.

Dacheng, T., Xuelong, L., Senior, M., Xindong, W. and Stephen, J. M. 2007. General Tensor Discriminate Analysis and Gabor Features for Gait Recognition. IEEE transactions on pattern analysis and machine intelligence, pp: 1700-1715.

Daoliang, T., Kaiqi H., Shiqi Y. and Tieniu T. 2007. Uniprojective Features for Gait Recognition. Advances in Biometrics Lecture Notes in Computer Science, 2007, Volume 4642/2007, pp: 673-682, DOI: 10.1007/978-3-540-74549-5_71.

Davrondzhon, G. and Einar, S. 2009. Gait Recognition Using Wearable Motion Recording Sensors. EURASIP Journal on Advances in Signal Processing Volume, 2009, pp: 1-16.

Davrondzhon, G., Kirsi, H. and Torkjel, S. 2006. Biometric Gait Authentication using Accelerometer Sensor. Proceedings of the 1st IEEE International Conference on Availability, Reliability and Security, pp: 51-59.

Dimosthenis, I., Dimitrios, T., Ioannis, G. D., Savvas, A. and Konstantinos, M. 2007. Gait Recognition Using Compact Feature Extraction Transforms and Depth Information. IEEE Transactions on Information Forensics and Security, VOL. 2, NO. 3, September 2007. pp: 623-630.

Dong, X., Shuicheng, Y., Dacheng, T., Lei, Z. L. and Hong-Jiang X. Z. 2006. Human Gait Recognition with Matrix Representation. IEEE Transactions on Circuits and Systems for Video Technology, Vol. 16, No. 7, July 2006, pp: 896-903.

Dong, X., Shuicheng, Y., Dacheng, T., Stephen, L. and Hong-Jiang, Z. 2007. Marginal Fisher Analysis and Its Variants for Human Gait Recognition and Content Based Image Retrieval. IEEE transaction on image processing, pp: 2811-2821.

Ekinci, M. and Gedikli E. 2005. Gait Recognition Using View Distance Vectors. Springer-Verlag Berlin Heidelberg, CIS 2005, Part I, LNAI 3801, pp. 973–978, 2005.

Fida El Baf, Thierry B. and Bertrand V. 2008. A Fuzzy Approach for Background Subtraction. ICIP 2008, pp: 2648-2651.

Fu, C.Y., Li, P., Wen, Y.M., Yuan, H.J. and Ye, B. 2008. Gait Silhouette Extraction Algorithm Using Gauss Model. Chinese Journal of Sensors and Actuators 21(7) (2008).

Gafurov, D. 2007. A Survey of Biometric Gait Recognition: Approaches, Security and Challenges, NIK-2007 conferences; URL http://www.nik.no/

Gafurov, D., Helkala K. and Soendrol, T. 2006. Gait Recognition Using Acceleration from MEMS. International Conference on Availability, Reliability and Security, ARES, pp: 1-6.

Gafurov, D., Snekkenes, E. and Bours, P. 2007. Gait Authentication and Identification Using Wearable Accelerometer Sensor. IEEE Workshop on Automatic Identification Advanced Technologies, pp: 220-225.

Gang, Q., Jiqing, Z. and Assegid, K. 2008. People identification Using Gait via Floor Pressure Sensing and Analysis. Smart Sensing and Context, Lecture Notes in Computer Science, 2008, Volume 5279/2008, pp: 83-98, DOI: 10.1007/978-3-540-88793-5_7.

Gross, R. and Shi, J. 2001. The CMU Motion of Body (MoBo) database. Technical Report CMU-RI-TR-01-08, Robotics institute, Carnegie Mellon University, June 2001.

Guoying, Z., Li, C., Hua, L. and Matti, P. 2006. Gait Recognition Using Fractal Scale and Wavelet Moments. The international conference on pattern recognition, pp: 453-456.

Han, S. and Feng-Gang, H. 2005. Human Gait Recognition Based on Motion Analysis. Machine Learning and Cybernetics, Proceedings of International Conference on pp: 4464 - 4468.

Hansung, K., Ryuuki, S., Itaru, K.,Tomoji, T. and Kiyoshi, K. 2007. Robust Silhouette Extraction Technique Using Background Subtraction, Opt. Eng. 46, 097004 (Sep 20, 2007); doi:10.1117/1.2779022.

Hao, Z. and Zhijing, L. 2009. Gait Representation and Recognition Using Haar Wavelet and Radon Transform. 2009 WASE International Conference on Information Engineering, pp: 83-86.

Hayder Ali, Jamal Dargham, Chekima Ali, and Ervin Gobin Moung, 2011, "Person Identification using Gait", International Journal of Computer and Electrical Engineering, vol. 3, no. 4, pp. 477- 482, 2011.

Hayder Ali, Jamal Dargham, Chekima Ali, and Ervin Gobin Moung; 2011, "Analysis of Gait Recognition System based on Silhouettes and GEI templates", International Journal of Computer and Electrical Engineering, Accepted.

Hayder Ali, Jamal Dargham, Chekima Ali, Ervin Gobin Moung, 2011, "Gait Recognition using Gait Energy Image", International Journal of Signal Processing, Image Processing and Pattern (IJSIP), vol. 4, no. 3, pp. 141-152, 2011.

Hayder Ali, Jamal Dargham, Chekima Ali, Ervin Gobin Moung; "A Comparison of Gait Recognition using PCA with and without Radon Transform", 3rd International Conference on Signal Acquisition and Processing (ICSAP 2011), Singapore, February 26-28, vol. 2, pp. 28-31, 2011.

Hayder Ali, Jamal Dargham, Chekima Ali, Ervin Gobin Moung; "Gait Recognition using Principal Component Analysis", 3rd International Conference on Machine Vision (ICMV), Hong Kong, China, December 28-30, pp. 539-543, 2010.

Hayder Ali, Jamal Dargham, Chekima Ali, Ervin Gobin Moung; "Gait Recognition using Radon Transform with Principal Component Analysis", 3rd International Conference on Machine Vision (ICMV), China, Hong Kong, December 28-30, pp. 585-589, 2010.

Hayder, A., Jamal, D., Chekima, A. and Ervin, G. M. 2010a. Gait Recognition using Radon Transform with Principal Component Analysis. 3rd International Conference on Machine Vision (ICMV), China, Hong Kong, December 28-30, 2010, pp: 585-589.

Hayder, A., Jamal, D., Chekima, A. and Ervin, G. M. 2010b. Gait Recognition using Principal Component Analysis. 3rd International Conference on Machine Vision (ICMV), China, Hong Kong, December 28-30, 2010, pp: 539-543.

Heesung, L., Sungjun, H. and Euntai, K. 2009. An Efficient Gait Recognition with Backpack Removal. Hindawi Publishing Corporation, EURASIP Journal on Advances in Signal Processing, Volume 2009, Article ID 384384, 7 pages, doi:10.1155/2009/384384, pp: 1-7.

Heesung, L., Sungjun, H., Imran, F. N. and Euntai K. 2009. A Noise Robust Gait Representation: Motion Energy Image. International Journal of Control, Automation, and Systems (2009) 7(4):638-643, DOI 10.1007/s12555-009-0414-2, pp: 638-643.

Henty, J.R., Wood, D.E. and Ewins, D.J. 2001. An Experimental Evaluation of The Gyroscope as a Sensor in Fes Foot drop Correction Systems. Proceedings 7th Vienna International Workshop on Functional Electrical Stimulation. Vienna Austria, September 12-15, 2001, pp: 196-200.

Hong-Gui L., Cui-Ping S. and Xing-Guo L. 2005. LLE Based Gait Recognition. Proceedings of the Fourth International Conference on Machine Learning and Cybernetics, Guangzhou, 18-21 August 2005. pp: 4516-4521.

Honggui, L., Cuiping, S. and Xingguo, L. 2006. PCA Based Gait Segmentation. International Journal of Information Technology Vol. 12, No. 5, pp: 136-145.

Ibrahim, R. K., Ambikairajah, E. C., Branko, G. L. and Nigel, H. 2008. Gait Pattern Classification Using Compact Features Extracted From Intrinsic Mode Functions. Annual International Conference of the IEEE Engineering in Medicine and Biology Society, EMBS, pp: 3852-3855.

Ioannidis D., Tzovaras D., Damousis I.G., Argyropoulos S. and Moustakas K. 2007. Gait Recognition Using Compact Feature Extraction Transforms and Depth Information. IEEE Transactions on Information Forensics and Security, pp: 623-630.

Jaakko S., Kaori F. and Juha R. 2008. Gaussian Process Person Identification Based on Simple Floor Sensors. Lecture Notes in Computer Science, volume 5279/2008, pp: 55-68.

Jia, C., Lu, H. and Zhang, R. 2009. Aggressive Motion Detection Based on Normalized Radon Transform and Online AdaBoost. Electronics Letters, 26th February 2009, Vol. 45, No. 5, pp:257-258.

Jianyi, L. and Nanning, Z. 2007. Gait History Image: A Novel Temporal Template for Gait Recognition. IEEE International Conference on Multimedia and Expo, pp: 663 – 666.

Jin-Woo J., Dae-Jin K. and Zenn A. B. 2005. Realization of Personalized Services for Intelligent Residential Space based on User Identification Method using Sequential Walking Footprints. Systemic, Cybernetics, and Informatics, vol 3, no.2 pp: 90-95.

John P. S., Samara L. F. and Harry K. C. J. 2007. Biometric Identification from A Floor Based PVDF Sensor Array Using Hidden Markov Models. Sensors Application Symposium Technology Conference. pp: 1-5.

José-Luis, L., Montse, P. and Li-Qun, X. 2004. Shadow Removal with Morphological Reconstruction. In Proceedings of Jornades de Recerca en Automàtica, Visióí Robòtica (AVR), Barcelona (Spain), pp: 1-5.

Ju, H. and Bir, B. 2006. Individual Recognition using Gait Energy Image. IEEE Transactions on Pattern Analysis and Machine Intelligence, Vol. 28, No. 2, February 2006, pp: 316-322.

Jun Y., Xiaojuan W. and Zhang P. 2006. Gait Recognition Base on Difference Motion Slice. International Conference on Signal Processing (ICSP2006), volume: 4, Digital Object Identifier: 10.1109/ICOSP.2006.345931.

Junping, Z., Jian, P., Changyou, C. and Rudolf, F. 2010. Low-Resolution Gait Recognition. IEEE Transactions on Systems, Man, and Cybernetics—Part B: Cybernetics, Vol. 40, No. 4, August 2010, pp: 986-996.

Junqiu, W., Makihara, Y. and Yagi, Y. 2008. Human Tracking and Segmentation Supported By Silhouette-Based Gait Recognition. IEEE International Conference on Robotics and Automation (ICRA), pp: 1698-1703.

Jyoti, B. and Gupta, M.K. 2011. Human Gait Recognition using All Pair Shortest Path. 2011 International Conference on Software and Computer Applications IPCSIT vol.9 (2011) © (2011) IACSIT Press, Singapore, pp: 279-284.

Kanak, S. and Pratibha M. 2011. Human Gait Recognition using Local Binary Pattern Variance. International Journal of Advanced Engineering Sciences and Technologies (IJAEST), Vol. No. 7, Issue No. 2, 234 – 238, pp: 66-70.

Khalid B., Tao X. and Shaogang G. 2009. Gait Representation using Flow Fields. School of EECS, Queen Mary University of London, London E1 4NS, UK, pp: 1-11.

Khalid, B., Tao, X. and Shaogang, G. 2008. Feature Selection on Gait Energy Image for Human Identification. IEEE International Conference on Acoustics, Speech and Signal Processing, pp: 985 – 988.

Khalid, B., Tao, X. and Shaogang, G. 2010. Gait recognition without subject cooperation. Pattern Recognition Letters 31 (2010), pp: 2052–2060.

Khalid, B., Tao, X. and Shaogang, G. 2010. Gait Recognition without Subject Cooperation. Pattern Recognition Letters, Volume 31, Issue 13, 1 October 2010, pp: 2052-2060.

Khalid, B., Tao, X. and Shaogang, G. 2010. Gait Recognition without Subject Cooperation. Pattern Recognition Letters Volume 31, Issue 13, 1 October 2010, Meta-heuristic Intelligence Based Image Processing, pp: 2052–2060.

Kim K. (2003). Face Recognition using Principle Component Analysis, DCS, University of Maryland.

Landabaso J.L., Pardàs M. and Xu L.Q. 2004. Shadow Removal with Morphological Reconstruction. In Proceedings of Jornades de Recerca en Automàtica, Visió i Robòtica (AVR), Barcelona (Spain), 2004.

Lanshammar, H and Strandberg, L. 1981, Horizontal ¯oor reactions and heel movements during the initial stance phase, Eighth International Congress of Biomechanics, Nagoya, Japan, and July.

Lee M., Alex A. B., Alex B. and Mark S. N. 2005. A Floor Sensor System for Gait Recognition. Proceedings of the IEEE Workshop on Automatic Identification Advanced Technologies, pp: 171-176.

Lee M., Alex A. B., Alex B. and Mark S. N. 2005. A Floor Sensor System for Gait Recognition. Proceedings of the IEEE Workshop on Automatic Identification Advanced Technologies, pp: 171-176.

Lei, C., Yunhong, W., Yiding, W. and De, Z. 2009. Gender Recognition from Gait Using Radon Transform and Relevant Component Analysis. Proceeding ICIC'09 Proceedings of the 5th international conference on Emerging intelligent computing technology and applications, pp: 92-101.

Li F., Maylor K.H. L., Tejas S., Victor C. and Kean F. C. 2006. Palmprint. Classification, IEEE Int. Conf. on Systems, Man and Cybernetics, Vol. 4, 8-11 October 2006, pp: 2965-2969.

Liang, W., Tieniu, T., Huazhong, N. and Weiming, H. 2003. Silhouette Analysis-Based Gait Recognition for Human Identification. IEEE Transactions on Pattern Analysis and Machine Intelligence, Vol. 25, No. 12, December 2003, pp: 1505-1518.

Liang, W., Tieniu, T., Weiming, H. and Huanzhong, N. 2003. Autoomatic gait recognition based on statistical shape analysis. IEEE transactions on image processing, Vol. 12, No. 9, pp: 1-13.

Liang, Wa., Huazhong Ni., Tieniu T. and Weiming H. 2004. Fusion of Static and Dynamic Body Biometrics for Gait Recognition. IEEE Transactions on Circuits and Systems for Video Technology, pp: 149- 158.

Lili, L., Yilong, Y. and Wei, Q. 2010. Gait Recognition Based on Outermost Contour. Proceedings of the 5th international conference on Rough set and knowledge technology RSKT'10, pp. 395–402.

Ling-Feng, L., Wei. J. and Yi-Hai, Z. 2009a. Gait Recognition Using Hough Transform and Principal Component Analysis. With Aspects of Artificial Intelligence, Lecture Notes in Computer Science, Springer Berlin / Heidelberg, Volume no. 5755/2009, pp: 363-370.

Ling-Feng, L., Wei. J. and Yi-Hai, Z. 2009b. Survey of Gait Recognition, Emerging Intelligent Computing Technology and Applications. With Aspects of Artificial Intelligence, Lecture Notes in Computer Science, Springer Berlin / Heidelberg, Volume no. 5755/2009, pp: 652-659.

Liu R., Zhou J., Liu M. and Hou X. 2007. A Wearable Acceleration Sensor System for Gait Recognition. Industrial Electronics and Applications, ICIEA, IEEE Conference, pp: 2654-2659.

Liu, R., Zhou J., Liu M. and Hou X. 2007. A Wearable Acceleration Sensor System for Gait Recognition. Industrial Electronics and Applications, ICWAPR, International Conference, pp: 1067-1071.

M.H Ali, A. Chekima, M.A.L Razak, Jamal A. Dargham; "A Survey of Person Identification using Gait", 2nd Seminar on Engineering and Information Technology (SEIT2009), Sustainable Development through Engineering and Information Technology, University Malaysia Sabah, Kota Kinabalu, Malaysia, 8th – 9th July, 2009, pp. 338-341, 2009.

Mark S. Redfern{*, Rakieâ Cham{, Krystyna Gielo-Perczak{, Raoul Groè Nqvist}, Mikko Hirvonen}, Ha Ê Kan Lanshammar}, Mark Marpet{{, Clive Yi-Chung Pai{{and

Christopher Powers}}, Biomechanics of Slips. Ergonomics, 2001, Vol. 44, No. 13, 1138 – 1166.

Mark, R. D. 2002. Gait Recognition. Final Report, MEng Computing 4, Department of Computing Imperial College of Science, Technology & Medicine London, SW7 2BZ, pp: 16.

Mayu, O., Haruyuki, I., Yasushi, M. and Yasushi, Y. 2010. Performance Evaluation of Vision-based Gait Recognition using a Very Large-scale Gait Database. Biometrics: IEEE International Conference on Theory Applications and Systems (BTAS), pp: 1-6.

Mcfayden, B. J. and Winder, D. A. 1988, An integrated biomechanical analysis of normal stair ascent and descent, Journal of Biomechanics, 21, 733 - 744.

Michela, G., John N. C. and Mark S N. 2008. Front View Gait Recognition. IEEE International Conference on Biometrics: Theory, Applications And Systems, BTAS, pp: 1-6.

Miciak, M. 2010. Radon Transformation and Principal Component Analysis Method Applied in Postal Address Recognition Task. International Journal of Computer Science and Applications at techno mathematics Research Foundation, Vol. 7 No. 3, pp: 33 – 44.

Mircea, G. N., Robert J. H. and Jain L. C. 2004. Knowledge-Based Intelligent Information and Engineering Systems, 8th International Conference, KES 2004, Wellington, New Zealand, September 20-25, 2004. Proceedings, Part II. Lecture Notes in Artificial Intelligence, Vol. 3214, pp: 312-313.

Mirosław, M. 2010. Radon Transformation and Principal Component Analysis Method Applied in Postal Address Recognition Task, International Journal of Computer Science and Applications, Technomathematics Research Foundation, Vol. 7, No. 3, pp. 33 – 44.

Moeslunda, T. B., Adrian, H. and Volker, K. 2006. A survey of advances in vision-based human motion capture and analysis, Computer Vision and Image Understanding, Volume 104, Issues 2-3, November-December 2006, pp: 90-126.

Moghaddam, B. 2002. Principal manifolds and probabilistic subspaces for visual recognition, IEEE Trans Pattern Anal Machine Intell 24 (2002), 780–788.

Mohiuddin, A., Irine, P. and Seong-Whan, L. 2010. Silhouette History and Energy Image Information for Human Movement Recognition, Journal of Multimedia, Vol. 5, No. 1, February 2010, pp: 12-21.

Mori, T. S., Asaki, T. K. Yoshimoto Y. and Kishimoto Y. One-Room-Type Sensing System for Recognition and Accumulation of Human Behavior., IROS Proceedings IEEE/RSJ International Conference on Intelligent Robots and Systems, pp: 344-350.

Murat, E. 2006. Gait Recognition Using Multiple Projections. Proceedings of the 7th International Conference on Automatic Face and Gesture Recognition (FGR'06), pp: 1-4.

Murat, E. 2006. Human Identification Using Gait. Turk J Elec Engin, Vol.14, No.2 2006, pp: 267-291.

Murat, E. and Eyup, G. 2005. Gait Recognition Using View Distance Vectors. Springer-Verlag Lecture Notes in Artificial Intelligence, LNAI Vol. 3801, pp: 973-978, December, 2005.

Nikolaos, V. b. and Zhiwei X. C. 2007. Gait Recognition Using Radon Transform and Linear Discriminant Analysis. IEEE Transactions on Image Processing. Vol. 16, No. 3, March 2007, pp: 731-740.

Nikolaos, V. B. and Zhiwei, X. C. 2007. Gait Recognition Using Radon Transform and Linear Discriminant Analysis. IEEE Transactions on Image Processing, Vol. 16, No. 3, pp: 731- 740.

Nini, L., Jiwen, L., Yap-Peng, T. and Zhenzhong, C. 2009. Enhanced Gait Recognition Based on Weighted Dynamic Feature. 2009 16th IEEE International Conference Image Processing (ICIP), pp: 3581 – 3584.

Orr, R. J. and Abowd, G. D. 2000. The Smart Floor: A Mechanism for Natural User Identification and Tracking". Conference on Human Factors in Computing Systems, pp: 275-276.

Patla, A. E. 1993, Age-related changes in visually guided locomotion over diVerent terrains: major issues, in G. E. H. Stelmach, Sensorimotor Impairment in the Elderly (Dordrecht: Kluwer), 231- 252.

Perkins, P. J. 1978, Measurement of slip between the shoe and ground during walking, in Walkway Surfaces: Measurement of Slip Resistance, ASTM STP 649, Philadelphia, PA.

Perkins, P. J. and Wilson, M. P. 1983, Slip resistance testing of shoesÐNew developments, Ergonomics, 26, 73 - 82.

Phillips, P.J, Sarkar S., Robledo I., Grother P. and Bowyer K. 2002. Baseline Results for the Challenge Problems of Human ID Using Gait Analysis. Proceedings of the Fifth IEEE International Conference on Automatic Face and Gesture Recognition, pp: 130-135, 2002.

Qiong, C., Bo, F. and Hui, C. 2009. Gait Recognition Based on PCA and LDA. Proceedings of the Second Symposium International Computer Science and Computational Technology (ISCSCT '09), China, 26-28, Dec. 2009, pp. 124-127.

Reports and Research > Biometrics Market and Industry Report 2009-2014; http://www.biometricgroup.com/reports/public/market_report.php

Ricardo, F., Luciano Da F. C., Julio C. T. and Odemir M. B. 2008. 2D Euclidean Distance Transform Algorithms: A Comparative Survey. ACM Computing Surveys, Vol. 40, No. 1, Article 2, Publication date: February 2008.

Rishi, R., Visell, Y. and Cooperstock, J.R. 2010. Probabilistic Tracking of Pedestrian Movements via In-Floor Force Sensing. 2010 Canadian Conference on Computer and Robot Vision (CRV), pp: 143 – 150.

Rong, H., Wei, S. and Hongyuan, W. 2010. Recursive spatio temporal subspace learning for gait recognition. Journal Neurocomputing, Volume 73, Issue 10-12, June 2010, pp: 1892-1899.

Rosalyn, R. P., Ali, C., Farrah, W. and Sainarayanan, G. 2009. Proceedings of the 2nd Seminar on Engineering and Information Technology, 8th - 9th July 2009, Kota Kinabalu, Sabah, Malaysia, pp: 348 – 351.

Saeid, R., Reihaneh M. and Kazemi, F. M. 2008. Gait Recognition Using Wavelet Transform. Fifth International conference on Information Technology: New Generations, pp: 932 – 936.

Schneider, J., W. and Borlund P. 2007. Matrix comparison, part 1: Motivation and important issues for measuring the resemblance between proximity measures or ordination results. Journal of the American Society for Information Science and Technology 58(11), pp: 1586–1595.

Seyyed, M. H., Abbas, N., Peyman, N. and Hasan, F. 2010. A Novel Human Gait Recognition System. International Journal of Computer and Electrical Engineering, Vol.2, No.6, December, 2010, pp: 1793-8163.

Shamsher, S. and Biswas, K.K. 2009. Biometric Gait Recognition with Carrying and Clothing Variants. Proceedings of the 3rd International Conference on Pattern Recognition and Machine Intelligence PReMI '09, pp: 446-451.

Shi, C. and Youxing G. 2007. An Invariant Appearance Model for Gait Recognition. 2007 IEEE International Conference on Multimedia and Expo 2007, pp: 1375 – 1378.

Shutler, J., Grant M., Nixon M.S. and carter J. N. 2002. A large sequence based human gait database. In proc int conf recent advances in soft computing, pp: 66-72, 2002, http://www.gait.ecs.soton.ac.uk/

Siva, M. S. and Mathivanan, B. 2011. Performance Evaluation of LDA & RADON in Gait Recognition. International Journal of Computer Applications (0975 – 8887), Volume 13– No.8, January 2011, pp: 1-5.

Song-Zhi, S., Li W. and Shao-Zi L. 2008. Interframe Variation Vector Based Gait Recognition. International Conference on Intelligent System and Knowledge Engineering, pp: 707-712.

Strandberg, L. 1983, On accident analysis and slip-resistance measurement, Ergonomics, 26, 11 - 32.

Su-li, X. and Qian-jin, Z. 2010. Gait Recognition using Fuzzy Principal Component Analysis. 2nd International Conference on e-Business and Information System Security (EBISS), pp: 1-4.

Sungjun, H., Heesung, L., Kyongsae, O., Mignon, P. and Euntail, K. 2006. Gait Recognition using Sampled Point Vectors. Proceeding of the International Joint Conference on SICE-ICASE, pp: 3937-3940.

Takeda, R., Tamano S., Todoh M. and Yoshinari S. 2009. Human Gait Analysis Using Wearable Sensors of Acceleration and Angular Velocity. IFMBE, Proceedings Vol.23, pp: 1069-1072.

Tanaya, G. and Rahab, W. 2010. Differential Radon Transform for Gait Recognition. IEEE International Conference on Acoustics Speech and Signal Processing (ICASSP), pp: 834-837.

Tao, D. 2008. A Robust identification Approach to Gait Recognition. Proceeding of the IEEE Conference on computer Vision and Pattern Recognition, pp: 1-8.

Tee, C., Andrew, T., Michael, G. and David, N. 2003. Palmprint Recognition with PCA and ICA. Image and vision computing NZ, pp: 227-232.

Vili, K., Guoying, Z., Stan, Z. L. and Matti, P. 2009. Dynamic Texture Based Gait Recognition. Proceedings of the Third International Conference on Advances in Biometrics ICB '09, pp: 1000-1009.

Wenxin, L., David, Z. and Zhuoqun, X. 2003. Image Alignment Based on Invariant Features for Palmprint Identification. Signal Processing: Image Communication, Volume 18, Issue 5, pp: 373-379.

Winter, D. A. 1991, The Biomechanics and Motor Control of Human Gait: Normal, Elderly and Pathological, 2nd edn (Waterloo, Ontario: University of Waterloo Press).

Woollacott, M. H. and Tang, P.-F. 1997, Balance control during walking in the older adult: research and its implications, Physical Therapy, 77, 646 - 660.

Xiang-tao, C., Zhi-hui F., Hui W. and Zhe-qing L. 2010. 2010 International Conference on Biomedical Engineering and Computer Science (ICBECS), 23-25 April 2010, pp: 1-4. Doi-10.1109/ICBECS.2010.5462298.

Xiaochao, Y., Ji, D., Yue, Z. and Jie, Y. 2008. Gabor Based Discriminative Common Vector For Gait Recognition. Proceedings of the Congress on Image and Signal Processing, pp: 191-195.

Xiaochao, Y., Yue, Z., Tianhao, Z., Guang, S. and Jie, Y. 2008. Gait recognition based on dynamic region analysis. Signal Processing, Volume 88, Issue 9, September 2008, pp:2350-2356.

Xiaxi, H. and Boulgouris, N.V. 2008. Gait Recognition using Multiple Views. Proceeding of the IEEE International Conference on Acoustics, Speech, and Signal Processing, pp: 1705-1708.

Xiaxi, H. and Nikolaos, V. B. 2010. Gait Recognition Using Linear Discriminant Analysis with Artificial walking Conditions. Proceedings of 2010 IEEE 17th International Conference on Image Processing September 26-29, 2010, Hong Kong, pp: 2461-2464.

Xu, H., Jiwei, L., Lei, L. and Zhiliang, W. 2006. Gait Recognition Considering Direction of Walking. IEEE Conference on Cybernetics and Intelligent Systems, pp: 1-5.

Xu, L.Q., Landabaso, J.L. and Pardàs, M. 2005. Shadow Removal with Blob-Based Morphological Reconstruction for Error Correction. Proceedings of International Conference on Acoustics, Speech and Signal Processing (ICASSP). IEEE Computer Society, Philadelphia, PA, USA, March 2005, pp: 229-232.

Yangming, G. and Guangjian, T. 2008. Gait Recognition Based on Anatomical Knowledge. 7th World Congress on Intelligent Control and Automation, WCICA, pp: 6803 – 6806.

Yi, H., Dong X. and Tat-Jen C. 2010. Face and Human Gait Recognition Using Image-to-Class Distance. IEEE Transactions on Circuits and Systems for Video Technology, Vol. 20, No. 3, March 2010, pp: 431-438.

Zhang, R., Christian, V. and Dimitris, M. 2004. Human Gait Recognition. Proceedings of the 2004 IEEE Computer Society Conference on Computer Vision and Pattern Recognition Workshops (CVPRW'04), June 2004, PP: 18-28.

Zongyi, L. and Sarkar, S. 2006. Improve Gait Recognition by Gait Dynamics Normalization. IEEE Transactions on Pattern Analysis and Machine Intelligence, pp: 863-876.

Zongyi, L. and Sudeep, S. 2005. Effect of Silhouette Quality on Hard Problems In Gait Recognition. IEEE Transaction on System, Man and Cybernetics, vol. 35. no.2.

PUBLICATIONS FROM PROJECT

Journal Papers:

Hayder Ali, Jamal Dargham, Chekima Ali, and Ervin Gobin Moung; 2011, "Analysis of Gait Recognition System based on Silhouettes and GEI templates", International Journal of Computer and Electrical Engineering, **Accepted**.

Hayder Ali, Jamal Dargham, Chekima Ali, and Ervin Gobin Moung, 2011, "Person Identification using Gait", International Journal of Computer and Electrical Engineering, vol. 3, no. 4, pp. 477- 482, 2011.

Hayder Ali, Jamal Dargham, Chekima Ali, Ervin Gobin Moung, 2011, "Gait Recognition using Gait Energy Image", International Journal of Signal Processing, Image Processing and Pattern (IJSIP), vol. 4, no. 3, pp. 141-152, 2011.

Conference Papers:

Hayder Ali, Jamal Dargham, Chekima Ali, Ervin Gobin Moung; "A Comparison of Gait Recognition using PCA with and without Radon Transform", 3rd International Conference on Signal Acquisition and Processing (ICSAP 2011), Singapore, February 26-28, vol. 2, pp. 28-31, 2011.

Hayder Ali, Jamal Dargham, Chekima Ali, Ervin Gobin Moung; "Gait Recognition using Principal Component Analysis", 3rd International Conference on Machine Vision (ICMV), Hong Kong, China, December 28-30, pp. 539-543, 2010.

Hayder Ali, Jamal Dargham, Chekima Ali, Ervin Gobin Moung; "Gait Recognition using Radon Transform with Principal Component Analysis", 3rd International Conference on Machine Vision (ICMV), China, Hong Kong, December 28-30, pp. 585-589, 2010.

M.H Ali, A. Chekima, M.A.L Razak, Jamal A. Dargham; "A Survey of Person Identification using Gait", 2nd Seminar on Engineering and Information Technology (SEIT2009), Sustainable Development through Engineering and Information Technology, University Malaysia Sabah, Kota Kinabalu, Malaysia, 8th – 9th July, 2009, pp. 338-341, 2009.

APPENDICES

APPENDIX A: PCA PROGRAM PSEDUCODE

1.1 PCA ALGORITHM APPLIED FOR FACE RECOGNITION

A 2-D facial image can be represented as 1-D vector by concatenating each row (or column) into a long thin vector.

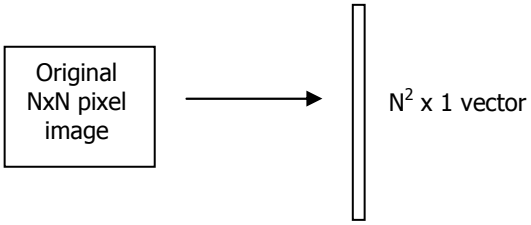

Figure 1.1: An NxN pixel image of a face, represented as a vector of size N^2-dimensional image space.

Supposed we have I_1, I_2 … I_M images in the training set, where M is the number of total images in training set. All images represented as N^2-dimensional vectors. Each image I_i represented as a vector Γ_i.

$$I_i = \begin{bmatrix} a_{11} & a_{12} & \dots & a_{1N} \\ a_{21} & a_{22} & \dots & a_{2N} \\ \vdots & \vdots & \ddots & \vdots \\ a_{N1} & a_{N2} & \dots & a_{NN} \end{bmatrix}_{N \times N} \xrightarrow{\text{concatenation}} \begin{bmatrix} a_{11} \\ \vdots \\ a_{1N} \\ \vdots \\ a_{2N} \\ \vdots \\ a_{NN} \end{bmatrix}_{N^2 \times 1} = \Gamma_i$$

Average face vector Ψ calculated.

$$\Psi = \frac{1}{M} \sum_{i=1}^{M} \Gamma_i$$

(1)

Each face vector Γ_i were subtracted the mean face Ψ, to get a set of vectors Φ_i. The purpose of subtracting the mean image from each image vector is to be left with only the distinguishing features from each face and "removing" information that is common.

$$\Phi_i = \Gamma_i - \Psi$$

(2)

Covariance matrix C calculated.

$C = AA^T$, where $A = [\Phi_1, \Phi_2 \ldots \Phi_M]$

(3)

Note that C is an N^2xN^2 matrix and A is an N^2xM matrix. Eigenvectors u_i of C need to be calculated. However note that C is an N^2xN^2 matrix and it would return N^2 Eigenvectors each being N^2 dimensional. For an image this number is huge. Instead of the Matrix AA^T, consider the matrix A^TA. Remember A is an N^2xM matrix, thus A^TA is an MxM matrix. If the Eigenvectors of this matrix were found, it would return M Eigenvectors, each of dimensions Mx1.Tthese Eigenvectors will be called v_i. Consider the eigenvectors v_i of A^TA such that

- $A^TA\ v_i = \lambda\ v_i$
- v_i is the eigenvector of A^TA, and λ is the eigenvalue.
- Multiplying both sides by A, we have $AA^T\ (Av_i) = \lambda(Av_i)$.
- From the new equation, it can be seen that Av_i is the eigenvector of AA^T.
- So, the eigenvector of $C=AA^T$, is $u_i = Av_i$.

This implies that using v_i we can calculate the M largest Eigenvectors of AA^T. Remember that M << N^2 as M is simply the number of training images. Find the best M Eigenvectors of $C = AA^T$ by using the relation discussed above. That is: $u_i = Av_i$. The eigenvectors were then normalize so that $\| u_i \| = 1$. Select the best K Eigenvectors, where $K \leq M$. Since these eigenvectors have the same dimension as the original image, they have a face like appearance, which were called Eigenfaces.

Now each face in the training set (minus the mean), Φ_i can be represented as a linear combination of these Eigenvectors u_i.

$\Phi_i = \sum_{j=1}^{K} w_j u_j$

(4)

where u_j are eigenfaces. These weights can be calculated as

$w_j = u_j^T \Phi_i$

(5)

Each normalized training image is represented in this basis as a vector.

$$\Omega_i = \begin{bmatrix} w_1 \\ w_2 \\ \vdots \\ w_k \end{bmatrix}$$

Where i = 1, 2… M. This means we have to calculate such a vector corresponding to every image in the training set and store them as templates.

APPENDIX B: ALGORITHM OF EUCLIDEAN DISTANCE

2.1 DISCUSSION OF EFFECT OF THRESHOLD TUNING PARAMETER ON RECOGNITION RATE

As can be seen from the recall correct classification rate is decreasing while the rejection correct classification rate is increasing as Tcpara increase. However, the False Acceptance Rate for both recall and rejection decrease as Tcpara value increases. Thus, the value of the threshold tuning parameter can be used to tune the performance of the system to have either high recall with high false acceptance rate for application such as boarder monitoring or high rejection rate for unknown persons for application such as access control.

2.2 DISTANCE MEASUREMENT

The Euclidean distance measure is used for the classification task. If the Euclidean distance between test image y and image x in the training database d(x,y) is smaller than a given threshold t then images y and x are assumed to be of the same person. The threshold t is the largest Euclidean distance between any two face images in the training database, divided by a threshold tuning value (Tcpara) as given in Equation 1.

The distance threshold Θ_{tc} is the largest distance between any two face images, and divided by a threshold tuning value (Tcpara).

$$\Theta_{tc} = \frac{[\max_{j,k}\{\|\Omega_j - \Omega_k\|\}]}{\text{Tcpara}} \quad (1)$$

Where j, k = 1, 2 … M

M = total number of training image

Ω = the reduced dimension images

2.3 The Euclidean distance algorithm

Euclidean distance is calculated from the center of the source cell to the center of each of the surrounding cells. True Euclidean distance is calculated in each of the distance tools. Conceptually, the Euclidean algorithm works as follows: for each cell, the distance to each source cell is determined by calculating the hypotenuse with x_max and y_max as the other two legs of the triangle. This calculation derives the true Euclidean distance, rather than the cell distance. The shortest distance to a source is determined, and if it is less than the specified maximum distance, the value is assigned to the cell location on the output raster.

Determining true Euclidean distance

The output values for the Euclidean distance raster are floating-point distance values. If the cell is at an equal distance to two or more sources, the cell is assigned to the source that is first encountered in the scanning process. You cannot control this scanning process.
The above description is only a conceptual depiction of how values are derived. The actual algorithm computes the information using a two-scan sequential process. This process makes the speed of the tool independent from the number of source cells, the distribution of the source cells, and the maximum distance specified. The only factor that influences the speed with which the tool executes is the size of the raster. The computation time is linearly proportional to the number of cells in the Analysis window.

2.4 Measures of distance between samples: Euclidean

Pythagoras' theorem

The photo shows Michael in July 2008 in the town of Pythagorion, Samos island, Greece, paying homage to the one who is reputed to have made almost all the content of this book possible Pythagoras the Samian. The illustrative geometric proof of Pythagoras' theorem stands carved on the marble base of the statue – it is this theorem that is at the heart of most of the multivariate analysis presented in this book, and particularly the graphical approach to data analysis that we are strongly promoting. When you see the word "square" mentioned in a statistical text (for example, chi square or least squares), you can be almost sure that the corresponding theory has some relation to this theorem. We first show the theorem in its simplest and most familiar two-dimensionalform, before showing how easy it is to generalize it to multidimensional space. In a right 4- 2 angled triangle, the square on the hypotenuse (the side denoted by A in figure 1) is equal to the sum of the squares on the other two sides (B and C); that is, $A^2 = B^2 + C^2$.

Figure 1 Pythagoras' theorem in the familiar right-angled triangle, and the monument to this triangle in the port of Pythagorion, Samos island, Greece, with Pythagoras himself forming one of the sides. Figure 1 Pythagoras' theorem in the familiar right-angled triangle, and the monument to this triangle in the port of Pythagorion, Samos island, Greece, with Pythagoras himself forming one of the sides.

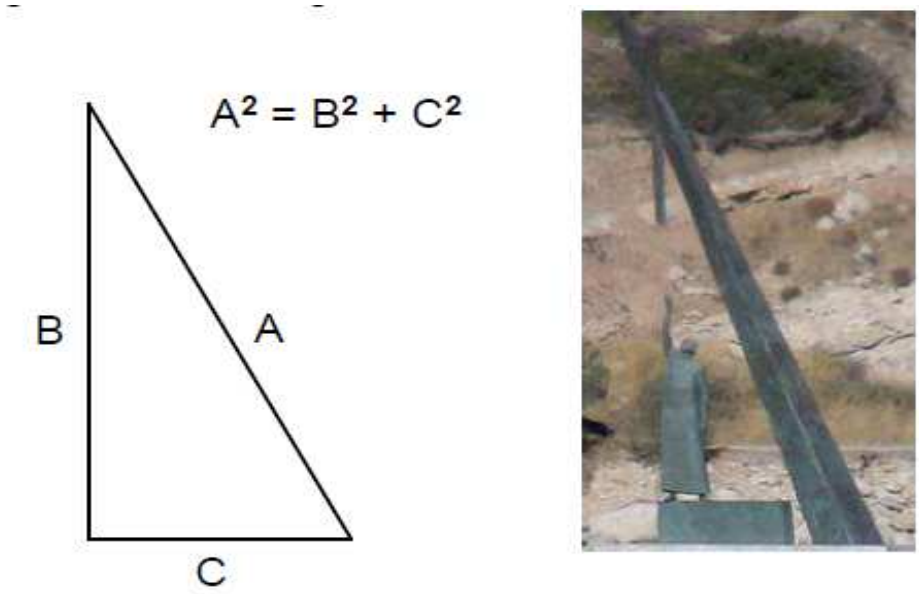

Figure 1 Pythagoras' theorem in the familiar right-angled triangle, and the monument to this triangle in the port of Pythagorion, Samos island, Greece, with Pythagoras himself forming one of the sides.

2.5 Euclidean distance

The immediate consequence of this is that the squared length of a vector $x = [\, x_1\ x_2\,]$ is the sum of the squares of its coordinates (see triangle OPA in figure 2, or triangle OPB – $|OP|^2$ denotes the squared length of x, that is the distance between point O and P); and the figure 2 Pythagoras' theorem applied to distances in two-dimensional space.

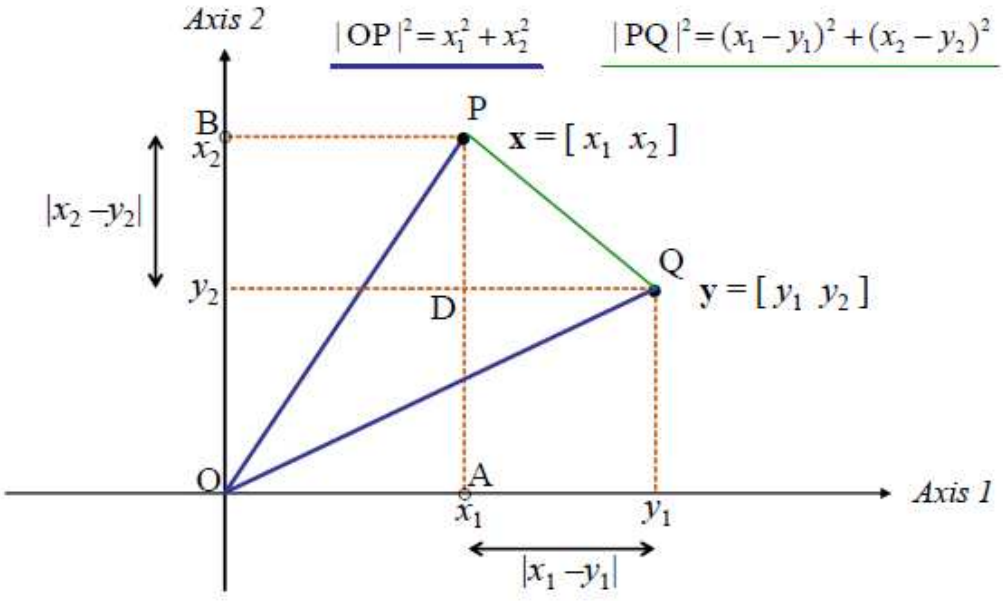

Figure 2: Pythagoras' theorem applied to distances in two-dimensional space.

squared distance between two vectors x = [x_1 x_2] and y = [y_1 y_2] is the sum of squared differences in their coordinates (see triangle PQD in figure 2; $|PQ|^2$ denotes the squared distance between points P and Q). To denote the distance between vectors x and y we can use the notation x, y d so that this last result can be written as:

$$d^2_{x,y} = (x_1 - y_1)^2 + (x_2 - y_2)^2$$

that is, the distance itself is the square root

$$d_{x,y} = \sqrt{(x_1 - y_1)^2 + (x_2 - y_2)^2}$$

What we called the squared length of x, the distance between points P and O in figure 2, is the distance between the vector x = [x_1 x_2] and the zero vector 0 = [0 0] with coordinates all zero:

$$d_{x,0} = \sqrt{(x_1^2 + x_2^2}$$

which we could just denote by dx . The zero vector is called the origin of the space.

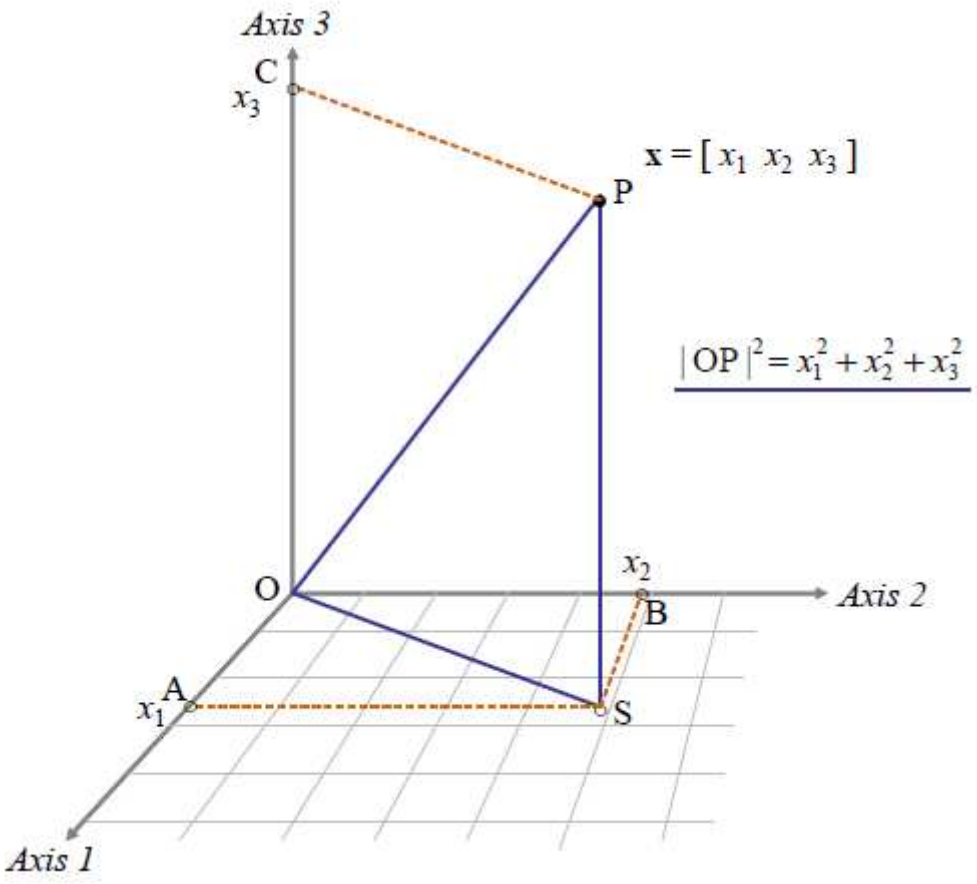

Figure 3: Pythagoras' theorem extended into three dimensional space

We move immediately to a three-dimensional point $x = [\, x_1 \; x_2 \; x_3 \,]$, shown in figure 3. This figure has to be imagined in a room where the origin O is at the corner – to reinforce this idea 'floor tiles' have been drawn on the plane of axes 1 and 2, which is the 'floor' of the room. The three coordinates are at points A, B and C along the axes, and the angles AOB, AOC and COB are all 90° as well as the angle OSP at S, where the point P (depicting vector x) is projected onto the 'floor'.

Using Pythagoras' theorem twice we have:

$|OP|^2 = |OS|^2 + |PS|^2$ (because of right-angle at S)

$|OS|^2 = |OA|^2 + |AS|^2$ (because of right-angle at A)

and so

$|OP|^2 = |OA|^2 + |AS|^2 + |PS|^2$

that is, the squared length of x is the sum of its three squared coordinates and so

$$d_x = \sqrt{x_1^2 + x_2^2 + x_3^2}$$

(1)

It is also clear that placing a point Q in figure 3 to depict another vector y and going through the motions to calculate the distance between x and y will lead to

$$d_{x,y} = \sqrt{(x_1 - y_1)^2 + (x_2 - y_2)^2 + (x_{13} - y_3)^2}$$

(2)

Furthermore, we can carry on like this into 4 or more dimensions, in general J dimensions, where J is the number of variables. Although we cannot draw the geometry any more, we can express the distance between two J-dimensional vectors x and y as:

$$d_{x,y} = \sqrt{\sum_{j=1}^{j} (x_j - y_j)^2}$$

(3)

This well-known distance measure, which generalizes our notion of physical distance in two- or three-dimensional space to multidimensional space, is called the Euclidean distance (but often referred to as the 'Pythagorean distance' as well).

Source: http://www.econ.upf.edu/~michael/stanford/maeb4.pdf
Wikipedia http://en.wikipedia.org/wiki/Euclidean_distance

APPENDEX C: RADON TRANSFORM AND ALL MATLAB CODES

3.1 RADON TRANSFORM

The Radon transform is an integral transform whose inverse is used to reconstruct images from medical CT scans. A technique for using Radon transforms to reconstruct a map of a planet's polar regions using a spacecraft in a polar orbit has also been devised (Roulston and Muhleman 1997).

The Radon transform can be defined by

$$R(p,\tau)[f(x,y)] = \int_{-\infty}^{\infty} f(x,\tau+px)\,dx \quad (1)$$

$$= \int_{-\infty}^{\infty}\int_{-\infty}^{\infty} f(x,y)\,\delta[y-(\tau+px)]\,dy\,dx \quad (2)$$

$$= U(p,\tau), \quad (3)$$

where p is the slope of a line and τ is its intercept. The inverse Radon transform is

$$f(x,y) = \frac{1}{2\pi}\int_{-\infty}^{\infty}\frac{d}{dy}H[U(p,y-px)]\,dp, \quad (4)$$

where H is a Hilbert transform. The transform can also be defined by

$$R'(r,\alpha)[f(x,y)] = \int_{-\infty}^{\infty}\int_{-\infty}^{\infty} f(x,y)\,\delta(r-x\cos\alpha-y\sin\alpha)\,dx\,dy, \quad (5)$$

where r is the perpendicular distance from a line to the origin and α is the angle formed by the distance vector.

Using the identity

$$\mathcal{F}_{\omega\alpha}[R[f(\omega,\alpha)]](x,y) = \mathcal{F}_{u,v}^{2}[f(u,v)](x,y), \quad (6)$$

where $\mathcal{F}$ is the Fourier transform, gives the inversion formula

$$f(x,y) = c\int_{0}^{\pi}\int_{-\infty}^{\infty}\mathcal{F}_{\omega\alpha}[R[f(\omega,\alpha)]]\,|\omega|\,e^{i\omega(x\cos\alpha+y\sin\alpha)}\,d\omega\,d\alpha.$$

(7)

The Fourier transform can be eliminated by writing

$$f(x,y) = \int_0^{\pi} \int_{-\infty}^{\infty} R[f(r,\alpha)]\, W(r,\alpha,x,y)\, d\, r\, d\,\alpha, \tag{8}$$

where W is a weighting function such as

$$W(r,\alpha,x,y) = h(x\cos\alpha + y\sin\alpha - r) \tag{9}$$

$$= \mathcal{F}^{-1}[|\omega|]. \tag{10}$$

Nievergelt (1986) uses the inverse formula

$$f(x,y) = \frac{1}{\pi}\lim_{c\to 0}\int_0^{\pi}\int_{-\infty}^{\infty} R[f(r + x\cos\alpha + y\sin\alpha, \alpha)]\, G_c(r)\, d\, r\, d\,\alpha, \tag{11}$$

where

$$G_c(r) = \begin{cases} \dfrac{1}{\pi c^2} & \text{for } |r| \le c \\ \dfrac{1}{\pi c^2}\left(1 - \dfrac{1}{\sqrt{1 - c^2/r^2}}\right) & \text{for } |r| > c. \end{cases} \tag{12}$$

Ludwig's inversion formula expresses a function in terms of its Radon transform. $R'(r,\alpha)$ and $R(p,\tau)$ are related by

$$p = \cot\alpha \quad \tau = r\csc\alpha \tag{13}$$

$$r = \frac{\tau}{1+p^2} \quad \alpha = \cot^{-1} p. \tag{14}$$

The Radon transform satisfies superposition

$$R(p,\tau)[f_1(x,y) + f_2(x,y)] = U_1(p,\tau) + U_2(p,\tau), \tag{15}$$

linearity

$$R(p,\tau)[a\, f(x,y)] = a\, U(p,\tau), \tag{16}$$

scaling

$$R(p,\tau)\left[f\left(\frac{x}{a},\frac{y}{b}\right)\right]=|a|\,U\left(p\,\frac{a}{b},\frac{\tau}{b}\right), \tag{17}$$

rotation, with R_ϕ rotation by angle ϕ

$$R(p,\tau)\left[R_\phi f(x,y)\right]=\frac{1}{|\cos\phi+p\sin\phi|}\,U\left(\frac{p-\tan\phi}{1+p\tan\phi},\frac{\tau}{\cos\phi+p\sin\phi}\right), \tag{18}$$

and skewing

$$R(p,\tau)\left[f(a\,x+b\,y,c\,x+d\,y)\right]=\frac{1}{|a+b\,p|}\,U\left[\frac{c+d\,p}{a+b\,p},\frac{\tau\,(a\,b+b\,c)}{a+b\,p}\right] \tag{19}$$

(Durrani and Bisset 1984; correction in Durrani and Bisset 1985).

The line integral along p,τ is

$$I=\sqrt{1+p^2}\;U(p,\tau). \tag{20}$$

The analog of the one-dimensional convolution theorem is

$$R(p,\tau)\left[f(x,y)*g(y)\right]=U(p,\tau)*g(\tau), \tag{21}$$

the analog of Plancherel's theorem is

$$\int_{-\infty}^{\infty}U(p,\tau)\,d\tau=\int_{-\infty}^{\infty}\int_{-\infty}^{\infty}f(x,y)\,dx\,dy, \tag{22}$$

and the analog of Parseval's theorem is

$$\int_{-\infty}^{\infty}R(p,\tau)\left[f(x,y)\right]^2\,d\tau=\int_{-\infty}^{\infty}\int_{-\infty}^{\infty}f^2(x,y)\,dx\,dy. \tag{23}$$

If f is a continuous function on $\mathbb{C}$, integrable with respect to a plane Lebesgue measure, and

$$\int_l f\,ds=0 \tag{24}$$

for every (doubly) infinite line l where s is the length measure, then f must be identically zero. However, if the global integrability condition is removed, this result fails (Zalcman 1982, Goldstein 1993).

Sources:

Anger, B. and Portenier, C. Radon Integrals. Boston, MA: Birkhäuser, 1992.

Armitage, D. H. and Goldstein, M. "Nonuniqueness for the Radon Transform." *Proc. Amer. Math. Soc.* 117, 175-178, 1993.

Deans, S. R. The Radon Transform and Some of Its Applications. New York: Wiley, 1983.

Zalcman, L. "Uniqueness and Nonuniqueness for the Radon Transform." Bull. London Math. Soc. 14, 241-245, 1982.

http://mathworld.wolfram.com/RadonTransform.html

Flow Chart of Radon Transform

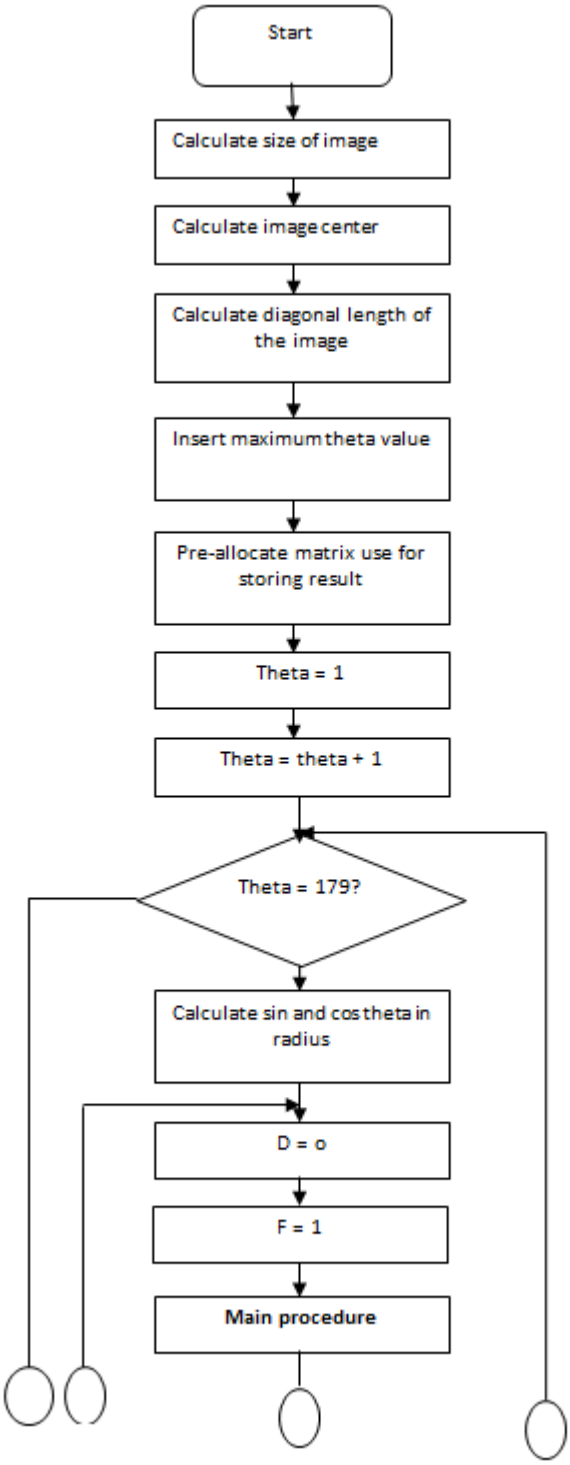

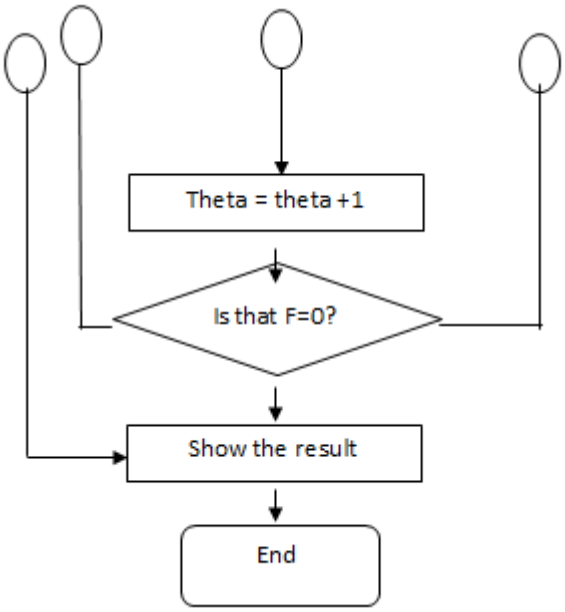

Figure 3.1 : Flow chart of Radon Transform technique

Mail procedure

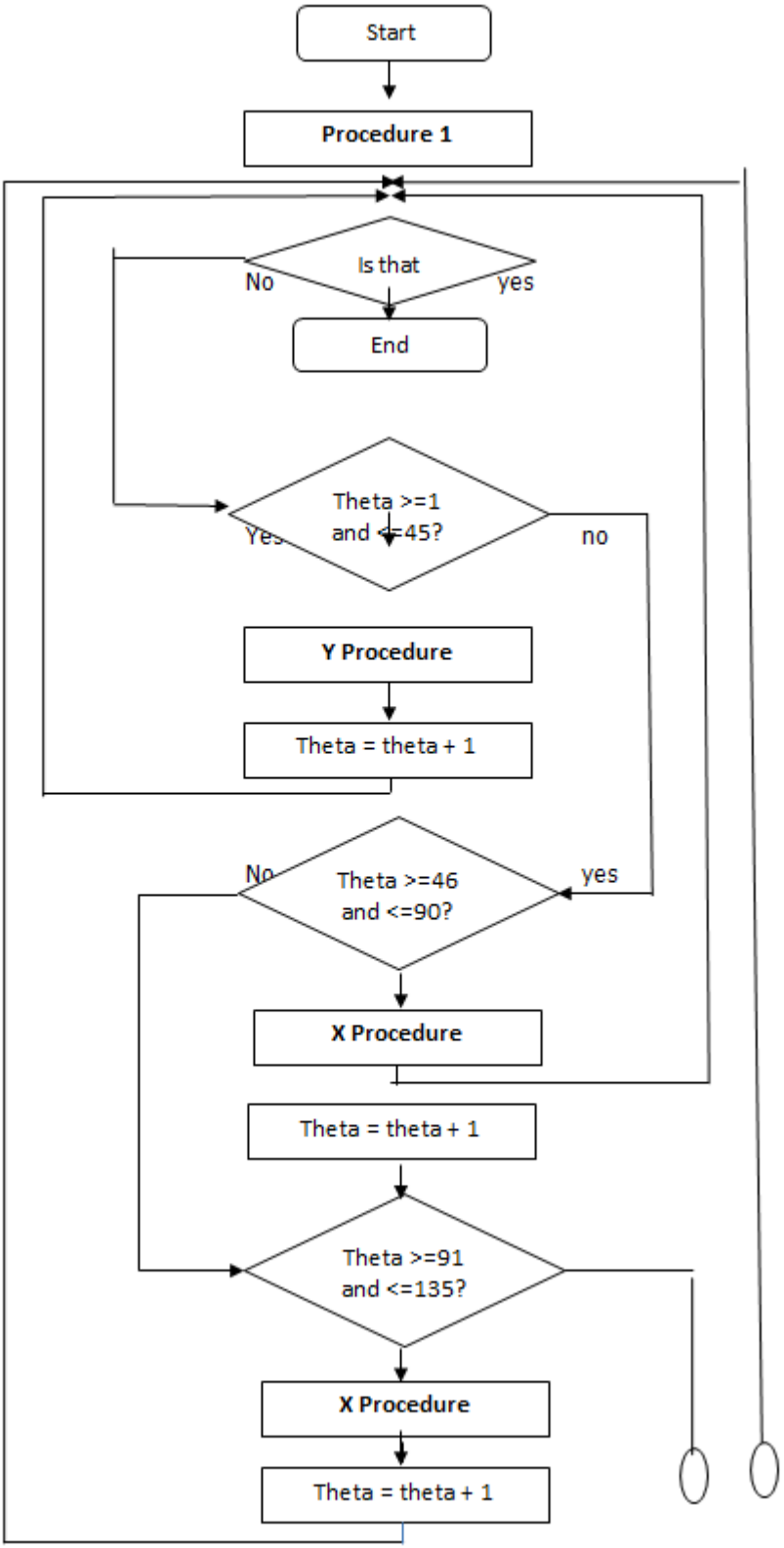

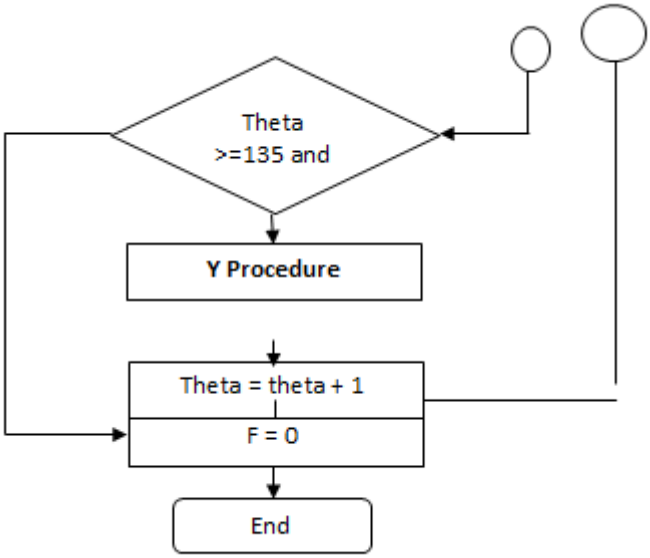

Figure 3.2: Flow chart of main procedure

Procedure 1

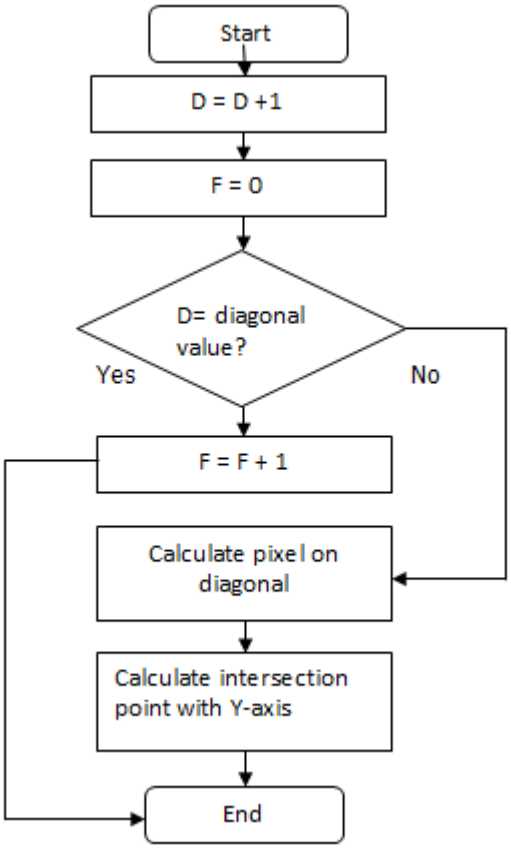

Figure 3.3: Flow chart of Procedure 1

X procedure

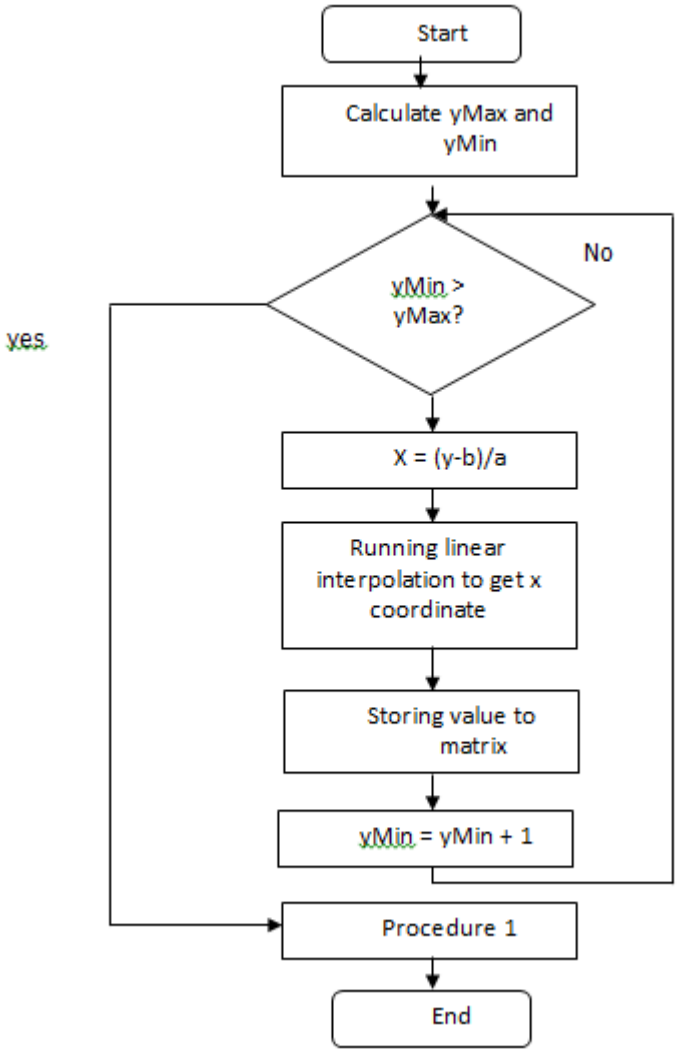

Figure 3.4: Flow chart of X procedure

Y procedure

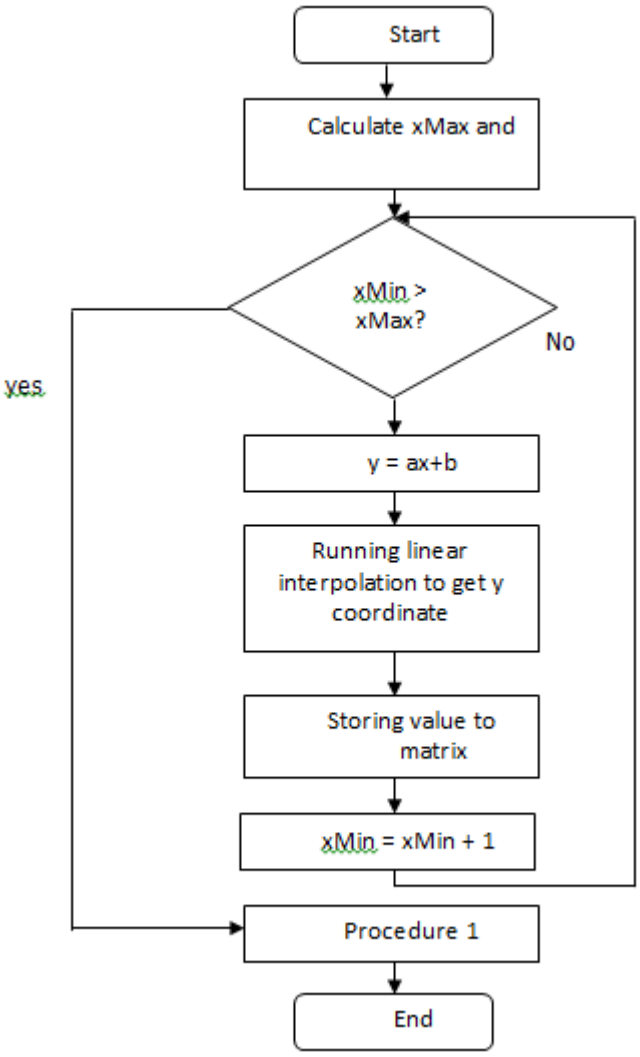

Figure 3.5: Flow chart of Y procedure

PROGRAM CODE

EUCLIDEAN DISTANCE

```
tic
clc
close all
clear all

M = input('Load how many image: ');

img=imread('test1.jpg');
if isrgb(img)
img = rgb2gray(img);
end

row=100;
col=100;
% [row col]=size(img);

fprintf('\nPreparing test image\n');
EU = []; % storing the images in a matrix
checkloop=0;
for i=1:M
str=strcat('test',int2str(i),'.jpg');
eval('img=imread(str);');
if isrgb(img)
img = rgb2gray(img);
end
img=histeq(img,255);
img=imresize(img, [row col]);
temp=reshape(img',row*col,1);
EU=[EU temp];

fprintf('%d  ', i);
checkloop = checkloop+1;
if checkloop == 10
fprintf('\n');
```

```
checkloop = 0;
end
end

EU = double(EU);

checkloop=0;
fprintf('\nCalculating euclidean distance\n');
distance=[];
frame=[];
for i=1:M;
temp = norm(EU(:,1)-EU(:,i));
distance = [ distance; temp ];

fprintf('%d  ', i);
checkloop = checkloop+1;
if checkloop == 10
fprintf('\n');
checkloop = 0;
end
frame=[frame i];
end

figure(1);
axes1 = axes('Parent',figure(1),'FontSize',14);
hold on
plot1 = plot(frame,distance,'Parent',axes1,'MarkerSize',3,'LineWidth',2);
set(plot1,'MarkerFaceColor',[0 0 0],'Marker','o',...
'DisplayName','Distance value',...
'Color',[0 0 0]);
legend('show');
set(legend,'Location','NorthOutside');
xlabel('Frame number','FontSize',16);
ylabel('Euclidean distance value','FontSize',16);
hold off
```

```
fprintf('\nProgram end - Image size [%dx%d]\n',col,row);
elapsed=toc/60;
fprintf('Elapsed time is: %d minutes %2.1f seconds\n',fix(elapsed), (elapsed-fix(elapsed))*60);
```

DATA INPUT

```
clc
clear

fprintf('\n[TRAINING SET DETAIL]\n');
fprintf('How many person in training set\t: ');
trainperson_no = input(' ');

train_person_detail=[]; % to store amount of images used for each person
for i=1:trainperson_no
fprintf('Person [%d]\tgot how many image\t: ',i);
temp = input(' ');
train_person_detail=[train_person_detail;temp];
end
fprintf('For LDA - Each person got how many image? ');
population = input(' ');
class_number=trainperson_no; % total class/person

looptrain=0; % default training image size
for i=1:trainperson_no
looptrain = looptrain + train_person_detail(i);
end
fprintf('Your training set size is: %d\n',looptrain);


fprintf('\n[TESTING SET (KNOWN) DETAIL]\n');
fprintf('How many person in testing set\t: ');
testperson_no1 = input(' ');

test_person_detail1=[]; % to store amount of images used for each person
for i=1:testperson_no1
```

```
fprintf('Person [%d]\tgot how many image\t: ',i);
temp = input(' ');
test_person_detail1=[test_person_detail1;temp];
end

no_test1=0;  % default test image size
for i=1:testperson_no1
no_test1=no_test1+test_person_detail1(i);
end
fprintf('Your testing set size is: %d\n',no_test1);

fprintf('\n[TESTING SET (UNKNOWN) DETAIL]\n');
fprintf('How many person in testing set\t: ');
testperson_no2 = input(' ');

test_person_detail2=[]; % to store amount of images used for each person
for i=1:testperson_no2
fprintf('Person [%d]\tgot how many image\t: ',i);
temp = input(' ');
test_person_detail2=[test_person_detail2;temp];
end

no_test2=0;  % default test image size
for i=1:testperson_no2
no_test2=no_test2+test_person_detail2(i);
end
fprintf('Your testing set size is: %d\n',no_test2);

save data\training_and_testing_data_input
save data\forlda population class_number
```

PROMOSING

```
clear
tic
clc
close all
load data\training_and_testing_data_input

DisplayTrainingSet=[];
TrainingSet=[];

DisplayTestSet1=[];
DisplayTestSet2=[];
TestSet1=[];
TestSet2=[];

fprintf('LOAD AND STORE IMAGE IN MATRIX\n');
fprintf('______________________________________________');

str1='F:\provided silhouettes for known and unknown\known_unknown_silhouettes\carrying a ball walk\train\';
str2='F:\provided silhouettes for known and unknown\known_unknown_silhouettes\carrying a ball walk\test\';
str3='F:\provided silhouettes for known and unknown\known_unknown_silhouettes\carrying a ball walk\unknown\';

fprintf('\nResize image -\nRow: ');
rowused = input(' ');
fprintf('Col: ');
colused = input(' ');

fprintf('\nLoad training images\t\t- [          ');
% Preparing training images
for i=1:looptrain
strimg=strcat(str1,'train', int2str(i),'.jpg');
eval('img=imread(strimg);');
if size(img,3)==3
```

```
img=rgb2gray(img);
end
img=histeq(img,255);
img=imresize(img, [rowused colused]);
temp=reshape(img', rowused*colused,1);
TrainingSet=[TrainingSet temp]; % training image set
percent=(i/looptrain)*100;
fprintf('\b\b\b\b\b\b\b\b\b%6.2f%% ]', percent);
end
clear temp

fprintf('\nLoad test images (known)\t- [          ');
% Preparing testing images (known)
for i=1:no_test1
strimg=strcat(str2,'test',int2str(i),'.jpg');
eval('img=imread(strimg);');
if size(img,3)==3
img=rgb2gray(img);
end
img=histeq(img,255);
img=imresize(img, [rowused colused]);
temp=reshape(img', rowused*colused,1);
TestSet1=[TestSet1 temp]; % training image set
percent=(i/no_test1)*100;
fprintf('\b\b\b\b\b\b\b\b\b%6.2f%% ]', percent);
end
clear temp

fprintf('\nLoad test images (unknown)\t- [          ');
% Preparing testing images (unknown)
for i=1:no_test2
strimg=strcat(str3,'unknown',int2str(i),'.jpg');
eval('img=imread(strimg);');
if size(img,3)==3
img=rgb2gray(img);
end
```

```
img=histeq(img,255);
img=imresize(img, [rowused colused]);
temp=reshape(img', rowused*colused,1);
TestSet2=[TestSet2 temp]; % training image set
percent=(i/no_test2)*100;
fprintf('\b\b\b\b\b\b\b\b\b%6.2f%% ]', percent);
end
clear temp
fprintf('\n');

N = size(TrainingSet,1); % dimension of the image

save data\prosimgdata N TestSet1 TestSet2 TrainingSet colused looptrain no_test1 no_test2
rowused trainperson_no testperson_no1 testperson_no2 train_person_detail test_person_detail1
test_person_detail2
fprintf('\nProgram end - Data saved!\nImage size [%dx%d]\nTrainig & Testing size - [%d, %d,
%d]\n',colused,rowused,looptrain,no_test1, no_test2);
elapsed=toc/60;
fprintf('Elapsed time is: %d minutes %2.1f seconds\n',fix(elapsed), (elapsed-fix(elapsed))*60)
```

PROGRAM PCA

```
tic
clear all
close all
load data\prosimgdata
load data\data_train
clear DisplayTrainingSet DisplayTestSet1 DisplayTestSet2

fprintf('\n\nPCA WITH RADON\n');
fprintf('¯¯¯¯¯¯¯¯¯¯¯¯¯¯¯¯\n');


%
============================================================
=============
```

```
% S=resmat_train; % radon + pca
S=TrainingSet; % pca only
%
=============================================================
=============


fprintf(' Finding mean image\n');
% Getting mean image
S=double(S);
tmimg=mean(S,2);  % obtains the mean of each row instead of each column

fprintf(' Finding zero-mean matrix of the image set\n');
% Step 3: Subtract the mean
Sdiff = S - repmat(tmimg,1,looptrain); % zero-mean image set

fprintf(' Finding covariance matrix C=AA''\n');
% Step 4: Find covariance matrix
% Find eigenvector if C = AA'
% Consider C = A'A
covariance = double(Sdiff') * double(Sdiff);
% Find v=eigenvector, d=eigenvalue
% A'A(v) = d(v)
% But use AA'(Av) = d(Av) method
% So Av is the eigenvector for C=AA'
% I have proove this myself
% With this, i will get the best M's eigenvector of C=AA'

fprintf(' Finding eigenvectors & eigenvalues\n');
% Step 5: Find eigenvectors and eigenvalues of C=AA'
[ v d ] = eig(covariance);
d = diag(d);

fprintf(' Sorting eigenvalues for C=A''A - [          ');
for i=1:looptrain-1
j=1;
```

```
while j<looptrain
if d(j) < d(j+1)
temp1 = d(j);
temp2 = v(:,j);
d(j) = d(j+1);
v(:,j) = v(:,j+1);
d(j+1) = temp1;
v(:,j+1) = temp2;
else
end
j=j+1;
end
percent=(i/(size(d,1)-1))*100;
fprintf('\b\b\b\b\b\b\b\b%6.2f%% ]', percent);
end
clear temp1 temp2;
fprintf('\n');
% d --> M's highest eigenvalues, sorted from HI to LO.
% v --> M's best eigenvectors, ordered by eigenvalue, HI to LO.

% normalizing ||v|| = 1
for i=1:looptrain;
v(:,i)=v(:,i)/norm(v(:,i));
end
eigenface = double(Sdiff) * v; % this is the best M eigenvector of C=AA'


no_of_fevec = looptrain; % the best K's eigenvector
d=d(1:no_of_fevec);
eigenface=eigenface(:,1:no_of_fevec);
% select the best K's eigenvector
% normaly K <= M
fprintf(' Number of eigenfaces used: %d \n', no_of_fevec);

fprintf(' Normalizing ||eigenface|| = 1\n');
% Step 6: Getting the eigenfaces
```

```
% normalizing ||eigenface|| = 1
for i=1:no_of_fevec;
eigenface(:,i)=eigenface(:,i)/norm(eigenface(:,i));
end


fprintf(' Getting weight vector (kernel set) of training images');
% Step 7: Finding weights vector of the training images
W=[];
W=eigenface'*double(Sdiff);
fprintf('\n');

% used for fusion of system
W_pca_with_radon = W;
eigenface_pca_with_radon = eigenface;
tmimg_pca_with_radon = tmimg;


save data/rdpcadata W_pca_with_radon eigenface_pca_with_radon looptrain no_test1 no_test2
tmimg_pca_with_radon;
fprintf('\nProgram end\nImage size [%dx%d]\nNumber of eigenvector used
[%d]\n',colused,rowused,no_of_fevec);
elapsed=toc/60;
fprintf('Elapsed time is: %d minutes %2.1f seconds\n',fix(elapsed), (elapsed-fix(elapsed))*60);
```

PROGRAM RADON

```
tic
clear
close all

fprintf('\n\nPERFORMING RADON TRANSFORM\n');
fprintf('¯¯¯¯¯¯¯¯¯¯¯¯¯¯¯¯¯¯¯¯¯¯¯¯¯¯¯¯¯¯¯¯¯¯\n');

% fprintf('theta step size, 1 to 10?\n: ');
% increament = input(' ');
increament = 1;
```

```
% fprintf('rho step size, 1 to 10?\n: ');
% increa2 = input(' ');
increa2 = 1;
save data\radonincrea increament increa2

load data\prosimgdata
% ------------------------------------------------
% || PERFORM RADON TRANSFORM ON TRAINING IMAGES ||
% ------------------------------------------------
resmat_train = []; % empty matrix
rhomat_train = [];
fprintf('Perform radon transform on Training Image Set\n');
fprintf('Progress [          ');
for i=1:looptrain
f=TrainingSet(:,i);
f=(reshape(f,colused,rowused))';
f=double(f);
[M N] = size(f);

% Center of the image
m = round(M/2);
n = round(N/2);

% The total number of rho's is the number of pixels on the diagonal, since
% this is the largest straight line on the image when rotating
rhomax = ceil(sqrt(M^2 + N^2));
rc = round(rhomax/2);

theta = 0:180;
mt = max(theta);

res = cast(zeros(rhomax+1,mt),'double'); % add 1 to be sure,
% could also be subtracted when
% checking bounds

for t = 1:increament:45 % below 45 degrees, use y as variable
```

```
costheta = cos(t*pi/180);
sintheta = sin(t*pi/180);
a = -costheta/sintheta; % y = ax + b

for r = 1:rhomax
rho = r - rc;
b = rho/sintheta; % y = ax + b

ymax = min(round(-a*m+b),n-1);
ymin = max(round(a*m+b),-n);

for y = ymin:increa2:ymax

x = (y-b)/a;
xfloor = floor(x); % The integer part of x
xup = x - xfloor; % The decimals of x
xlow = 1 - xup; % What is says
x = xfloor;
x = max(x,-m);
x = min(x,m-2);

% Flip the image horizontally:
res(rhomax - r + 1,mt-t) = res(rhomax - r + 1,mt-t) + xlow*f(y+n+1,x+m+1);
res(rhomax - r + 1,mt-t) = res(rhomax - r + 1,mt-t) + xup*f(y+n+1,x+m+2);
end
end
end

for t = 46:increament:90

costheta = cos(t*pi/180);
sintheta = sin(t*pi/180);
a = -costheta/sintheta; % y = ax + b
for r = 1:rhomax
rho = r - rc;
```

```
b = rho/sintheta; % y = ax + b
xmax = min(round((-n-b)/a),m-1);
xmin = max(round((n-b)/a),-m);
for x = xmin:increa2:xmax
y = a*x+b;
yfloor = floor(y);
yup = y - yfloor;
ylow = 1 - yup;
y = yfloor;
y = max(y,-n);
y = min(y,n-2);
res(rhomax - r + 1,mt-t) = res(rhomax - r + 1,mt-t) + ylow*f(y+n+1,x+m+1);
res(rhomax - r + 1,mt-t) = res(rhomax - r + 1,mt-t) + yup*f(y+n+2,x+m+1);
end
end
end

for t = 91:increament:135
costheta = cos(t*pi/180);
sintheta = sin(t*pi/180);
a = -costheta/sintheta; % y = ax + b
for r = 1:rhomax
rho = r - rc;
b = rho/sintheta; % y = ax + b
xmax = min(round((n-b)/a),m-1);
xmin = max(round((-n-b)/a),-m);
for x = xmin:increa2:xmax
y = a*x+b;
yfloor = floor(y);
yup = y - yfloor;
ylow = 1 - yup;
y = yfloor;
y = max(y,-n);
y = min(y,n-2);
res(rhomax - r + 1,mt-t) = res(rhomax - r + 1,mt-t) + ylow*f(y+n+1,x+m+1);
res(rhomax - r + 1,mt-t) = res(rhomax - r + 1,mt-t) + yup*f(y+n+2,x+m+1);
```

```
end
end
end

for t = 136:increament:179 % above 135 degrees, use y as variable
costheta = cos(t*pi/180);
sintheta = sin(t*pi/180);
a = -costheta/sintheta; % y = ax + b
for r = 1:rhomax
rho = r - rc;
b = rho/sintheta; % y = ax + b
ymax = min(round(a*m+b),n-1);
ymin = max(round(-a*m+b),-n);
for y = ymin:increa2:ymax
x = (y-b)/a;
xfloor = floor(x);
xup = x - xfloor;
xlow = 1 - xup;
x = xfloor;
x = max(x,-m);
x = min(x,m-2);
res(rhomax - r + 1,mt-t) = res(rhomax - r + 1,mt-t) + xlow*f(y+n+1,x+m+1);
res(rhomax - r + 1,mt-t) = res(rhomax - r + 1,mt-t) + xup*f(y+n+1,x+m+2);
end
end
end
for t = 180 % the sum-line is vertical
rhooffset = round((rhomax - M)/2);
for x = 1:M % cannot use r as x in both res and f since they are not the same size
r = x+rhooffset;
r = rhomax - r + 1;
for y = 1:N
res(r,t) = res(r,t) + f(y,x);
end
end
end
```

```
rhoaxis = (1:rhomax+1) - rc; %original
% rhoaxis = rhoaxis'; % original
theta = 1:180; % original

% store all the res to single matrix
[rowres colres]=size(res);
temp=reshape(res',rowres*colres,1);
resmat_train=[resmat_train temp]; % store all the res image <---- main data

[rowrho colrho]=size(rhoaxis);
temp=reshape(rhoaxis',rowrho*colrho,1);
rhomat_train=[rhomat_train temp]; % store all the rhoaxis


percent=(i/looptrain)*100;
fprintf('\b\b\b\b\b\b\b\b\b%6.2f%% ]', percent);
end
fprintf('\n');
save data\data_train resmat_train rhomat_train colres rowres colrho rowrho;


clear
close all
load data\radonincrea
load data\prosimgdata
% -------------------------------------------------------
% || PERFORM RADON TRANSFORM ON TESTING (KNOWN) IMAGES ||
% -------------------------------------------------------
resmat_test1 = [];
rhomat_test1  = [];
fprintf('\nPerform radon transform on KTB\n');
fprintf('Progress [          ');
for i=1:no_test1
f=TestSet1(:,i);
```

```
f=(reshape(f,colused,rowused))';
f=double(f);

[M N] = size(f);
% Center of the image
m = round(M/2);
n = round(N/2);

% The total number of rho's is the number of pixels on the diagonal, since
% this is the largest straight line on the image when rotating
rhomax = ceil(sqrt(M^2 + N^2));
rc = round(rhomax/2);

theta = 1:180;
mt = max(theta);

res = cast(zeros(rhomax+1,mt),'double'); % add 1 to be sure,
% could also be subtracted when
% checking bounds


for t = 1:increament:45 % below 45 degrees, use y as variable

costheta = cos(t*pi/180);
sintheta = sin(t*pi/180);
a = -costheta/sintheta; % y = ax + b

for r = 1:rhomax
rho = r - rc;
b = rho/sintheta; % y = ax + b

ymax = min(round(-a*m+b),n-1);
ymin = max(round(a*m+b),-n);

for y = ymin:increa2:ymax
x = (y-b)/a;
```

```
xfloor = floor(x); % The integer part of x
xup = x - xfloor; % The decimals of x
xlow = 1 - xup; % What is says
x = xfloor;
x = max(x,-m);
x = min(x,m-2);

% Flip the image horizontally:
res(rhomax - r + 1,mt-t) = res(rhomax - r + 1,mt-t) + xlow*f(y+n+1,x+m+1);
res(rhomax - r + 1,mt-t) = res(rhomax - r + 1,mt-t) + xup*f(y+n+1,x+m+2);
end
end
end

for t = 46:increament:90
costheta = cos(t*pi/180);
sintheta = sin(t*pi/180);
a = -costheta/sintheta; % y = ax + b
for r = 1:rhomax
rho = r - rc;
b = rho/sintheta; % y = ax + b
xmax = min(round((-n-b)/a),m-1);
xmin = max(round((n-b)/a),-m);
for x = xmin:increa2:xmax
y = a*x+b;
yfloor = floor(y);
yup = y - yfloor;
ylow = 1 - yup;
y = yfloor;
y = max(y,-n);
y = min(y,n-2);
res(rhomax - r + 1,mt-t) = res(rhomax - r + 1,mt-t) + ylow*f(y+n+1,x+m+1);
res(rhomax - r + 1,mt-t) = res(rhomax - r + 1,mt-t) + yup*f(y+n+2,x+m+1);
end
end
end
```

```
for t = 91:increament:135
costheta = cos(t*pi/180);
sintheta = sin(t*pi/180);
a = -costheta/sintheta; % y = ax + b
for r = 1:rhomax
rho = r - rc;
b = rho/sintheta; % y = ax + b
xmax = min(round((n-b)/a),m-1);
xmin = max(round((-n-b)/a),-m);
for x = xmin:increa2:xmax
y = a*x+b;
yfloor = floor(y);
yup = y - yfloor;
ylow = 1 - yup;
y = yfloor;
y = max(y,-n);
y = min(y,n-2);
res(rhomax - r + 1,mt-t) = res(rhomax - r + 1,mt-t) + ylow*f(y+n+1,x+m+1);
res(rhomax - r + 1,mt-t) = res(rhomax - r + 1,mt-t) + yup*f(y+n+2,x+m+1);
end
end
end
for t = 136:increament:179 % above 135 degrees, use y as variable
costheta = cos(t*pi/180);
sintheta = sin(t*pi/180);
a = -costheta/sintheta; % y = ax + b
for r = 1:rhomax
rho = r - rc;
b = rho/sintheta; % y = ax + b
ymax = min(round(a*m+b),n-1);
ymin = max(round(-a*m+b),-n);
for y = ymin:increa2:ymax
x = (y-b)/a;
xfloor = floor(x);
xup = x - xfloor;
xlow = 1 - xup;
```

```
x = xfloor;
x = max(x,-m);
x = min(x,m-2);
res(rhomax - r + 1,mt-t) = res(rhomax - r + 1,mt-t) + xlow*f(y+n+1,x+m+1);
res(rhomax - r + 1,mt-t) = res(rhomax - r + 1,mt-t) + xup*f(y+n+1,x+m+2);
end
end
end
for t = 180 % the sum-line is vertical
rhooffset = round((rhomax - M)/2);
for x = 1:M % cannot use r as x in both res and f since they are not the same size
r = x+rhooffset;
r = rhomax - r + 1;
for y = 1:N
res(r,t) = res(r,t) + f(y,x);
end
end
end

rhoaxis = (1:rhomax+1) - rc; %original
% rhoaxis = rhoaxis'; % original
theta = 1:180; % original

% store all the res to single matrix
[rowres colres]=size(res);
temp=reshape(res',rowres*colres,1);
resmat_test1=[resmat_test1 temp]; % store all the res image <---- main data

[rowrho colrho]=size(rhoaxis);
temp=reshape(rhoaxis',rowrho*colrho,1);
rhomat_test1=[rhomat_test1 temp]; % store all the rhoaxis

percent=(i/no_test1)*100;
fprintf('\b\b\b\b\b\b\b\b\b%6.2f%% ]', percent);
end
fprintf('\n');
```

```
save data\data_test1 resmat_test1  rhomat_test1;



clear
close all
load data\radonincrea
load data\prosimgdata
% ---------------------------------------------------------
% || PERFORM RADON TRANSFORM ON TESTING (UNKNOWN) IMAGES ||
% ---------------------------------------------------------
resmat_test2 = [];
rhomat_test2  = [];
fprintf('\nPerform radon transform on UTB\n');
fprintf('Progress [          ');
for i=1:no_test2
f=TestSet2(:,i);
f=(reshape(f,colused,rowused))';
f=double(f);

[M N] = size(f);
% Center of the image
m = round(M/2);
n = round(N/2);

% The total number of rho's is the number of pixels on the diagonal, since
% this is the largest straight line on the image when rotating
rhomax = ceil(sqrt(M^2 + N^2));
rc = round(rhomax/2);

theta = 1:180;
mt = max(theta);

res = cast(zeros(rhomax+1,mt),'double'); % add 1 to be sure,
% could also be subtracted when
% checking bounds
```

```
for t = 1:increament:45 % below 45 degrees, use y as variable

costheta = cos(t*pi/180);
sintheta = sin(t*pi/180);
a = -costheta/sintheta; % y = ax + b

for r = 1:rhomax
rho = r - rc;
b = rho/sintheta; % y = ax + b

ymax = min(round(-a*m+b),n-1);
ymin = max(round(a*m+b),-n);

for y = ymin:increa2:ymax
x = (y-b)/a;
xfloor = floor(x); % The integer part of x
xup = x - xfloor; % The decimals of x
xlow = 1 - xup; % What is says
x = xfloor;
x = max(x,-m);
x = min(x,m-2);

% Flip the image horizontally:
res(rhomax - r + 1,mt-t) = res(rhomax - r + 1,mt-t) + xlow*f(y+n+1,x+m+1);
res(rhomax - r + 1,mt-t) = res(rhomax - r + 1,mt-t) + xup*f(y+n+1,x+m+2);
end
end
end

for t = 46:increament:90
costheta = cos(t*pi/180);
sintheta = sin(t*pi/180);
a = -costheta/sintheta; % y = ax + b
for r = 1:rhomax
```

```
rho = r - rc;
b = rho/sintheta; % y = ax + b
xmax = min(round((-n-b)/a),m-1);
xmin = max(round((n-b)/a),-m);
for x = xmin:increa2:xmax
y = a*x+b;
yfloor = floor(y);
yup = y - yfloor;
ylow = 1 - yup;
y = yfloor;
y = max(y,-n);
y = min(y,n-2);
res(rhomax - r + 1,mt-t) = res(rhomax - r + 1,mt-t) + ylow*f(y+n+1,x+m+1);
res(rhomax - r + 1,mt-t) = res(rhomax - r + 1,mt-t) + yup*f(y+n+2,x+m+1);
end
end
end
for t = 91:increament:135
costheta = cos(t*pi/180);
sintheta = sin(t*pi/180);
a = -costheta/sintheta; % y = ax + b
for r = 1:rhomax
rho = r - rc;
b = rho/sintheta; % y = ax + b
xmax = min(round((n-b)/a),m-1);
xmin = max(round((-n-b)/a),-m);
for x = xmin:increa2:xmax
y = a*x+b;
yfloor = floor(y);
yup = y - yfloor;
ylow = 1 - yup;
y = yfloor;
y = max(y,-n);
y = min(y,n-2);
res(rhomax - r + 1,mt-t) = res(rhomax - r + 1,mt-t) + ylow*f(y+n+1,x+m+1);
res(rhomax - r + 1,mt-t) = res(rhomax - r + 1,mt-t) + yup*f(y+n+2,x+m+1);
```

```
end
end
end
for t = 136:increament:179 % above 135 degrees, use y as variable
costheta = cos(t*pi/180);
sintheta = sin(t*pi/180);
a = -costheta/sintheta; % y = ax + b
for r = 1:rhomax
rho = r - rc;
b = rho/sintheta; % y = ax + b
ymax = min(round(a*m+b),n-1);
ymin = max(round(-a*m+b),-n);
for y = ymin:increa2:ymax
x = (y-b)/a;
xfloor = floor(x);
xup = x - xfloor;
xlow = 1 - xup;
x = xfloor;
x = max(x,-m);
x = min(x,m-2);
res(rhomax - r + 1,mt-t) = res(rhomax - r + 1,mt-t) + xlow*f(y+n+1,x+m+1);
res(rhomax - r + 1,mt-t) = res(rhomax - r + 1,mt-t) + xup*f(y+n+1,x+m+2);
end
end
end
for t = 180 % the sum-line is vertical
rhooffset = round((rhomax - M)/2);
for x = 1:M % cannot use r as x in both res and f since they are not the same size
r = x+rhooffset;
r = rhomax - r + 1;
for y = 1:N
res(r,t) = res(r,t) + f(y,x);
end
end
end
```

```
rhoaxis = (1:rhomax+1) - rc; %original
% rhoaxis = rhoaxis'; % original
theta = 1:180; % original

% store all the res to single matrix
[rowres colres]=size(res);
temp=reshape(res',rowres*colres,1);
resmat_test2=[resmat_test2 temp]; % store all the res image <---- main data

[rowrho colrho]=size(rhoaxis);
temp=reshape(rhoaxis',rowrho*colrho,1);
rhomat_test2=[rhomat_test2 temp]; % store all the rhoaxis

percent=(i/no_test2)*100;
fprintf('\b\b\b\b\b\b\b\b\b%6.2f%% ]', percent);
end
fprintf('\n');
save data\data_test2 resmat_test2  rhomat_test2;


fprintf('\nProgram end - Data saved!\n');
elapsed=toc/60;
fprintf('Elapsed time is: %d minutes %2.1f seconds\n',fix(elapsed), (elapsed-fix(elapsed))*60)
```

PROGRAM END

```
tic
close all
clear all
load data\prosimgdata
load data\rdpcadata
load data\data_test1;
load data\data_test2;

ccmat1 = [];
farmat1 = [];
```

```
frrmat1 = [];
ccmat2=[];
farmat2=[];
decide = 3;

fprintf('\n\n(PCA WITH RADON) RECOGNITION TASK\n');
fprintf('                                        \n');
tcstart = input('Start of TCPARA value: ');
tcend = input('End   of TCPARA value: ');
stepval=input('Step value          : ');
TCPARA = [];
y=1;
tccheck=0;
while tccheck<tcend
TCPARA(y) = tcstart+(stepval*(y-1));
tccheck=TCPARA(y);
y=y+1;
end

fprintf('\n[] Total TCPARA to be tested: %d', size(TCPARA,2));
fprintf('\n[] Program start\n');

bigloop=1;
while bigloop<3
selection = bigloop;
if selection == 1
fprintf('\n[] Processing on Known Database - [          ');
else
fprintf('\n[] Processing on Unknown Database - [          ');
end

loading=0;
for z=1:size(TCPARA,2)

Tcpara=TCPARA(z);
```

```
if selection == 1
rmdir('result\PCA(with radon)\','s');
mkdir('result\PCA(with radon)\');
mkdir('result\PCA(with radon)\[known]CorrectMatching\');
mkdir('result\PCA(with radon)\[known]FAR\');
mkdir('result\PCA(with radon)\[known]FRR\');
mkdir('result\PCA(with radon)\[unknown]CorrectReject\');
mkdir('result\PCA(with radon)\[unknown]FAR\');

%
==========================================================
=============
%     T=[resmat_test1]; % radon + pca
T=TestSet1; % pca only
%
==========================================================
=============

% Step 3: Subtract the mean
T=double(T);
Tdiff = T - repmat(tmimg_pca_with_radon,1,no_test1);
elseif selection == 2
rmdir('result\PCA(with radon)\[unknown]CorrectReject','s');
rmdir('result\PCA(with radon)\[unknown]FAR','s');
mkdir('result\PCA(with radon)\[unknown]CorrectReject\');
mkdir('result\PCA(with radon)\[unknown]FAR\');

%
==========================================================
=============
%     T=[resmat_test2]; % radon + pca
T=TestSet2; %pca only
%
==========================================================
=============
```

```
% Step 3: Subtract the mean
T=double(T);
Tdiff = T - repmat(tmimg_pca_with_radon,1,no_test2);
else
end


if selection == 1
no_test=no_test1;
test_person_detail=test_person_detail1;
elseif selection == 2
no_test=no_test2;
test_person_detail=test_person_detail2;
end

% Step 4: Finding weight vector of the test image
w=[]; % Storing the weight of training images in matrix
for i=1:no_test;
temp = eigenface_pca_with_radon' * double(Tdiff(:,i));
w=[w temp];
loading=loading+1; % LOADING
percent=(loading/(size(TCPARA,2)*(no_test+looptrain+no_test)+size(TCPARA,2)))*100;
fprintf('\b\b\b\b\b\b\b\b%6.2f%% ]', percent);
end
clear temp

Tc = 0;
for j=1:looptrain;
for k=1:looptrain;
% euclidean distance start
temp = max(norm(W_pca_with_radon(:,j)-W_pca_with_radon(:,k)));
% euclidean distance end
if temp > Tc
Tc = temp;
end
end
```

```
loading=loading+1; % LOADING
percent=(loading/(size(TCPARA,2)*(no_test+looptrain+no_test)+size(TCPARA,2)))*100;
fprintf('\b\b\b\b\b\b\b\b%6.2f%% ]', percent);
end
Tc = Tc/Tcpara;
clear temp

success=0;
frr=0;
CC=0;
far=0;

testflag = test_person_detail(1);
TestPerson = 1;

for h=1:no_test;
if h<= testflag
% do nothing
else
testflag=testflag+test_person_detail(TestPerson+1);
TestPerson=TestPerson+1;
end

E = [];
for i=1:looptrain;
temp = norm(w(:,h)-W_pca_with_radon(:,i));
E = [ E; temp ];
end
[Emin person] = min(E);
clear temp

trainflag = train_person_detail(1);
TrainPerson=1;
for k=1:person
if k<= trainflag
% do nothing
```

```
else
trainflag=trainflag+train_person_detail(TrainPerson+1);
TrainPerson=TrainPerson+1;
end
end

if Emin < Tc
success=success+1;
if selection == 1
img=uint8(TestSet1(:,h));
img=reshape(img,(colused),(rowused));
img1=img';
elseif selection == 2
img=uint8(TestSet2(:,h));
img=reshape(img,(colused),(rowused));
img1=img';
end
img=uint8(TrainingSet(:,person));
img=reshape(img,(colused),(rowused));
img2=img';
img3=[img1 img2];
img3=imresize(img3, [(rowused*10) (colused*10)]);
if selection == 1
if TrainPerson==TestPerson
CC=CC+1;
str=strcat('result\PCA(with radon)\[known]CorrectMatching\','Test[',int2str(h),'] -
Train[',int2str(person),'].jpg');
eval('imwrite(img3,str)');

else
far=far+1;
if selection == 1
str=strcat('result\PCA(with radon)\[known]FAR\','Test[',int2str(h),'] -
Train[',int2str(person),'].jpg');
eval('imwrite(img3,str)');
```

```
end
end
elseif selection == 2
str=strcat('result\PCA(with radon)\[unknown]FAR\','Test[',int2str(h),'] -
Train[',int2str(person),'].jpg');
eval('imwrite(img3,str)');

end
else
frr=frr+1;
if selection == 1
img=uint8(TestSet1(:,h));
img=reshape(img,(colused),(rowused));
img1=img';
elseif selection == 2
img=uint8(TestSet2(:,h));
img=reshape(img,(colused),(rowused));
img1=img';
end
img=imread('unknown.jpg');
img=rgb2gray(img);
img2=imresize(img, [(rowused) (colused)]);
img3=[img1 img2];
img3=imresize(img3, [(rowused*10) (colused*10)]);
if selection == 1
str=strcat('result\PCA(with radon)\[known]FRR\','Test[',int2str(h),'].jpg');
eval('imwrite(img3,str)');

elseif selection == 2
str=strcat('result\PCA(with radon)\[unknown]CorrectReject\','Test[',int2str(h),'].jpg');
eval('imwrite(img3,str)');

else
end
end
loading=loading+1; % LOADING
```

```
percent=(loading/(size(TCPARA,2)*(no_test+looptrain+no_test)+size(TCPARA,2)))*100;
fprintf('\b\b\b\b\b\b\b\b\b%6.2f%% ]', percent);
end

% results in percentage (%)
success=(success/no_test)*100;
CC=(CC/no_test)*100;
far=(far/no_test)*100;
frr=(frr/no_test)*100;


if selection == 1
ccmat1 = [ccmat1 CC];       % correct classification for known database
farmat1 = [farmat1 far];        % FAR for known database
frrmat1 = [frrmat1 frr];       % FRR for known database
else
ccmat2 = [ccmat2 frr];      % correct classification for unknown database
farmat2 = [farmat2 success]; % FAR for unknown database
end
loading=loading+1; % LOADING
percent=(loading/(size(TCPARA,2)*(no_test+looptrain+no_test)+size(TCPARA,2)))*100;
fprintf('\b\b\b\b\b\b\b\b\b%6.2f%% ]', percent);
end

if selection == 1
recall=[TCPARA; ccmat1; farmat1; frrmat1];
save('recall.mat','ccmat1','farmat1','frrmat1','recall');
elseif selection == 2
reject=[TCPARA; ccmat2; farmat2];
end

bigloop=bigloop+1;
end
xcross=[TCPARA; ccmat1; ccmat2];
true=1;
while(true)
```

```
fprintf('\n\nShow result''s graph?\n1. Yes\n2. No\nchoise: ');
showgraph = input('');
if showgraph == 1

figure(1);
axes1 = axes('Parent',figure(1),'FontSize',14);
hold on
plot1 = plot(TCPARA,ccmat1,'Parent',axes1,'MarkerSize',8,'LineWidth',3);
set(plot1,'MarkerFaceColor',[0 0 0],'Marker','o',...
'DisplayName','Recall Correct Classification',...
'Color',[0 0 0]);
plot2 = plot(TCPARA,farmat1,'Parent',axes1,'MarkerSize',12,'LineWidth',3);
set(plot2,'MarkerFaceColor',[0 0 0],'Marker','x',...
'DisplayName','Recall FAR',...
'Color',[1 0 0]);
legend('show');
set(legend,'Location','NorthOutside');
xlabel('TCPARA','FontSize',16);
ylabel('Percentage (%)','FontSize',16);
hold off

figure(2);
axes1 = axes('Parent',figure(2),'FontSize',14);
hold on
plot1 = plot(TCPARA,ccmat2,'Parent',axes1,'MarkerSize',8,'LineWidth',3);
set(plot1,'MarkerFaceColor',[0 0 0],'Marker','o',...
'DisplayName','Reject Correct Classification',...
'Color',[0 0 0]);
plot2 = plot(TCPARA,farmat2,'Parent',axes1,'MarkerSize',12,'LineWidth',3);
set(plot2,'MarkerFaceColor',[0 0 0],'Marker','x',...
'DisplayName','Reject FAR',...
'Color',[1 0 0]);
legend('show');
set(legend,'Location','NorthOutside');
xlabel('TCPARA','FontSize',16);
ylabel('Percentage (%)','FontSize',16);
```

```
hold off

load recall.mat
figure(3);
axes1 = axes('Parent',figure(3),'FontSize',14);
hold on
plot1 = plot(TCPARA,ccmat1,'Parent',axes1,'MarkerSize',8,'LineWidth',3);
set(plot1,'MarkerFaceColor',[0 0 0],'Marker','o',...
'DisplayName','Recall Correct Classification',...
'Color',[0 0 0]);
plot2 = plot(TCPARA,ccmat2,'Parent',axes1,'MarkerSize',12,'LineWidth',3);
set(plot2,'MarkerFaceColor',[0 0 0],'Marker','x',...
'DisplayName','Reject Correct Classification',...
'Color',[1 0 0]);
legend('show');
set(legend,'Location','NorthOutside');
xlabel('TCPARA','FontSize',16);
ylabel('Percentage (%)','FontSize',16);
hold off

load recall.mat
figure(4);
axes1 = axes('Parent',figure(4),'FontSize',14);
hold on
plot1 = plot(TCPARA,farmat1,'Parent',axes1,'MarkerSize',8,'LineWidth',3);
set(plot1,'MarkerFaceColor',[0 0 0],'Marker','o',...
'DisplayName','Recall FAR',...
'Color',[0 0 0]);
plot2 = plot(TCPARA,farmat2,'Parent',axes1,'MarkerSize',12,'LineWidth',3);
set(plot2,'MarkerFaceColor',[0 0 0],'Marker','x',...
'DisplayName','Reject FAR',...
'Color',[1 0 0]);
legend('show');
set(legend,'Location','NorthOutside');
xlabel('TCPARA','FontSize',16);
ylabel('Percentage (%)','FontSize',16);
```

```
hold off
true=0;
elseif showgraph==2
true=0;
else
fprintf('[No such option!]');
end
end

fprintf('\nProgram end - Image size [%dx%d]\n',(colused),(rowused));
elapsed=toc/60;
fprintf('Elapsed time is: %d minutes %2.1f seconds\n',fix(elapsed), (elapsed-fix(elapsed))*60);
```